PUBLICATIONS OF
THE UNIVERSITY OF EASTERN FINLAND

Dissertations in Health Sciences

UNIVERSITY OF
EASTERN FINLAND

NIKO KIVINEN

THE ROLE OF AUTOPHAGY IN AGE-RELATED MACULAR DEGENERATION

The Role of Autophagy in Age-related Macular Degeneration

NIKO KIVINEN

The Role of Autophagy in Age-related Macular Degeneration

Studies into the pathogenesis of AMD

To presented by permission of the Faculty of Health Sciences, University of Eastern Finland for public examination in MS302, Medistudia building, of the University of Eastern Finland, Kuopio, on 10th February, 2017 at 12 noon.

Publication of the University of Eastern Finland
Dissertation in Health Sciences
400

Department of Ophthalmology, Institute of Clinical Medicine, School of Medicine
Faculty of Health Sciences
University of Eastern Finland
Kuopio
2017

Grano Oy
Jyväskylä, 2017

Distributor:
University of Eastern Finland
Kuopio Campus Library
P.O.Box 1627
FI-70211 Kuopio, Finland
http://www.uef.fi/kirjasto

ISBN (print): 978-952-61-2413-1
ISBN (pdf): 978-952-61-2414-8
ISSN (print): 1798-5706
ISSN (pdf): 1798-5714
ISSN-L: 1798-5706

Author's address: Department of Ophthalmology
University of Eastern Finland
KUOPIO
FINLAND

Supervisors: Professor Kai Kaarniranta, M.D., Ph.D.
Department of Ophthalmology
University of Eastern Finland
KUOPIO
FINLAND

Adjunct Professor Reijo Sironen, M.D., Ph.D.
Department of Pathology
University of Eastern Finland
KUOPIO
FINLAND

Reviewers: Docent Olli Arjamaa, M.D., Ph.D.
Zoological Museum, Section of Biodiversity and Environmental Science
University of Turku
TURKU
FINLAND

Adjunct Professor Jerzy Mackiewicz, M.D., Ph.D.
Department of Vitreoretinal Surgery
Medical University of Lublin
LUBLIN
POLAND

Opponent: Professor Morten C. Moe, M.D., Ph.D.
Department of Ophthalmology
University of Oslo
OSLO
NORWAY

Kivinen Niko
The Role of Autophagy in Age-related Macular Degeneration, Studies into the pathogenesis of AMD
University of Eastern Finland, Faculty of Health Sciences
Publications of the University of Eastern Finland. Dissertations in Health Sciences Number 400. 2017. 117p

ISBN (print): 978-952-61-2413-1
ISBN (pdf): 978-952-61-2414-8
ISSN (print): 1798-5706
ISSN (pdf): 1798-5714
ISSN-L: 1798-5706

ABSTRACT

Age-related macular degeneration (*AMD*) is the leading cause of irreversible blindness in the developed countries. The prevalence of disease is expected to triple in the approaching decades. At the moment, only those cases which present choroidal neovascularization, a hallmark of wet AMD, are treatable with antiproliferative therapeutic agents. Unfortunately, these cases account for only 10-15 % of all AMD patients, i.e. most patients are still without any treatment options. The key role in the development of AMD can be traced the degeneration of retinal pigment epithelium cells (*RPE*) which are the caretakers of photoreceptor rod and cones.

The aim of the study was to clarify the role of autophagy in the pathogenesis of AMD. Ocular samples from knock-out mice and human cadavers were used in the experiments in conjunction with laboratory grown RPE-cell lines; samples were examined by modern cell and molecular biological techniques as well as immunohistochemical methods. Finally, a test series with collagen 18 total knock-out (*Col18a1*$^{-/-}$) mice was conducted. The above methods were used to evaluate proteostasis of RPE in the mouse model.

The levels of SQSTM1/p62 protein were elevated in macular areas of AMD cadaver samples; this was interpreted as evidence that a dysfunction of autophagy is involved in AMD pathogenesis. We also noted that the molecular chaperone, Hsp70, which has a strong cytoprotective capacity, evades autophagic clearance. The current standard-of-care for AMD has no effect on the activity of autophagy in RPE cells. An age-related insufficiency of proteostasis was observed together with RPE degeneration in *Col18a1*$^{-/-}$ mice.

We conclude that SQSTM1/p62 is a good marker for impaired autophagy. Furthermore, Hsp70 upregulation could be used as a therapeutic target against retinal pigment epithelium (*RPE)* degeneration and in the development novel treatments for AMD. Finally, *Col18a1*$^{-/-}$ mice, which display AMD-like tissue alterations may represent a relevant animal model for impaired autophagy and AMD.

National Library of Medicine Classification: WW 270, QU 375, QZ 140

Medical Subject Headings: Age-related Macular Degeneration; AMD pathophysiology; Autophagy; Animal model; Mouse model; Ocular disease; Blindness; Visual impairment

Kivinen Niko
Autophagian rooli silmänpohjan ikärappeumassa, tutkimuksia AMD:n patogeneesistä
Itä-Suomen yliopisto, terveystieteiden tiedekunta
Publications of the University of Eastern Finland. Dissertations in Health Sciences Numero 400. 2017. 117 s.

ISBN (print): 978-952-61-2413-1
ISBN (pdf): 978-952-61-2414-8
ISSN (print): 1798-5706
ISSN (pdf): 1798-5714
ISSN-L: 1798-5706

TIIVISTELMÄ

Silmänpohjan ikärappeuma (engl. *Age-related macular degeneration, AMD*) on yleisin näkövammaisuuteen johtava silmäsairaus länsimaissa. Sen esiintyvyys tulee kolminkertaistumaan tulevien vuosien aikana. Tällä hetkellä ainoastaan ne tapaukset, joissa on mukana uudissuonitusta, ovat hoidettavissa verisuonten kasvua estävillä lääkkeillä. Nämä tapaukset kattavat ainoastaan noin 10-15 % kaikista tapauksista ja siten suurin osa AMD-potilaista on vailla hoitoa. Merkittävä rooli sairauden synnyssä on valoa aistivien solujen hyvinvoinnista huolehtien verkkokalvon pigmenttiepiteelisolujen (engl. *Retinal pigment epithelium, RPE*) rappeuma.

Tutkimuksen tarkoituksena oli selvittää solujen itsesyönnin eli autophagian roolia ikärappeuman synnyssä. Käytimme laboratorio-olosuhteissa kasvatettujen solujen lisäksi silmänäytteitä kadaveri-ihmisiltä ja geenimuunnelluista hiiristä. Näytteitä tutkittiin modernein solu- ja molekyylibiologisin menetelmin sekä immunohistokemiallisesti. Lopuksi selvitimme näillä menetelmillä kollageeni 18 -poistogeenisten hiirten RPE-solujen valkuaisainehomeostaasia.

AMD-potilaiden silmänäytteiden makula-alueiden koholla olevat SQSTM1/p62-tasot osoittivat autofagian toimimattomuuden liittyvän AMD:n patogeneesiin. Näytimme myös vahvan soluja suojelevan kapasiteetin omaavan kaitsijaproteiini Hsp70 väistävän autofagisen hajotuksen. Nykyinen käypä hoito AMD:lle, eli silmän sisälle pistettävä verisuonien kasvua estävä tekijä ei vaikuttanut autofagiaan. Osoitimme selvän ikääntymiseen liittyvän RPE-solukon degeneraation ja proteiinisäätelyn toimintahäiriön *Col18a1*$^{-/-}$ hiirissä.

Havaitsimme SQSTM1/p62–proteiinitasojen olevan hyvä merkkiaine autophagian toimimattomuudelle. Lisäksi, nostamalla Hsp70 tasoja RPE-soluissa esimerkiksi laserin tai lääkkeiden avulla voitaisiin mahdollisesti estää niiden rappeutumista ja hidastaa AMD:n kehittymistä. Lopuksi, *Col18a1*$^{-/-}$ hiiri AMD:n kaltaisine muutoksineen voisi toimia eläinmallina toimimattomalle autophagialle ja silmänpohjan ikärappeumalle.

Luokitus: WW 270, QU 375, QZ 140
Yleinen Suomalainen asiasanasto: Silmänpohjan ikärappeuma; AMD tautioppi; Autofagia; Eläinmalli; Hiirimalli

To my wife and family

Acknowledgements

This study was completed in the Doctoral Program of Clinical Research of the University of Eastern Finland. The study was carried out in the Department of Ophthalmology, Institute of Clinical Medicine, University of Eastern Finland.

I express my deepest gratitude to my principal supervisor Professor Kai Kaarniranta. His guidance, expertise, enthusiasm and encouragement both in this study and ophthalmogy in general have been invaluable to this work.

I would also like to thank my supervisor Adjunct Professor Reijo Sironen for his recognized expertise and guidance both in microscopy, immunohistochemistry as well as in scientific writing. Without your help and guidance, I would have been completely lost.

Anne Seppänen and Anne-Mari Haapaniemi are warmly acknowledged for their help and technical assistance in sample collection. I thank Elisa Toropainen, Ph.D., Johanna Viiri, MSc., and Jussi Paterno, M.D., for all their help in scientific and non-scientific matters. I would also like to thank Niko Setälä, M.D., Ph.D., for all the guidance. A special thank you goes to all the collaborators who have participated in these studies. Ewen MacDonald, Ph.D., is warmly thanked for the linguistic revision of the thesis.

The reviewers of this thesis, Docent Olli Arjamaa, M.D., Ph.D., and Adjunct Professor Jerzy Mackiewicz, M.D., Ph.D., are warmly acknowledged for their expertise and comments, which helped to improve this work.

My family, and especially my dear wife Taija-Lotta, have helped me navigate through this project. I wouldn't have made it without you and for that I'm eternally grateful.

This study was supported by grands from University of Eastern Finland, Evald and Hilda Nissi Foundation, The Finnish Eye Foundation, The Finnish Medical Foundation and Suomen Silmälääkäriyhdistys which are gratefully acknowledged.

Kuopio, January 2017

Niko Kivinen

List of the original publications

This dissertation is based on the following original publications:

I Viiri J, Amadio M, Marchesi N, Hyttinen JMT, Kivinen N, Sironen R, Rilla K, Akhtar S, Provenzani A, D'Agostino VG, Govoni S, Pascale A, Agostini H, Petrovski G, Salminen A, Kaarniranta K. Autophagy Activation Clears ELAVL1/HuR-mediated Accumulation of SQSTM1/p62 During Proteasomal Inhibition in Human Retinal Pigment Epithelial Cells. *PLoS ONE 8(7):e69563. doi:10.1371/journal.pone.0069563, 2013.*

II Kivinen N, Hyttinen JMT, Viiri J, Paterno J, Felszheghy S, Kauppinen A, Salminen A, Kaarniranta K. Hsp70 Binds Reversible to Proteasome Inhibitor -induced Protein Aggregates and Avoid Autophagic Clearence in ARPE-19 Cells. *Journal of Biochemical and Pharmacological Research, Vol. 2 (1): 1-7, 2014.*

III Kivinen N, Dithmer M, Kinnunen K, Lucius R, Roider J, Kaarniranta K, Klettner A. Bevacizumab Does Not Affect Autophagy Clearance During Proteasomal Inhibition in Human Retinal Pigment Epithelial Cells. *Journal of Biochemical and Pharmacological Research, Vol. 2 (1): 44-53, 2014.*

IV Kivinen N, Felszaghy S, Kinnunen A, Setälä N, Aikio M, Kinnunen K, Sironen R, Pihlajaniemi T, Kauppinen A, Kaarniranta K. Absence of Collagen XVIII in Mice Causes Age-related Insufficiency in Retinal Pigment Epithelium Proteostasis. *Biogerontology. Vol. 17(4): 749-761, 2016. doi: 10.1007/s10522-016-9647-7*

Contents

Abbreviations

AD	Alzheimer's disease
ADP	Adenosine diphosphate
AE2	N-retinyl-N-retinylidene ethanolamine
AGE	Advanced glycation end-products
AICAR	5-Aminoimidazole-4-carboxamide ribonucleotide
AMD	Age-related macular degeneration
AMPK	AMP-activated protein kinase
ARE	adenine/uracil-rich elements
AREDS	Age-related eye disease study
ATCC	American type culture collection
ATP	Adenosine triphosphate
BAF	Bafilomycin
BCL-2	B-cell lymphoma 2
BCVA	Best corrected visual acuity
C3	Complement component 3
CHF	Complement factor H
CNV	Choroidal neovascularisation
ELAVL1	Embryonic Lethal, Abnormal Vision, Drosophila -Like 1
FAG	Fluorescein angiography
Hsp	Heat-shock protein
Hur	Human antigen R
LC3	Microtubule-associated protein light chain 3
LPP	Lysosomal proteolysis
MG-132	Carbobenzoxy-Leu-Leu-leucinal
MMP	Matrix metalloproteinase
mTOR	mammalian target of rapamycin
NFKB	Nuclear factor kappa-B
NRF2	Nuclear factor E2-related factor 2
OCT	Optical coherence tomography
ORF	Open reading frame
PDT	Photodynamic therapy
p62	Nucleoporin p62
RAGE	Receptor for AGE
ROS	Reactive oxygen species
RPE	Retinal pigment epithelium
SDS	Sodium dodecyl sulphate
SQSTM1	Sequestome 1
TNFα	Tumor necrosis factor alpha
UB	Ubiquitin

UPP	Ubiquitin-proteasome pathway
VCAM-1	Vascular cell adhesion molecule-1
VEGF	Vascular endothelial growth factor

1 Introduction

Age-related macular degeneration (*AMD*) is the leading cause for irreversible visual impairment and blindness (i.e. best corrected visual acuity (*BCVA*) < 0.3 in better eye) in the developed countries. Its prevalence is expected to increase in the future [Pascolini et al. 2002, Gongdon et al. 2004, Rein et al. 2009]. The disease affects mainly the central or macular area of the eye (Figure 1), the part of the eye which is responsible for detailed vision. The macula has the highest concentration of photoreceptor cells, and thus AMD causes a loss of central vision whereas the peripheral vision usually remains normal [Cheung and Eaton 2013]. The loss of vision is directly linked to the damage and death of photoreceptor cells; this is primarily caused by degeneration of the retinal pigment epithelium (*RPE*) (Figure 2) [Klettner et al. 2013]. RPE is a part of the blood-ocular barrier and furthermore it performs many functions such as transporting nutrients and oxygen between the retina and the choroid as well as producing growth factors and cytokines [Cheung and Eaton 2013].

Phenotypically AMD can be divided into dry (atrophic) and wet (exudative) forms [Kaarniranta et al. 2013]. Dry AMD is more common and is responsible for 80-85 % of all cases [Kaarniranta et al. 2009a]. In the early stages of dry AMD, one can detect small, yellow deposits called drusen (sing. *druse*) in the fundus of the eye. These deposits are mainly composed of protein derivates, essentially cellular waste products, and they gradually grow in size from small, less than 63 μm diameter deposits to larger than 125 μm deposits [Bird et al. 1995]. The dry form usually progresses slowly over years [Sunnes et al. 1997, Kaarniranta and Salminen 2009]. The wet form is more aggressive as it can progress in a much shorter time frame, days or weeks, leading to a complete loss of central vision if not treated [Klettner 2014]. In the wet form of AMD, new, abnormal blood vessels (so-called neovascularization) grow from the choroidal capillaries through Bruch's membrane into the retina. These new blood vessels tend to leak, leading to edema in the retina and damage to the photoreceptor cells [Kaarniranta et al. 2003, Mannermaa et al. 2007]. Currently, there is no cure for dry AMD, although nutrient supplements are usually recommended [AREDS 2000]. The wet form is treated with anti-VEGF agents, which may stop or retard the progression of the disease [Klettner 2014].

Although the pathogenesis of AMD is still partly unknown, the decline of cellular autophagy (literally meaning "self-eating") plays a key role in the development of AMD [Kaarniranta et al. 2011]. Autophagy is a central degradation process in mammalian cells [Lilienbaum 2013], and it is known to be impared in aged RPE cells [Li et al. 2008].

The purpose of this study was to investigate the role of autophagy in the regulation of proteostasis in *in vitro* and *in vivo* models and in human samples. We postulate that autophagy might be a novel therapy target in AMD.

2 Review of Literature

2.1 AGE-RELATED MACULAR DEGENERATION

Age-related macular degeneration is the leading cause of visual impairment in the developed countries [Pascolini et al. 2002]. It has been estimated that about 50000 Finns have BCVA (*best corrected visual acuity*) below of 0.3 and approximately 40 % of these suffer from AMD [Ojamo 2014]. The prevalence of fundus findings (eg. drusen) correlating with AMD has been shown to be as high as 20 % in individuals aged 43-86 years, although this may not correlate with clinically significant AMD. Approximately 1.6 % of the population develop late stage AMD (Beaver Dam eye study) [Klein et al. 2014]. The prevalence of AMD increases exponentially with every decade after 50 years [Cheung and Eaton 2013]. Globally the annual costs associated with AMD are estimated 340 billion US dollars [Klein et al. 2010, Biarnés et al. 2011]. The loss of central vision can be devastating and crippling to patients and cause other severe complications such as falling down [Klein et al. 2003] and depression [Casten et al. 2004]. Considering its impact on quality of life, then AMD appears to be at the same level as other chronic diseases (eg. chronic cardiac diseases or arthritis) [Williams et al. 1998].

2.1.1 Etiology

AMD is a multifactorial disease and it evolves from complex genetic and environmental interactions. However, aging is the strongest risk factor for AMD. The risk increases exponentially with every decade after 50 years of age [Rudnicka et al. 2012]. In particular, the Caucasian race has been documented to be at risk for AMD [Klein et al. 2004]. Since females usually live longer than males, they have an increased risk of developing AMD [Hyman and Neborsky 2004]. However, many epidemiological findings are controversial and might be based on population differences [Klein et al. 2004]. Smoking, hypertension, high dietary intake of fats, obesity and low intake of anti-oxidants and zinc have been shown to be associated with the disease [Maguire et al. 1997, Klein et al. 2001, Seddon et al. 2003 Thornton et al. 2005]. Several studies have revealed that over 70 % of AMD cases are associated with polymorphisms in complement factor H (*CFH*), complement factor B and complement component 2 (*C2*) genes [Gold et al. 2006, Fritsche et al. 2013]. Genetic pathways have been linked to complement systems, cholesterol and lipid metabolism, oxidative stress and angiogenesis [Ratnapriya and Chew 2013].

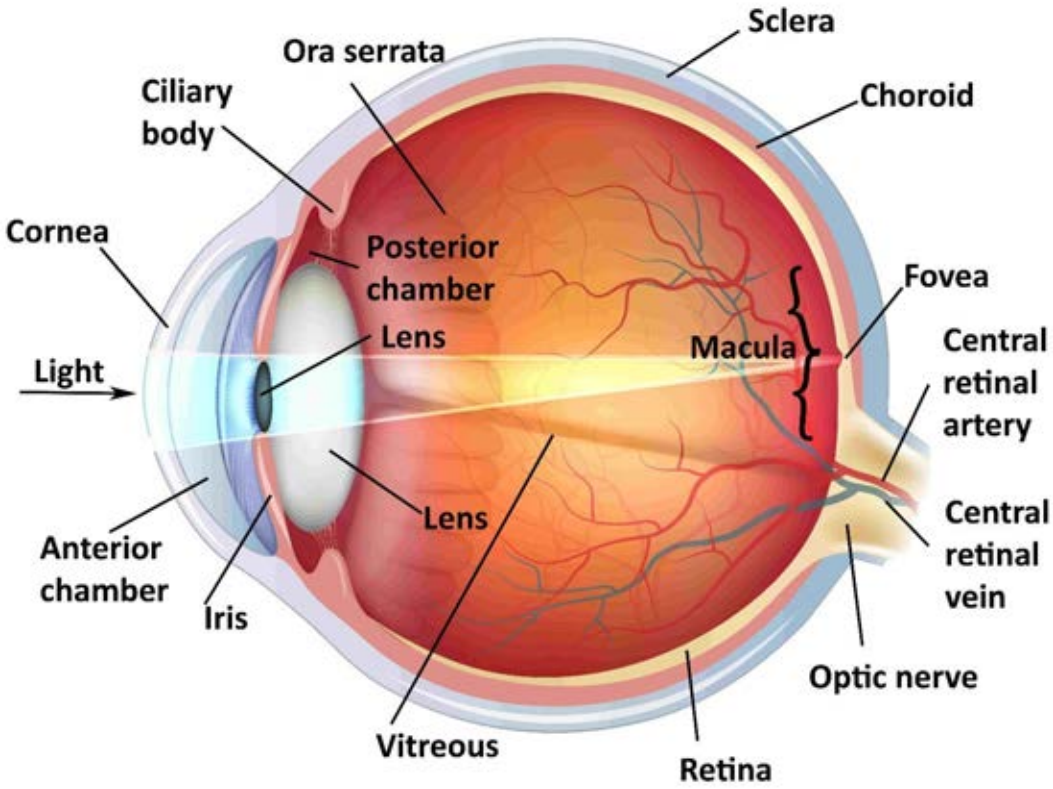

Figure 1. Anatomy of the human eye. Modified from Shutterstock images, www.shutterstock.com

2.1.2 Clinical findings and diagnostic criteria

The clinical examination can incorporate slit-lamp biomicroscopy, optical coherence tomography (*OCT*) (Figure 3) and fluorescein angiography (*FAG*). The first signs of AMD are small, white-yellow deposits called drusen situated between the RPE and the underlying basement membrane (Bruch's membrane) [Cheung and Eaton 2013]. Drusen can be subdivided according to their size and appearance. Small drusen have a diameter less than 63 μm, intermediates are sized between 63-125 μm and large are over 125 μm in diameter [Bird et al. 1995, Klein et al. 2014]. In addition to their size, drusen can be classified based on their form. Hard drusen are small and have well defined margins where as soft ones are larger and have diffuse, cloud-like margins [Sarks et al. 1994]. At the same time with drusen RPE hypo- and/or hyperpigmentation can be observed by fundus biomicrosopy [Fine et al. 2000]. The presence of choroidal neovascularization is a clinical criterion for wet AMD. Retinal hemorrhages and oedema can be observed by biomicroscopy and OCT (Figure 5). FAG-imaging shows leaking new blood vessels sprouting from the choriocapillaries [Mannermaa et al. 2007].

AREDS (The Age-Related Eye Disease Study) criteria [AREDS 2000] are widely used in the AMD classification. According to AREDS, AMD can be divided into early, intermediate and late forms of AMD. In the early stage, there are several small drusen, nonextensive

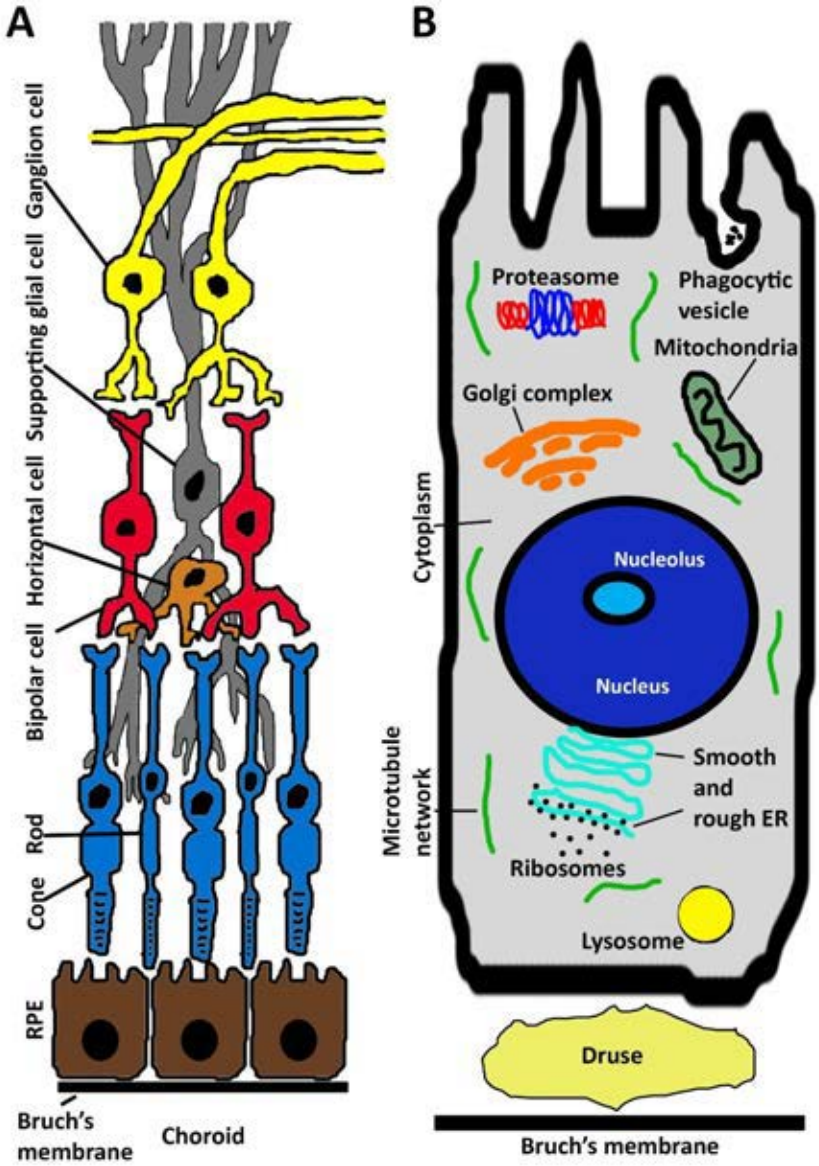

Figure 2. Retinal cells and RPE-cell organelles.

intermediate drusen or pigment abnormalities (hypo/hyperpigmentation) at least in one eye. In the intermediate stage, there are large drusen, several intermediate drusen or noncentral (i.e. not affecting the fovea) geographic atrophy at least in one eye. The term "geographic atrophy" is used when there are no RPE or photoreceptor cells in the area of interest [Bird 2010]. Late stage disease has geographic atrophy, choroidal neovascularization and/or fibrosis in the fovea. Depending on the severity level of AMD, patients experience difficulties in reading, facial recognition and in driving a motorized vehicle [Fine et al. 2000].

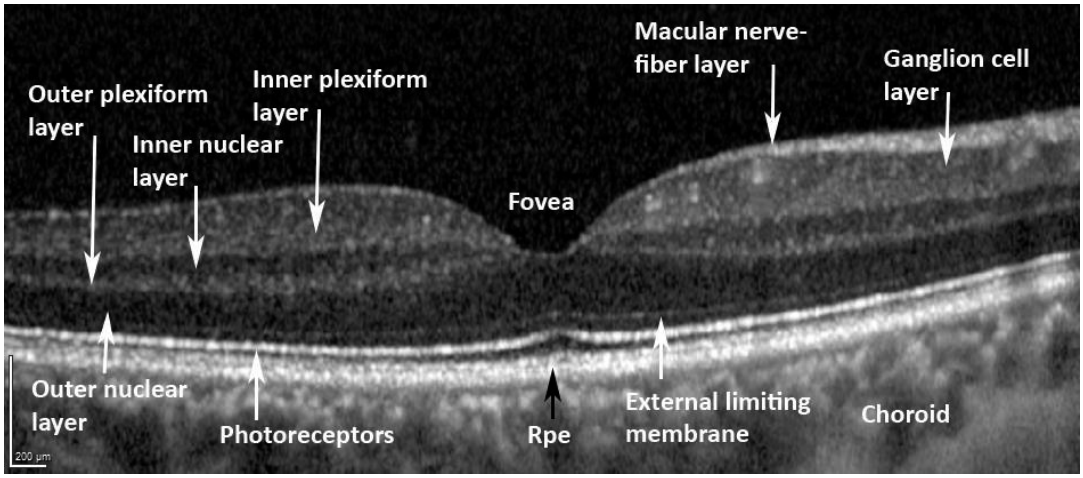

Figure 3. OCT-image of the human macula showing retinal cell layers.

2.1.3 Pathogenesis

The fundamental cellural pathophysiological events are increased oxidative stress, protein aggregation and inflammation (Figure 4). RPE cells function as the caretakers of the retinal outer segment which is mainly composed of photoreceptors. They maintain the blood-retina-barrier, regulate ion balance, participate in the visual cycle and secrete several growth factors [Kinnunen et al. 2012]. They also have a distinctive role in the clearance of used photoreceptor outer-segments (the part of the retina that wears out during the visual cycle) by a process called phagocytosis [Strauss 2005]. During phagocytosis, a cell engulfs and takes up a particle within a plasma-membrane envelope (a form of endocytosis) [Gordon et al. 2016].

The RPE cells are constantly exposed to oxidative stress. Firstly, they phagocytose lipid-rich retinal outer segments derived from photoreceptors, rods and cones. This predisposes the RPE to oxidation because the process generates reactive oxygen species (*ROS*) [Gordon 2016]. At the same time, the RPE is exposed to light combined with a high oxygen consumption due to its high metabolic activity. All of these properties increase oxidative stress [Tate et al. 1995, Beatty et al. 2000]. The dysfunction of phagocytosis leads to a

failure in the clearance of used photoreceptor outer segments, which on the other hand causes intracellular accumulation of lipofuscin, a lipid-protein-aggregate [Kennedy et al. 1995]. Lipofuscin is the product of the oxidation of unsaturated fatty acids [Algvere et al. 2016]. Around 90 % of the accumulated lipofuscin in

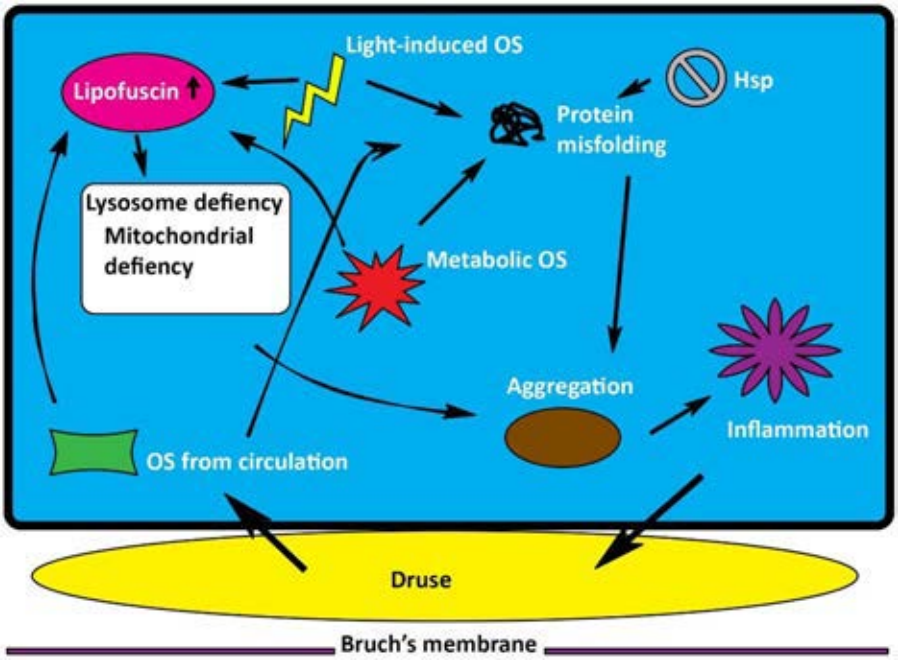

Figure 4. The vicious cycle in AMD. Lipofuscin accumulation leads to lysosome and mitochondrial defiency. This is worsened by the constant oxidative stress (OS). Oxidative stress also causes increased protein misfolding, which is impaired in AMD by a dysfunction of molecular chaperones (Hsp). These properties lead to protein aggregation and ultimately to inflammation, which in turn leads to drusen formation. The formation of drusen decreases cellular homeostasis, and the vicious cycle is completed.

the RPE originates from the retinoids (rich in unsaturated fatty acids) used in the visual cycle [Sparrow et al. 2013]. Lipofuscin is a toxic compound, which increases the formation of ROS when exposed to light [Algvere and Seregard 2002, Roth et al. 2004]. Vitamin A -derived fluorophores in the lipofuscin pigment cause protein misfolding and inhibition of mitochondrial respiration [Algvere and Seregard 2002, Brunk and Terman 2002]. In addition, nuclear factor kappaB, a master regulator of both innate and adaptive immune systems is triggered by many stimuli such as the accumulation of advanced glycation end-products (*AGE*) and receptor for AGE (*RAGE*). Interleukin 6 (*IL-6*) is transcriptionally regulated by nuclear factor kappaB and it is a regulator for choroidal neovascularization (*CNV*) [Izumi-Nagai et al. 2007]. Interestingly, activation of RAGE in RPE produces vascular endothelial growth factors (*VEGF*) and RAGE is highly accumulated in the late phase AMD but not in normal retina. Thus, the AGE-RAGE-nuclear factor kappaB –axis

can lead to CNV [Howes et al. 2004, Bierhaus et al. 2005, Paimela et al. 2007, Oskolkova et al. 2008, Javitt and Javitt 2009]. RPE degeneration caused by the dysfunction of phagocytosis, protein degradation and metabolic insufficiency all play a key role in the pathogenesis of AMD (Kinnunen et al. 2012]. This loss of retinal homeostasis distinguishes AMD from the normal degenerative changes that occur with aging [Ardeljan and Chan 2013].

Drusen are the hallmarks of AMD; they have both intra- and extraocular sources [Buschini et al. 2011]. Components, such as ubiquitin, integrins, beta-amyloid, complement components, collagens and fibronectins have been identified in drusen [Johnson et al. 2000]. Interestingly, beta-amyloid has been identified in the senile plaques of individuals with Alzheimer's disease (*AD*). AD also shares pathophysiological similarities with AMD e.g. oxidative stress and degeneration leading to cell death; in fact it has been hypothesized that AMD and AD might be two representations of the same disease [Vladan and Panfoli 2012]. Regardless of the AD connection, it seems that drusen are caused by local inflammation, activation of the complement system and systemic immune (eg. acute, autoimmune, coagulation, cytokine etc.) mechanisms [Hageman et al. 2001]. The formation and accumulation of drusen causes hypoxia in the retinal pigment epithelium by decreasing the flow of oxygen from the choriocapillaries to the RPE, which secondarily leads to degeneration [Arjamaa et al. 2009].

2.1.4 Current treatments of AMD

Currently, there is no treatment available for dry AMD [Bowes et al. 2013]. Oral supplementation with vitamins C and E, lutein, zeaxanthin and zinc according to AREDS and The Age-Related Eye Disease Study 2 (*AREDS2*) formulation may delay the progress of AMD from earlier stages to wet disease but not to late stage atrophic AMD [AREDS 2001, AREDS2 2013].

Laser photocoagulation of drusen has also been outconsidered as a therapeutic device, because the disappearance of drusen has been observed after laser photocoagulation [Cleasby et al. 1979, Gross-Jendroska et al. 1998]. In 2009, one study group showed that laser photocoagulation of drusen was not useful, although it had no adverse effects, and thus it could not be recommended [Frenneson et al. 2009]. This was later confirmed by a Cochrane review [Virgili et al. 2015].

Some years ago, photodynamic therapy (*PDT*) was widely used in the treatment of wet AMD. In PDT-treatment, intravenously administered verteporfin (a benzoporphyrin derivative) is activated with an infrared laser beam focused above the macula. Verteporfin concentrates in new blood vessels and its activation triggers the formation of free oxygen radicals, ultimately leading to local thrombosis [Scott and Goa 2000]. The use of PDT is less effective than treatment with VEGF inhibitors but it reduces the loss of vision [Kaiser 2006]. In rare cases, laser photocoagulation of CNV can be used as a treatment, but in those cases the lesion must be at least 200 μm from the fovea because of the risk of central

scotoma [Macular Photocoagulation Study Group 1991]. PDT is still a worthwhile option, for example, in cases where intravitreal injections are relatively (post-endophthalmitis, inflammation) or absolutely contraindicated (such as in macular ischemia).

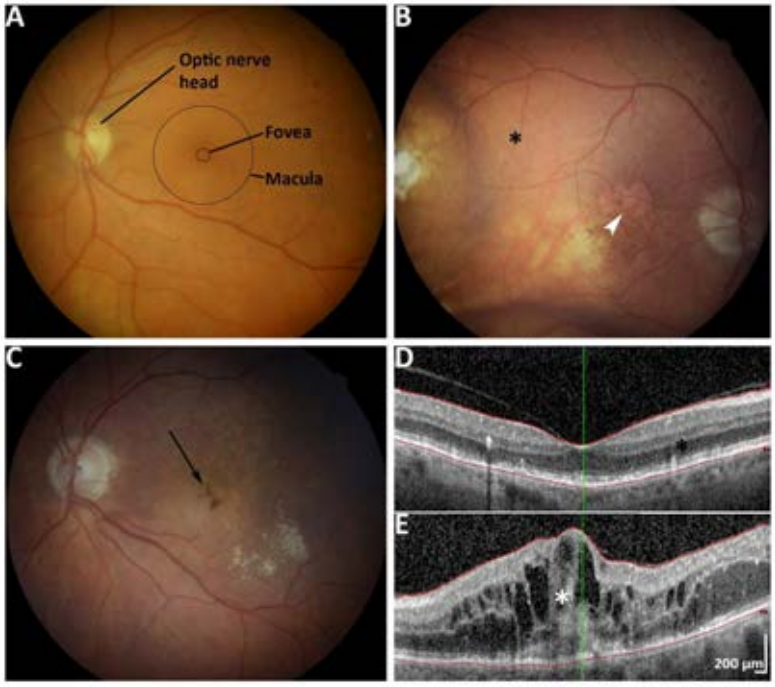

Figure 5. A: Normal fundus showing the papilla, macula and the fovea. B: Fundus with dry AMD. Drusen (black asterisk) and geographic atrophy (white arrow head). C: Retinal hemorrhage (black arrow) in the fundus of a patient with wet AMD. D: OCT-image from B, showing drusen with no oedema. E: OCT-image from C, showing massive intraretinal oedema (white asterisk).

Currently anti-VEGF –injections are the first option for the treatment of wet AMD [Klettner 2014]. Clinicians can administer four different VEGF-therapies for AMD [Cheung and Eaton 2013]. Bevacizumab was first developed for the treatment of metastatic colorectal carcinoma, but subsequently has been used intravitreally for the treatment of wet AMD as an off-label product [Brechner et al. 2011]. Bevacizumab binds to all active VEGF-A isoforms [Klettner and Roider 2009] and its safety and efficacy have been proved [Tufail et al. 2010]. Ranibizumab is the binding fragment of bevacizumab; it works similarly to bevazicumab binding to all active VEGF-A isoforms [Ferrara et al. 2006]. Aflibercept differs from the former two agents by binding to two sites on the VEGF-dimer and and thus trapping the growth factor. It also binds placental growth factor as well as all VEGF-A isoforms [Dixon et al. 2009]. The fourth currently used drug is pegaptanib, which prevents the VEGF-165 isoform from binding to VEGF receptors [Singerman et al. 2008]. Because the efficacy of pegaptanib has been proved to be inferior to the other options, it is used as a second-line therapy [Cheung and Eaton 2013]. In all of the therapies, an interval

of 4-8 weeks is generally applied although there are studies that recommend intravitreal injections to be given at 6-7 week intervals [Zhu et al. 2008]. In cases of resistance, treatment time-outs and/or switching between therapeutics can be useful [Bressler 2009, Arjamaa and Minn 2012].

2.1.5 Trials for new AMD treatments

Since AMD has a multifactorial background, several targets for treatment have been proposed. The systemic use of an antibody against amyloid-beta in a mouse model seems to preserve RPE integrity and visual function [Ding et al. 2011]. Complement-based therapeutics, such as inhibitory peptides, antibodies, aptamers, corticosteroids and non-steroidal anti-inflammatory drugs, have been widely studied but without any breakthroughs [Ambati et al. 2013]. For example, a recent PHASE II –trial showed that C5-inhibition was well tolerated but did not reduce the progression of geographic atrophy [Yehoshua et al. 2014]. Interestingly, inactivation of the complement factor D reduced geographic atrophy by approximately 20 % [Jack et al. 2016]. As oxidative stress has a significant role in the development of AMD, therapeutic agents aimed towards lessening oxidative stress are being evaluated. A topically administered disubstituted hydroxylamine, an anti-oxidant and anti-inflammatory molecule, was proven to be tolerated but not benefical in a PHASE II trial. As beta-amyloid is known to be pro-inflammatory, topically and intravenously delivered agents targeted against beta-amyloid are undergoing PHASE I and II trials on the hypothesis that this would be RPE protective [Hanus et al. 2016]. Agents targeting the visual cycle and lipofuscin, especially against the formation of vitamin A derivatives, are also under evaluation [Jack et al. 2016, Hanus et al. 2016]. Since AMD is associated with protein accumulation and dysfunction of RPE autophagy activity, autophagy regulating kinases are also thought to be potential targets for the treatment [Kaarniranta et al. 2012].

It has also been proposed that atrophic AMD would be amenable to treatment with stem cells. Stem cell –derived RPE would replace the damaged RPE and provide sufficient function to ensure the survival of other retinal cells. The first clinical trials with human embryonic stem cell –derived RPE cells transplanted subretinally were promising [Becker et al. 2012] and phase I/II trials showed improvement of BCVA [Schwartz et al. 2015]. Further results are awaited.

2.1.6 Current models for AMD

Cultured RPE cells are used in *in vitro* –studies with most of them being mouse, rat, pig and human primary and secondary cell cultures and cell lines [Pfeffer and Philp 2014]. One of the first RPE cell lines, which was clonable and did not lose its pigmentation, was derived from chicken embryos [Cahn and Cahn 1966]. In the 1970s and 1980s, RPE from human donor samples as well as cultured human RPE became available for us in experimental studies [Mannagh et al. 1973, Del Monte and Maumenee 1980]. Another

model originated from fetal human RPE [Aronson 1983]. Later, RPE cell lines from other animals have also been introduced (eg. pig) [Akeo et al. 1988]. Nowdays *in vitro* –experiments are mostly performed in ARPE-19 cells. ARPE-19 is a human RPE-cell line obtained from a 19-year old male donor. The cell line is spontaneously immortal, forms polarized monolayers in culture and displays similar physiological properties as found in RPE cells *in vivo* [Dunn et al. 1996]. Thus, ARPE-19 cells share a similar efflux protein profile with primary RPE cells [Mannermaa et al. 2009]. Recently, the use of human stem cell-derived RPE cells have been introduced into *in vitro* –studies. These cells share a similar efflux protein profile to ARPE-19, for example, this makes them suitable for drug research [Juuti-Uusitalo et al. 2012, Sorkio et al. 2014]

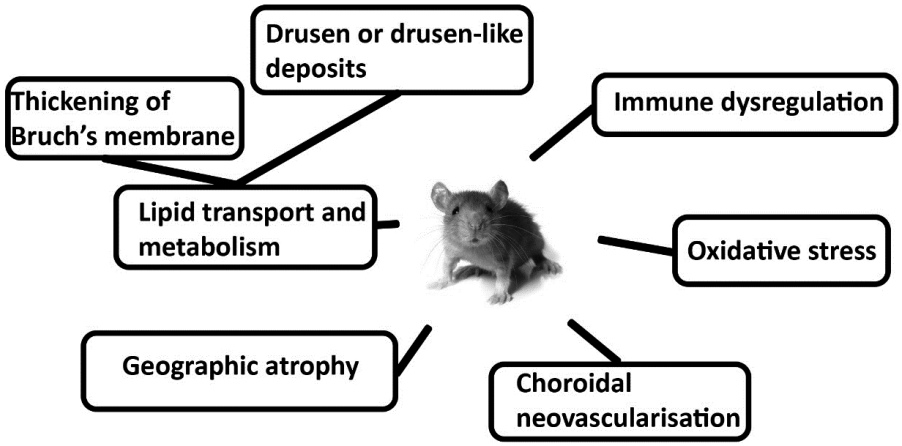

Figure 6. Currently used mouse models in AMD. Animal image from www.shutterstock.com.

There are also animal models of AMD that mimick some of the pathological features observed in AMD (Figure 6), but none of them capture all of the features of the disease [Pennesi et al. 2012]. As inflammation and the complement system play a major role in AMD, several mouse lines have been developed with genetic alterations in their complement factor pathway. These include mice lacking complement factor H or overexpressing C3, which both show degenerative changes, alterations in the outer segment (e.g. loss of the segment) and problems with visual functions [Coffey et al. 2007, Cashman et al. 2011]. Other models include chemokine receptor knock-outs [Ambati et al. 2003] and oxidative damage models [Imamura et al. 2006]. Both models exhibit AMD-like changes, the first with a deficiency in chemoattractant protein or its receptor ultimately leading to impaired macrophage recruitment and the latter with a deficiency in copper-zinc-superoxide dismutase leading to excess oxidative stress.

Mice fed with high-fat diets as well as high glycemic diets show age-related lesions earlier than low-intake controls [Cousins et al. 2002, Weikel et al. 2012]. For example, ApoE4 transgenic mice provided with a high-fat diet displayed drusen like deposits

[Ramkumar et al. 2010]. In addition to rodents, non-human primates have also been used to model AMD, notably older rhesus macaque monkeys [Bellhorn et al. 1981]. For example, more than half of aged rhesus monkeys have drusen [Gouras et al. 2008]. It has been shown that rhesus monkeys and humans share similar genetic polymorphisms (HTRA1 (*high-temperature requirement factor A1*) and ARMS2 (*age-related maculopathy susceptibility 2*)) indicating that they carry similar genetic risk factors [Fletcher et al. 2014].

2.2 PROTEOSTASIS IN THE DEVELOPMENT OF AMD

AMD pathophysiology consists of oxidative stress, protein aggregation and inflammation. Overall, every cell is constantly degrading and resynthesizing proteins in order to maintain homeostasis. The process of controlling protein has been termed proteostasis [Dokladny et al. 2015].

2.2.1 Heat-shock proteins in protein folding

If a protein is damaged (eg. inappropriate aggregation) or misfolded, the cell's primary response is to repair the protein through refolding. This is mediated by heat shock proteins (*Hsps*) [Hartl et al. 2011]. The Hsps are subdivided into several families according to their molecular size, function and structure [Kaarniranta et al. 2009b]. Hsp70 is the most highly conserved and ubiquitously expressed of this family [Dokladny et al. 2015]. It is involved in the folding of newly synthesized proteins as well as in post-translational folding, in translocation across membranes, and in the above-mentioned refolding process [De Los Rios et al. 2006, Piri et al. 2016]. Interestingly, if the Hsp system is inhibited in RPE cells, the aggregates formed are cleared nevertheless [Ryhänen et al. 2009]. This confirms the presence of parallel clearance systems. In addition, the heat shock and lysosome-dependent protein degradation interact with each other. For example, endoplasmic reticulum stress leads to an increase in autophagy related apoptosis [Qin et al. 2010]. Morever, the overexpression of Hsp70 inhibits autophagy [Dokladny et al. 2013]. Autophagy only exists in eukaryotic cells, whereas the Hsp chaperone system is featured in both prokaryotes and eukaryotes [Dokladny et al. 2015].

Hsp levels are evelated in response to cell stress, such as exposure to excess heat, cold, possible toxins, mechanical damage and oxidation. Increased levels of Hsps have also been detected in AMD, evidence of the involvement of cellular stress [Kaarniranta et al. 2009b]. Because lipofuscin accumulation has adverse effects in lysosomal function, the Hsp system, especially Hsp70, is an important protective factor in RPE homeostasis [Holz et al. 1999, Bergmann et al. 2004, Kaarniranta et al. 2005, Kaarniranta et al. 2009b, Ryhänen et al. 2009].

2.2.2 Proteasomes and RPE

Normal structure and function of proteins are essential for RPE health. Damaged proteins are degraded by the lysosomal pathway, such as autophagy, if the initial repair attempt fails. If a protein has not been successfully repaired by molecular chaperones, it is tagged with a small polypeptide called ubiquitin and forwarded to the Ubiquitin-Proteasome degradation pathway (*UPP*) [Ding and Yin 2008, Kaarniranta et al. 2009b]. Usually more than one ubiquitin is conjugated and a polyubiquitin chain is formed enabling efficient targeting to the proteasome [Howes et al. 2004]. The eukaryotic proteasome is a multicatalytic proteolytic complex present in cytosol, nucleus and microsomes, and it accounts for 1% of all cytosolic proteins [Tanaka et al. 1986]. The proteasome recognizes and selectively degrades oxidatively damaged and ubiquitinated proteins. It is also involved in part of cell-cycle regulation and synaptic plasticity as well as in signal transduction, especially in the activation and inhibition of nuclear factor kappaB [Ferrington and Gregerson 2011].

The UPP is a vital cellular system in removing damaged proteins caused by oxidative stress [Pickart 2001, Goettsch and Bayer 2002]. UPP and lysosomal proteolysis (*LPP*) usually work independently from each other and have different substrate spesificities [Shang and Taylor 2012]. In general, short lived regulatory proteins and soluble abnormal, denatured or otherwise damaged proteins are targeted to UPP whereas proteins associated with membranes or organelles are targeted to LPP [Ravid and Hochstrasser 2008, Korolchuk et al. 2009a, Korolchuk et al. 2009b, Ciechanover 2012].

As recently demonstrated by our group [Ryhänen et al. 2009], proteasome inhibition in RPE cells causes accumulation of ubiquitinated proteins, which are cleared by autophagocytosis. This implies that the dysfunction of protein degradation has a role in the pathogenesis of AMD [Ferrington et al. 2015].

2.2.3 Autophagic clearance in RPE

Protein aggregation has a role in AMD pathophysiology. The RPE is constantly combatting this process by activating its chaperones as well as its disposal systems i.e. UPP and LPP.

Autophagocytosis, literally meaning “self-eating”, is a basic cellular lysosomal clearance system. This process was first discovered in the 1960s [Arstila and Trump 1969] but its role in cellular pathology was not understood until recently. Autophagy has a key role in maintaining cellular homeostasis [Frost et al. 2014]. Since it clears aged and aggregated proteins, lipid-droplets and organelles from the cytoplasm of all eukaryotic cells [Kaarniranta et al. 2012]. Three different autophagic routes have been discovered: 1) macroautophagy (hereafter called autophagy), 2) microautophagy and 3) chaperone-mediated autophagy [Mizushima et al. 2008]. Microautophagy, in which small particles are transported directlyto the lysosome, is not common in mammalian cells but does occus in plants and fungi [Ahlberg et al. 1982, van Doorn and Papini 2013]. The autophagic

process begins with the formation of phagophores (Figure 7). These phagophores then encircle a portion of cytosol and form a distinctive double-membrane autophagosome. Lastly, the autophagosomes fuse with lysosomes and the contained waste is degraded by lysosomal enzymes [Kaarniranta et al. 2012]. This process is regulated by over 30 autophagy-related proteins [Blasiak et al. 2014]. There are two important regulators i.e. AMP-activated protein kinase (*AMPK*) and mammalian target of rapamycin (*mTOR*), the first being a master promoter and the latter an inhibitor [Kim et al. 2011]. AMPK can be activated by the use of 5-aminoimidazole-4-carboxamide ribonucleotide (*AICAR*). Interestingly, a recent study revealed that a commercial supplement containing resveratrol was capable of inducing autophagy in ARPE19 –cells [Koskela et al. 2016]. This happens by a direct inhibition of mTOR [Park et al. 2015].

Recently, in AMD donor samples, upregulation of autophagic markers (Atg12-Atg5 and LC3B) was observed along with a decrease in lysosomal activity and mitochondrial damage [Wang et al. 2009c]. Furthermore, if lysosomal activity is repressed, autophagic clearance does not function properly in RPE cells [Ryhänen et al. 2009]. Increased lipofuscinogenesis is attributable to the reduced autophagy activity in RPE cells [Krohne et al. 2010c]. Higher levels of lysosomal activity have been observed in the macular area; this would explain why dysfunction of autophagy would exert the mos damage in the macula and has been proposed as a reason why AMD affects mostly the macular area of the retina [Boulton et al. 1994, Strauss 2005]. Lipofuscinogenesis, the decrease in lysosomal activity, mitochondrial damage and the vulnerability to oxidative stress all have an association with autophagy [Mitter et al. 2012] by affecting the autophagic flux (i.e. the whole process of autophagy including up- and downregulation [Zhang et al. 2013]). As the decrease in autophagic flux can exert and effect on RPE homeostasis, dysfunction of autophagy has been postulated to play a major role in the development of AMD, and for this reason, autophagy can be a potential therapeutic target in the battle against AMD [Kaarniranta et al. 2013].

2.2.3.1 Ubiquitin in the regulation of proteostasis

Ubiquitin, a small protein of 8.5 kDa, was first documented in 1975 [Goldstein et al. 1975]. In the 1980s, it was discovered to be a regulator of protein degradation [Hershko et al. 1980]. The attachment of ubiquitin, or *ubiquitination*, may activate or inhibit enzymes and other cellular processes. It has been shown to take a part in the regulation of endocytosis, cell cycle, signal transduction, gene regulation and DNA repair [Welchman et al. 2005, Kirkin and Dikic 2007, Jung et al. 2009].

Protein degradation begins by ubiquitination of the harmful substrate which is then forwarded either to UPP or targeted for degradation by lysosomal proteolytic pathway, such as autophagy. SQSTM1/p62 (discussed later) works as a shuttling factor in this process. LC3 (*Microtubule-associated protein 1A/1B-light chain 3*), is 17 kDa protein mediating the interaction between cytoskeletal components and microtubules [Tanida et al. 2008]. In

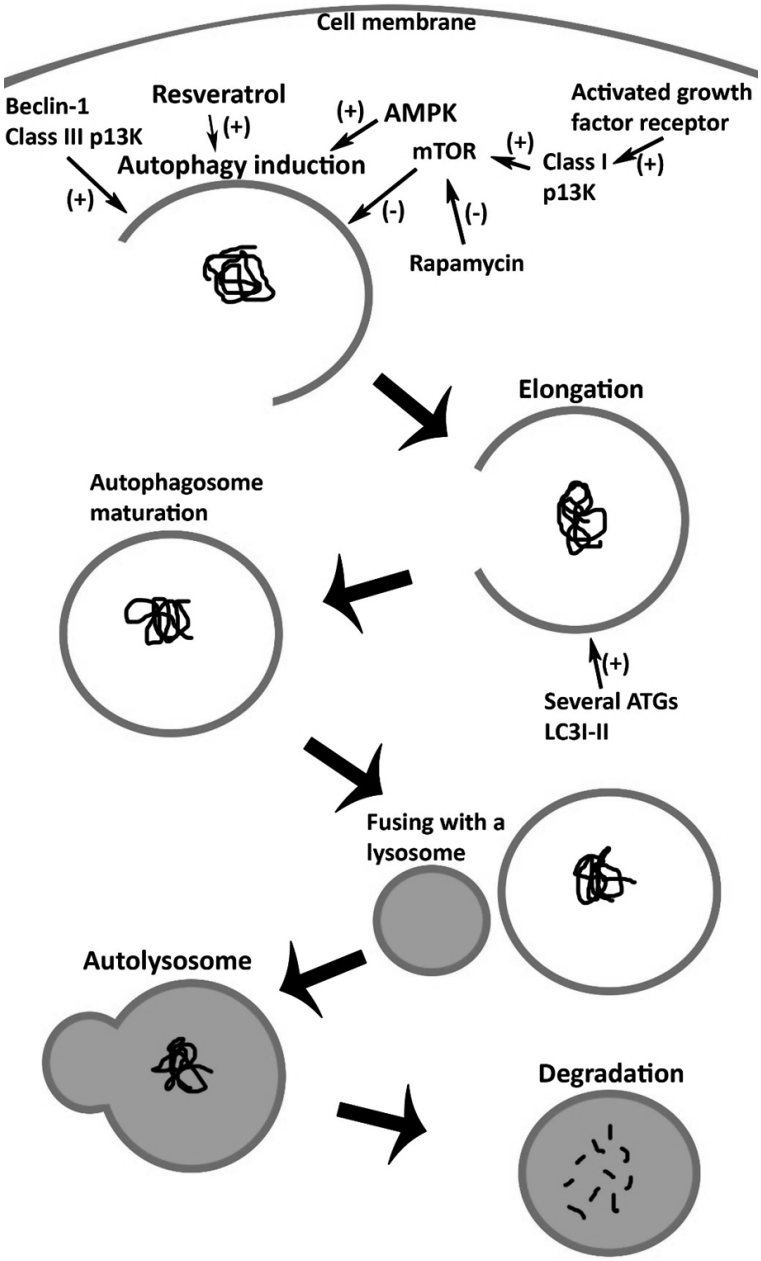

Figure 7. Autophagocytosis. The process of autophagy begins when it is induced by a phagophore. Induction has several promotors (+) and inhibitors (-), e.g. the downregulation of mTOR (a cellular regulator for growth) induces autophagy. Next, the phagophore elongates and finally matures. Then, the formed mature autophagosome fuses with a lysosome which permits to the degradation of engulfed waste.

the absence of LC3, the ubiquitin labeled proteins are targeted to UPP and in the presence of LC3, they are subjected to autophagocytic degradation (Figure 8) [Ichimura et al. 2008]. Inhibition of the UPP increases p62-mediated autophagy [Viiri et al. 2010]. Similarly, to the situation with p62, ubiquitin tends to accumulate and form aggregates if there is a dysfunction of autophagy [Knaevelsrud and Simonsen 2010, Rogov et al. 2014].

2.2.3.2 HuR regulates Hsp70 response

The ELAV1/HuR protein is a post-transcriptional gene expression regulator in eukaryotic cells [Zucal et al. 2015]. The ELAV family of proteins have a distinctive role in various pathological processes including cancers and in inflammatory diseases. This is mainly due to their above-mentioned regulatory role in gene expression. For instance, HuR directly binds to Hsp70 mRNA, and the serine/threonine residues on HuR are then phosphorylated leading to post-transcriptional regulation of Hsp70. [Amadio et al. 2008]. HuR promotes inflammation by interacting with the encoding of pro-inflammatory proteins and its levels haven found to be elevated in various cancers, such as colon, brain and breast cancers. It has been proposed as a marker for these cancers, but clinical applications are absent at the moment [Srikantan and Gorospe 2012]. Notably, ELAV proteins derangements seem to have a role in neurodegenerative diseases, such as AD. HuR levels in the AD hippocampi are decreased whereas beta-amyloid levels are increased [Amadio et al. 2009]. The dysfunction of the aformentioned HuR-Hsp interaction might be a contributor to these stressful conditions [Amadio et al. 2008].

2.2.3.3 SQTM1/p62 as a shuttling protein between proteasomes and autophagy

SQSTM1/p62 (here after abbreviated to p62) is a stress-induced protein with a size of 61 kDa. It has a role in amino acid sensing as well as in the oxidative stress response as a signaling hub; it also functions as an autophagy receptor for ubiquinated cargos [Katsuragi et al. 2015]. It was first characterized in polyubiquitinated aggregates in cells which had been subjected to proteasomal depletion [Kuusisto et al. 2001b] and later found to be expressed in numerous neurodegenerative diseases, most notably AD [Salminen et al. 2012]. p62 activates protein Nrf2 (*nuclear factor E2-related factor 2*), which controls the expression levels of several antioxidant proteins and thus protects against oxidative damage [Komatsu et al. 2010]. When damaged or otherwise misfolded proteins have been polyubiquitinated, p62 shuttles them to the autophagosomes. LC3 presents the autophagosome membrane and after induced binding the aggregates are degraded (Figure 8) [Pankiv et al. 2010]. As p62 is itself degraded by autophagy, any dysfunction of autophagy might lead to p62 accumulation and subsequently to the formation of aggregates [Komatsu and Ichimura 2010]. Hence, p62 can be used as an autophagy marker, since the transcription of p62 is upregulated during impaired autophagy [Klionsky et al. 2016]. Inhibition of p62 transcription blocks proteasomal sequestration of

ubiquitinated proteins and blocks the enlargement of inclusions. Therefore, p62 plays a vital role in the defense of cells from the toxicity of misfolded proteins by augmenting aggregate formation [Nakaso et al. 2004, Paine et al. 2005].

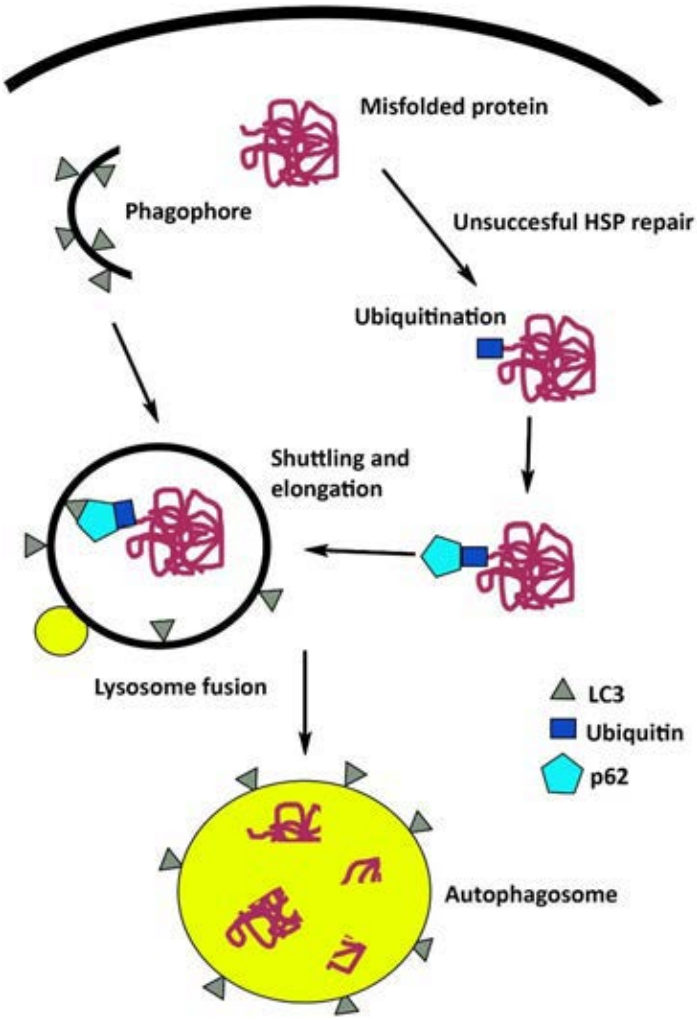

Figure 8. The interactions of ubiquitin, LC3 and p62 in autophagocytosis.

2.2.3.4 Beclin-1 as an inductor of autophagy

Beclin-1 is a 52 kDa protein that is essential for iniation of autophagocytic process [Salminen et al. 2013, Mei et al 2014] by Beclin-1 promoted vesicle nucleation [Suzuki et al 2001]. It was first discovered as a protein, which interacts with Bcl-2, a cellular antiapoptotic gene [Liang et al. 1998]. Beclin-1 is crucial for neuronal survival and it is widely expressed in the nervous system [O'Brien et al. 2015]. A Beclin-1 deficiency has worsened amyloid B induced pathology in a mouse model of AD by decreasing

autophagy, resulting in increased accumulation of amyloid B. In this model, representing heterozygous deletion of Beclin-1, the administration of a viral vector capable of triggering Beclin-1 overexpression, was able to reduce the amyloid B accumulation [Pickford et al. 2008]. There are indications that the amyloid B may be generated in autophagic vacuoles [Yu et al 2004]. It has been reported that the expression of Beclin-1 is reduced in patients with Alzheimer's disease [Pickford et al. 2008] and its dysfunction has a role in the pathogenesis of AD by affecting neuronal autophagy [Salminen et al. 2013]. In addition, pre-exposure of RPE cells to AE2, a component of lipofuscin, triggered the induction of autophagosomes and increased Beclin-1 expression [Zhang et al. 2015]. Since AD and AMD share similar pathophysiological backgrounds, it is possible that a dysfunction of Beclin has a role in the pathogenesis of AMD.

2.3 COLLAGEN XVIII AND ENDOSTATIN

As stated, AMD and AD share many pathophysiological features. The expression of collagen XVIII has been demonstrated in the plaques of AD patients [van Horssen et al. 2002]. Collagen XVIII belongs to a group of proteins, which make up a major proportion of the components of basement membranes [Ortega and Werb 2002]. Interestingly, collagen XVIII also has a role in the development of the brain and eyes by ensuring the correct function of basement membranes (*BMs*) [Fukai et al. 2002, Lakshmanachetty and Koster 2016]. Collagen XVIII is expressed in BMs throughout the body [Muragaki et al. 1995] and thus it is present nearly in every part of the human eye (Bowman's membrane, the lens capsule, the trabecular network and in all the endothelial and epithelial basal membranes in both anterior and posterior segments of the eye) [Ohlman et al. 2005].

Mutations (mostly nonsense mutations) in the *Col18a1* gene lead to Knobloch syndrome. This is an autosomal recessively inherited disease [Sertié et al. 2000]. The disease was first discovered in 1971 [Knobloch and Layer] and it is characterized by ocular manifestations and in some of the cases also occipital skull abnormalities are present. Ocular manifestations include severe myopia (when spherical equivalent refraction is less than -6,00 D [Koh et al. 2016]); subluxation of the lens; vitreoretinal degeneration which tends to lead to retinal detachment; and cataracts with an early onset [Khan et al. 2012]. The reported skull abnormalities include encephalocele, bone defects or cutis aplasia [Sniderman et al. 2000]. Since the first report, at least 85 cases have been identidied [Caglayan et al. 2014]. Interestingly, mice with collagen 18 depletion have been observed to display numerous ocular abnormalities and age-dependent loss of vision with accumulation of sub-RPE deposits [Fukai et al. 2002, Marneros et al. 2004]. Retinal neovascularization has also been observed [Hurskainen et al. 2005].

Another interesting feature of collagen XVIII is its C-terminal domain. This domain is called endostatin and it is produced via proteolytic cleavage [O'Reilly et al. 1997]. It has both anti-angiogenic and anti-proliferative effects [Behl and Kotwami 2015] and can

inhibit at least 65 different types of tumors [Folkman 2006]. Endostatin inhibits the migration and proliferation of new endothelial cells, which at least to some extent, explains its anti-angiogenic effects [Yamaguchi et al. 1999]. An interesting finding is that endostatin can also induce autophagy by increasing Beclin-1 levels [Nguyen et al. 2009]. It has been shown to be localized in the structures surrounding the vitreous and anterior chamber, which are normally avascular structures allowing light to pass undisturbed into the neural retina. The distribution of endostatin might indicate a possible role for these structures to guard against vascularization [Ohlman et al. 2005]. Endostatin is currently in phase II clinical trials as an angiogenesis inhibitor and it has been proposed to be used also in the treatment of diabetic retinopathy [Behl and Kotwani 2015].

3 Aims of Study

The general aim of the study was to evaluate the role of protein aggregation, especially dysfunction of autophagy in the pathogenesis of age-related macular degeneration.

The specific aims are:

I To evaluate the presence of protein degradation markers ubiquitin, LC3 and SQSTM1/p62 in ARPE19-cells and in the RPE of human cadaver AMD samples. (Publication I)

II To examine the connection between the proteostasis regulator Hsp70 and the autophagic clearance system. (Publication II)

III To determine whether the current standard of care for wet AMD (intravitreal aVEGF therapy with bevacizumab) has an effect on the autophagy clearance of RPE cells. (Publication III)

IV To study the role of autophagy in the pathogenesis of AMD-like structural changes in collagen XVIII knock-out mice. (Publication IV)

4 Autophagy Activation Clears ELAVL1/HuR-Mediated Accumulation of SQSTM1/p62 during Proteasomal Inhibition in Human Retinal Pigment Epithelial Cells

ABSTRACT

Age-related macular degeneration (AMD) is the most common reason of visual impairment in the elderly in the Western countries. The degeneration of retinal pigment epithelial cells (RPE) causes secondarily adverse effects on neural retina leading to visual loss. The aging characteristics of the RPE involve lysosomal accumulation of lipofuscin and extracellular protein aggregates called ''drusen''. Molecular mechanisms behind protein aggregations are weakly understood. There is intriguing evidence suggesting that protein SQSTM1/p62, together with autophagy, has a role in the pathology of different degenerative diseases. It appears that SQSTM1/p62 is a connecting link between autophagy and proteasome mediated proteolysis, and expressed strongly under the exposure to various oxidative stimuli and proteasomal inhibition. ELAVL1/HuR protein is a post-transcriptional factor, which acts mainly as a positive regulator of gene expression by binding to specific mRNAs whose corresponding proteins are fundamental for key cellular functions. We here show that, under proteasomal inhibitor MG-132, ELAVL1/HuR is up-regulated at both mRNA and protein levels, and that this protein binds and post-transcriptionally regulates SQSTM1/p62 mRNA in ARPE-19 cell line. Furthermore, we observed that proteasomal inhibition caused accumulation of SQSTM1/p62 bound irreversibly to perinuclear protein aggregates. The addition of the AMPK activator AICAR was pro-survival and promoted cleansing by autophagy of the former complex, but not of the ELAVL1/HuR accumulation, indeed suggesting that SQSTM1/p62 is decreased through autophagy-mediated degradation, while ELAVL1/HuR through the proteasomal pathway. Interestingly, when compared to human controls, AMD donor samples show strong SQSTM1/p62 rather than ELAVL1/HuR accumulation in the drusen rich macular area suggesting impaired autophagy in the pathology of AMD.

4.1 INTRODUCTION

Age-related macular degeneration (AMD) is the most common eye disease leading to visual impairment in the elderly in the developed countries [Pascolini et al. 2004]. The disease affects the central retina called the macula, the area that is responsible for the most important sharp and colour vision [Kaarniranta et al. 2011]. AMD is associated with aging, hereditary background, smoking, hypertension, hypercholesterolemia, arteriosclerosis, obesity and unhealthy diet. In global terms, 50 million people are affected by AMD with one third of them suffering severe visual loss [Geh et al. 2006, Gordois et al. 2012]. It is estimated that the number of AMD patients will triple during the next decades due to increased numbers of aged people [Friedman et al. 2004].

Primarily AMD is characterized by degeneration of the macular retinal pigment epithelial (RPE) cells that secondarily leads to cell death of photoreceptors (rods and cones) and visual loss [Kaarniranta et al. 2009]. AMD has a progressive character and may develop into either a dry (non-exudative) or wet (exudative) form [de Jong 2006, Jager et al. 2008]. Neovascularization, sprouting from the choriocapillaris into the retina, is one of the clinical hallmarks of wet AMD. The dry form of the disease is more prevalent and it accounts for as many as 90% of all cases. At present, no effective cure is available for dry AMD, although anti-oxidants and omega-fatty acids have been shown to have preventive properties in certain AMD patient groups [Kaarniranta and Salminen 2009, Sin et al. 2012]. In wet AMD, monthly applications of intravitreal injections of anti-VEGF antibodies havebeen used to suppress the activity of neovascularization [Martin et al. 2011].

AMD pathogenesis involves chronic oxidative stress, increased accumulation of lipofuscin in the lysosomes of RPE cells, as well as extracellular drusen formation and presence of chronic inflammation [Finneman et al. 2002, Terman et al. 2010, Kaarniranta et al. 2011]. The ability to prevent the accumulation of cytotoxic protein aggregates via autophagy may be decreased in aged post mitotic RPE cells leading to degenerative changes.

Autophagy is basic catabolic mechanism which ''self eats'' cellular components that are unnecessary or dysfunctional to the cell [Yang and Klionsky 2010a]. Autophagy comprises three intracellular pathways in eukaryotic cells, which are macroautophagy (hereafter referred to as autophagy), microautophagy and chaperone-mediated autophagy [Mizushima and Komatsu 2011]. Apart from its important role in cellular homeostasis, autophagy is also triggered as an adaptive response during AMD-associated stress conditions [Salminen and Kaarniranta 2009, Kaarniranta et al. 2009, Yang and Klionsky 2010b, Kaarniranta et al. 2011, Mizushima and Komatsu 2011]. Autophagy process begins with the formation of isolation membranes called phagophores; these latter then become elongated and surround portions of cytoplasm containing oligomeric protein complexes and organelles to form mature double membrane autophagosomes. The autophagosomes fuse with the lysosomes and their content is then degraded by lysosomal enzymes. Failure of autophagy in aged postmitotic cells, including RPE cells, can result in accumulation of aggregate-prone proteins, cellular degeneration and finally cell death [Kaarniranta et al. 2009].

SQSTM1/p62 (Sequestosome 1) is the best-characterized and ubiquitously expressed autophagy receptor that connects proteasomal clearance with lysosomes [Bjørkøy et al. 2005, Komatsu et al. 2007 Korolchuk et al. 2009b, Pankiv et al. 2010, Viiri et al. 2010]. Alleviation of autophagy is usually accompanied by an accumulation of SQSTM1/p62 mostly in large perinuclear aggregates or inclusion bodies which are also positive for ubiquitin, as reported in numerous neurodegenerative diseases (such as Alzheimer's disease, Parkinson's disease, and Huntington disease) [Kuusisto et al. 2001a, Kuusisto et al. 2002, Zatloukal et al. 2002, Braak et al. 2011, Salminen et al. 2012, Geetha et al. 2012].

The evidence indicates that SQSTM1/p62 is a stress response gene strongly induced at mRNA and protein levels by the exposure to various oxidative stimuli and proteasomal inhibitors [Ishii et al. 1997, Kuusisto et al. 2001b, Nagaoka et al. 2004, Jain et al. 2010].

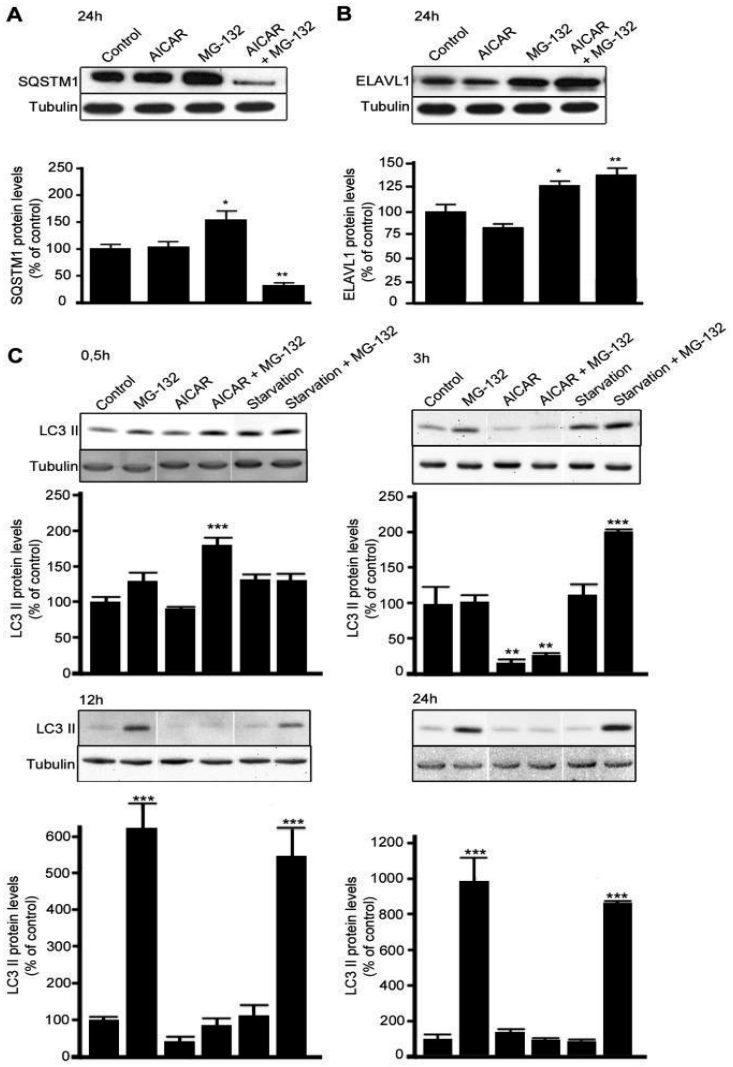

Figure 9. MG-132-induced increase of SQSTM1/p62 but not ELAVL1/HuR protein levels is counteracted by AICAR treatment. Representative western blotting (upper) and densitometric analysis (lower) of SQSTM1/p62 (A), ELAVL1/HuR (B) and MAP1LC3A/LC3-II (C) proteins in the total homogenates of ARPE-19 cells after starvation or/and exposure to AICAR (2 mM) or/and MG-132 (5 μM) for 0,5 h, 3 h, 12 h and 24 h. α-tubulin was used as a loading control. Control cells were exposed only to solvent (DMSO). Results are expressed as means ± S.E.M. The data were analyzed by ANOVA, followed by Dunnett's Multiple Comparison Test; *p<0.05, **p<0.01, control vs. treated, n=7 (SQSTM1/p62 and ELAVL1/HuR), n=3 (MAP1LC3A/LC3-II).

One of the most important post-transcriptional mechanisms involves ELAVL1/HuR (embryonic lethal, abnormal vision, Drosophila)-like 1 (Hu antigen R) protein, acting mainly as a positive regulator of gene expression by binding to and increasing the stability and/or translation of specific mRNAs whosecorrespondingproteins are fundamental for key cellular functions. It is noteworthy that ELAVL1/HuR, and in general ELAV family,

participates in various physio-pathological processes where oxidation and stress play a primary role [Amadio et al. 2009, Srikantan and Gorospe 2012, Pascale and Govoni 2012]. One of the main aims of our study was to investigate whether SQSTM1/p62

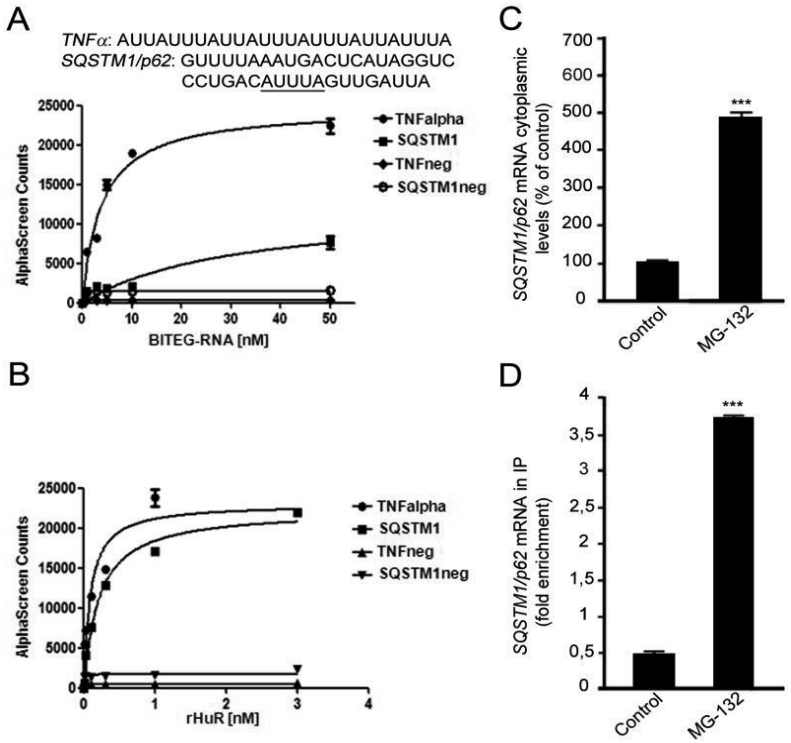

Figure 10. SQSTM1/p62 transcript as a new target of the RNA-binding ELAVL1/HuR protein. (A): RNA-binding activity of ELAVL1/HuR evaluated by AlphaScreen technology. Saturation binding experiments investigated by titrating a series of biotinylated single-stranded (BITEG-) RNAs, including *TNF*neg and *SQSTM1/p62*neg, that we designated as negative controls, against 1 nM of rELAVL1/HuR. Calculated dissociation constants (K_d) for *TNFalpha* (3.83±0.69 nM, R^2=0.97), and *SQSTM1/p62* (30.85±13.22 nM R^2 =0.91) are indicated. The plots represent mean ± SD of two independent experiments. (B): Saturation binding experiments as function of rELAVL1/HuR concentrations against four different type of RNA-substrates at 50 nM concentration. 1 nM of rELAVL1/HuR was enough to reach saturation of the binding. The plots represent Mean ± SD of two independent experiments. (C): Effect of MG-132 exposure on *SQSTM1/p62* gene expression. Determination of *SQSTM1/p62* mRNA by real-time qPCR in human ARPE-19 cells following treatments with solvent (control) or 5 μM MG-132 for 24 hrs. *SQSTM1/p62* mRNA expression in control cells was taken as 100%. The values obtained from total cellular mRNA have been normalized to the level of RPL6 mRNA and expressed as mean ± S.E.M. ***p<0.001; Student's t test; n=3. (D): The binding of ELAVL1/HuR protein to *SQSTM1/p62* transcript increases in the cytoplasm following MG-132 stimulus. Fold enrichment detected by quantitative real-time RT-PCR of *SQSTM1/p62* mRNA in control and 24 h MG-132 RPE cells following immunoprecipitation with anti-ELAV antibody (IP) in the cytoplasm. ***p<0.001, Student's t-test, n=3. The data of SQSTM1/p62 were normalized with respect to the data obtained from immunoprecipitation with an irrelevant antibody as a negative control.

mRNA would be a target of ELAVL1/HuR protein, and whether the binding between ELAVL1/HuR protein and SQSTM1/p62 transcript exists in human RPE

cells. We also investigated how proteasomal and autophagy modulation affects SQSTM1/p62 and ELAVL1/HuR expression. Moreover, their presence in drusen rich human cadaver AMD samples was studied.

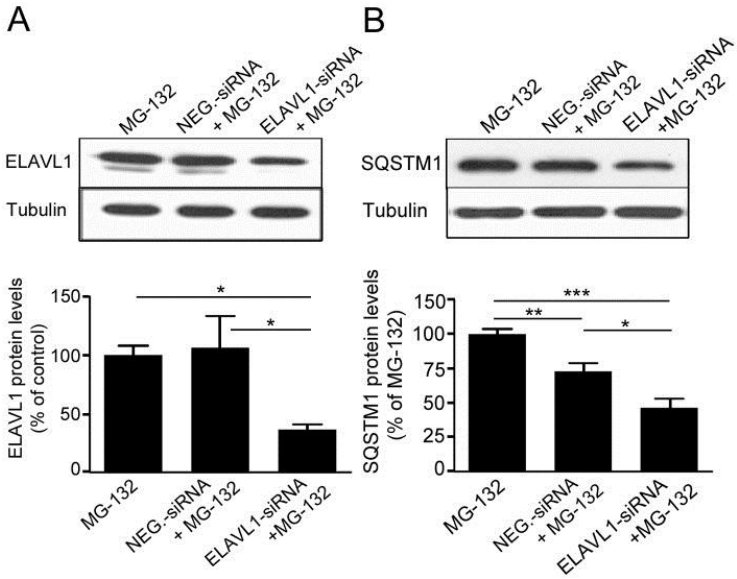

Figure 11. The MG-132-mediated upregulation of SQSTM1/p62 protein expression requires the specific presence of ELAVL1/HuR protein. Representative western blotting (upper) and densitometric analysis (lower) of ELAVL1/HuR (A) and SQSTM1/p62 (B) proteins in the total homogenates of ELAVL1/HuR silenced ARPE-19 cells and negative control (NEG-siRNA) cells after exposure to 5 μM MG-132 for 24 h. α-tubulin was used as a loading control. Results are expressed as means ± S.E.M. *p<0.05; **p<0.01; ***p<0.001, Tukey's multiple comparison test; n=5.

4.2 MATERIALS AND METHODS

4.2.1 Ethics Statement

The study was approved by the Ethics Committee of the Freiburg University Hospital, the University of Debrecen and the tenets of the Declaration of Helsinki were followed for human material. Participants provided their written informed consent for the human material in this study.

4.2.2 Cell Culture and Treatments

ARPE-19 human RPE cells were obtained from the American Type Culture Collection (ATCC). The cells were grown to confluence in a humidified 10% CO2 atmosphere at 37^{O}C in Dulbecco's MEM/Nut MIX F-12 (1:1) medium (Life Technologies, 21331) containing 10% inactivated fetal bovine serum (Hyclone, SV30160-03), 100 units/ml penicillin and 100 μg/ml streptomycin (Lonza, DE17-602E) and 2 mM L-glutamine (Lonza, BE17-605E). In proteasome experiments, the cells were exposed to 5 μM MG-132 proteasome inhibitor

(Calbiochem, 474790) for 0,5 hours, 3 hours, 12 hours and 24 hours (h). The cells were exposed to 50 nM bafilomycin A1 (Sigma, B1793) for 24 h. Additionally, the cells were treated with the AMPK (AMP-activated protein kinase) activator, AICAR 2 mM (5-aminoimidazole-4-carboxyamide ribonucleoside, Toronto Research Chemical, A611700) for 0,5 h, 3 h, 12 h and 24 h. Furthermore, the autophagy was induced with starvation by culturing cells in fetal bovine serum free medium for 0.5 h, 3 h, 12 h and 24 h.

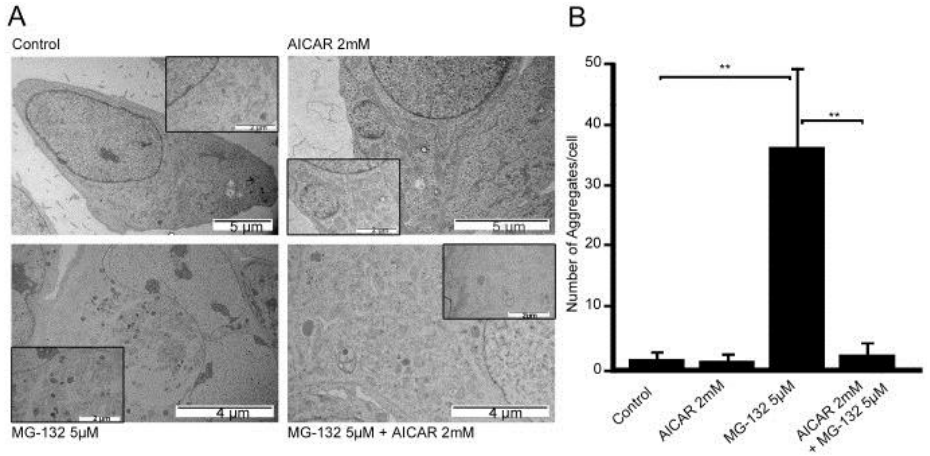

Figure 12. Transmission electron micrographs of ARPE-19 cells exposed to AICAR or/and MG-132 and aggregate quantification. (A) Representative transmission electron micrographs of ARPE-19 untreated control cells, cells exposed to AICAR 2 mM or/and MG-132 5 µM for 24 h. Aggregates are indicated by arrows. (B) Quantification of aggregates in ARPE-19 cells exposed to AICAR 2 mM or/and MG-132 5 µM for 24 h. Eight parallel samples were measured in all treatments. **p<0.01, Mann–Whitney.

4.2.3 Cellular Fractionation and Western Blotting

The nuclear extract kit (40010) from Active motif was used for the preparation of nuclear and cytoplasmic extracts from exposed ARPE-19 cells. Proteins were collected according to the manufacturer's protocol. The whole cell extracts were prepared in M-PER® (Mammalian Protein Extraction Reagent, Thermo Scientific, 78501) according to the manufacturer's protocol.

Proteins were diluted in 2X sodium dodecyl sulphate (SDS) protein gel loading solution, boiled for 5 minutes, separated on 12% SDS-polyacrylamide gel electrophoresis (SDS-PAGE) and processed following standard procedures. The mouse monoclonal antibodies were diluted as follows: the anti-ELAVL1/HuR (anti-ELAVL/Hu) antibody (Santa Cruz Biotech, sc-5261) at 1:1000; the anti-SQSTM1/p62 (anti-p62) antibody (Santa Cruz Biotech, sc-28359) at 1:1000; the anti-MAP1LC3A/LC3 (anti-LC3, microtubule-associated protein light chain 3A) antibody (Cell Signaling, 3868) at 1:1000 and the anti-α-tubulin (Sigma, T9026) at 1:1000. The nitrocellulose membranes signals were detected by chemiluminescence. Experiments were performed in duplicate for each different cell preparation and α-tubulin was used to normalize the data. Statistical analysis of western blot data was performed on the densitometric values obtained with the NIH image

software 1.61 (downloadable at http://rsb.info.nih.gov/nih-image) and Quantity One® software.

4.2.4 Fusion Plasmid Constructs

Human MAP1LC3A (LC3, light chain 3, NCBI gene bank no. AF303888) was amplified from DNase-treated (DNase I, Roche, 04716728001) total RNA extracted (Eurozol reagent, Euroclone, EMR055100) from human ARPE-19 cells. Initially, mRNA was reverse-transcribed (MultiScribe reverse transcriptase, Applied Biosystems, 4311235), and the MAP1LC3A/LC3 open reading frame (ORF) was amplified with a high-fidelity DNA polymerase (Phusion Hot start DNA polymerase, Finnzymes, F-530S). The following primers were used: sense 5′-ATA *CTCGAG* at **ATG** CCG TCG GAG AAG A and reverse 5′-TGT *AAG CTT* g **TTA** CAC TGA CAA TTT CAT CCC. The restriction sites for XhoI and HindIII are in italics. The translation initiation and termination sites are in boldface. The additional bases enabling in-frame cloning are in minuscules. The sticky ends for the amplified MAP1LC3A/LC3 ORFs as well as for the multiple cloning site of the vector pDendra2-C (Evrogen, FP821) were produced with restriction endonucleases XhoI and Hind III (MBI Fermentas, ER0691 and ER0501. respectively) [Gurskaya et al. 2006]. Ligated (T4 DNA Ligase, Roche, 10481220001) DNA, forming a fusion gene of Dendra2 and human MAP1LC3A/LC3 was transfected into competent DH5*α* E. coli cells, which were prepared using the protocol of Inoue and others and then cultured and purified [Inoue et al. 1990, Sambrook et al. 1990]. The integrity of the construct, named hereafter as pDendra2-hLC3 (MAP1LC3A/LC3), was determined initially by restriction endonuclease digestion analysis and finally sequencing of both the junction sites and the entire inserted MAP1LC3A/LC3 ORF.

Human Sequestosome 1, SQSTM1 (p62), NCBI gene bank no. NM_003900) was similarly inserted into the pDendra2 vector. The ORF insert was initially purchased from RZPD (Deutsches Ressourcenzentrum für Genomforschung, IRAUp969A0698D). The insert was amplified with the following primers: sense 5′-ATA *CTC GAG* at **ATG** GCG TCG CTC ACC; reverse 5′-TAT *AAG CTT* a **TCA** CAA CGG CGG GGG ATG. The restriction sites for XhoI and HindIII are shown in italics and the translation initiation and termination sites are in boldface. The additional bases enabling in-frame cloning are in minuscules. The final plasmid was named as pDendra2-hp62 (SQSTM1/p62).

4.2.5 Transfections and Confocal Imaging of pDendra2-hLC3 (MAP1LC3A/LC3) and pDendra2-hp62 (SQSTM1/p62)

ARPE-19 cells were cultured in 8-well plates (μ-Slide, ibiTreat, tissue culture treated, Ibidi, 80826) in a volume of 200 μl to a subconfluent density. In all transfection experiments, ExGen 500 in vitro Transfection Reagent (MBI Fermentas, R0511) was used and its protocol followed. The DNA content was 500 ng per single well and the transfection treatment lasted for 24 h. Chemical treatments with 5 μM MG-132 and/or 2 μM AICAR followed for 24 h in fresh medium.

Before the microscopic evaluation, the medium was always changed to a fresh medium without treatment. The nuclei were stained with DRAG5™ (Biostatus, DR50050), diluted

to 1/1000 in phosphate-buffered saline. The fluorescent images were obtained with a Zeiss Axio Observer inverted microscope (63xNA 1,4 oil objective) equipped with Zeiss LSM 700 confocal module (Carl Zeiss Microimaging). The change in the Dendra2 color from green to red was achieved by treatment of the cells with 405 nm UV-light [Inoue et al. 1990]. In the live cell imaging, a Zeiss XL-LSM S1 incubator with temperature and CO2 control was utilized. ZEN 2009 software (Carl Zeiss) was used for image processing.

4.2.6 Attenuation of the ELAVL1/HuR gene Expression by RNA Interference

A control siRNA (NEG-siRNA) having no known homology with any gene (Ambion, AM4641) and siRNA designed for the human ELAVL1/HuR gene (Ambion, s4610) were used. The ELAVL1/HuR siRNA has sense sequence GCG UUU AUC CGG UUU GAC ATT, and the binding site is at the bases 615–633 of the human ELAVL1/HuR gene (NCBI gene bank no. NM_001419) in exon 2, near to the 5′-end of the coding region. siRNAs were transfected into ARPE-19 cells using siPORT™ Amine transfection reagent (Ambion, AM4502) following the manufacturer's instructions. Cells were grown as described above. The concentration of siRNAs in cell cultures was 30 nM and duration of siRNA treatment was held for 24 h, followed by MG-132 treatment (5 μM) for 24 h. The decrease of ELAVL1/HuR expression was monitored using real time quantitative RT-PCR and western blotting.

4.2.7 Immunoprecipitation Followed by RNA Extraction

Immunoprecipitation on RPE cytoplasmic fractions was performed according to a previously published protocol with minor modifications [Tenenbaum et al. 2002]. Briefly, immunoprecipitation was performed at room temperature for 2 h using 1 μg of anti-Hu antibody per 50 μg of proteins diluted with an immunoprecipitation buffer (50 mM Tris pH 7.4, 150 mM NaCl, 1 mM MgCl2, 0.05% Igepal, 20 mM EDTA, 100 mM DTT, protease inhibitor cocktail and an RNAase inhibitor) in the presence of 50 μl of protein A/G plus agarose (Santa Cruz Biotech, sc-2003). The samples were finally subjected to RNA extraction. The negative control was obtained under the same conditions, but in the presence of an irrelevant antibody with the same isotype of the specific immunoprecipitating antibody. One hundred microliters of the immunoprecipitation mix were immediately collected from each sample and used as ''input signals'' to normalize the RT-PCR data.

4.2.8 Real-time Quantitative RT-PCR

RNA was extracted from total homogenates, immunoprecipitated pellets and relative ''input signals'' by using RNeasy MicroPlus Kit (Qiagen, 74034). The reverse transcription was performed following standard procedures. PCR amplifications were carried out using the Lightcycler instrument (Roche Molecular Biochemicals) in the presence of QuantiTect SYBR Green PCR mix (Qiagen, 204143) with primers designed by using the PRIMER3 software (www-genome.wi.mit.edu/cgi-bin/primer/primer3_www.cgi). Primer sequences were as follows: ELAVL1/HuR, 5′GAGGCTCCAGTCAAAAACCA -3′ (upstream), 5′-GTTGGCGTCTTTGATCACCT -3′ (downstream); SQSTM1/p62, 5′-

CTGGGACTGAGAAGGCTCAC -3′ (upstream), 5′- GCAGCTGATGGTTTGGAAAT -3′ (downstream); RPL6, 5′-AGATTACGGAGCAGCGCAAGATTG-3′(upstream),5′-GCAAACACAGATCGCAGGTAGCCC-3′ (downstream). The RPL6 mRNA was chosen as the reference on which the ELAVL1/HuR and SQSTM1/p62 values were normalized because it remained relatively stable during all the treatments and it does not bear adenine/uracil-rich elements (ARE) sequences (not shown).

In the statistical analysis the GraphPad Instat statistical package (version 3.05 GraphPad software, San Diego) was used. The data were subjected to analysis of variance (ANOVA) followed, when significant, by an appropriate test, in function of the number of samples. Differences were considered statistically significant when p values <0.05.

4.2.9 Preparation of the Vector Expressing HuR cMyc-His-tagged Protein

ELAVL1/HuR cDNA (NM 001419) was obtained and amplified from MCF7-cells retro-transcribed RNA and inserted into the pCMV6-AC-Myc-His PrecisionShuttle vector (PS100006; Origene Technologies) by using the forward (5′- GCC *GCGATCGC* CATGTCTAATGGTTATGA-3′) and reverse (5′- CGT *ACGCGT* TTTGTGGGACTTGTTGG-3′) primers containing the *SgfI* and the *MluI* restriction sites (in italics), respectively. The full-length open reading frame, with the Myc-His tag-encoding sequence located at the 3′-end, was confirmed by sequencing.

Recombinant vector pCMV6-HuR (ELAVL1/HuR) was transfected (3 mg per 10 cm tissue culture dish) in HEK293T cells by using Lipofectamine® 2000 transfection reagent (Life Technologies, 11668019) according to the manufacturer's protocol. Cells were harvested 48 h after transfection and sonicated (3x15 seconds, paused by 1 minute) with 75 of amplitude at 4^{O}C, in binding buffer (20 mM NaH2PO4, 0.5 M NaCl, 20 mM imidazole, pH 7.4) supplemented with Protease Inhibitor Cocktail (Sigma, P8340). Recombinant ELAVL1/HuR HuR-Myc-His proteins were purified by one-step affinity chromatography on HisTrap HP columns (GE Healthcare, 17-5247-01) following the recommended protocol and were eluted with 20 mM NaH2PO4, 0.5 M NaCl, 50 mM glycine, 300 mM imidazole, 10% glycerol, pH 7.5.

4.2.10 Amplified Luminescent Proximity Homogenous Assay

Amplified Luminescent Proximity Homogenous Assay (ALPHA) was applied to study the interaction between recombinant ELAVL1/HuR and two specific ARE-bearing RNA oligos designed from 3′UTRs of TNFalpha and SQSTM1/p62. Biotinylated single-stranded TNFalpha [40] (5′-AUUAUUUAUUAUUUAUUUA-UUAUUUA-3′), SQSTM1/p62 (5′-GUUUUAAAUGACU-CAUAGGUCCCUGACAUUUAGUUGAUU-3′), TNFneg (5′-ACCACCCACCACCCACCCACCACCCA-3′), SQSTM1/p62neg (5′-GCCCCAAACGACCCACAGGCCCCCGACACC-CAGCCGACC-3′) RNAs were purchased from Eurofins MWG Operon and recombinant ELAVL1/HuR HuR-MYC/DDK protein (TP301562) was purified from HEK293T cells transiently transfected with pCMV6-ELAVL1/HuR. The assays were performed in 384-well white OptiPlates (PerkinElmer, 6007299) using a final volume of 25 µl and optimized by titrating both interacting partners (in order to determine the optimal protein: RNA ratio). Values out of the ''hooking zone'',

where quenching of the signal was due to an excess of the binding partner, were used to determine the optimal concentrations of RNA-oligos and proteins. All reagents were tested in the nanomolar range using the Alpha Screen c-Myc detection kit (Perkin Elmer 6760611C) and reacted in a buffer containing 25 mM HEPES (pH 7.4), 100 mM NaCl, and 0.1% bovine serum albumin (BSA). Briefly, recombinant ELAVL1/HuR protein (range 0.1–300 nM tested, data not shown) was incubated with a biotinylated single-stranded RNA (range 0.1–300 nM) and with anti-c-Myc Acceptor beads (20 μg/ml final concentration) and, subsequently, the reaction was placed in the dark at room temperature for 30 min. The incubation in the same conditions was extended to 90 min after addition of streptavidin Donor beads (20 μg/ml final concentration). Specific interactions were quantified on a PerkinElmer Enspire plate reader by subtracting the signal of the background (non-specific binding). Dissociation constants (K_d) for TNFalpha (0.087±0.021), and SQSTM1/p62 (0.207±0.024) were determined from nonlinear regression fits of the data according to a 1-site binding model in GraphPad Prism®, version 5.0 (GraphPad Software, Inc.).

4.2.11 Transmission Electron Microscopy

For transmission electron microscopy, the cells were treated with 5 μM MG-132 and/or 2 mM AICAR for 3 h, 12 h and 24 h. Cell culture samples were prefixed with 2.5% glutaraldehyde in 0.1 M phosphate buffer pH 7.4 for 2 h at RT. After 15 min washing in 0.1 M phosphate buffer, the samples were post-fixed in 1% osmium tetraoxide and 0.1 M phosphate buffer for 1 hour, and again washed with phosphate buffer for 15 min prior to standard ethanol dehydration. Subsequently, the samples were infiltrated and embedded in LX-112 resin. Polymerization was carried out at 37^{O}C for 24 h and at 60^{O}C for 48 h. The sections were examined with a JEM-2100F transmission electron microscope (Jeol) at 200 kV.

Aggregates and autophagic vesicles were manually counted. Eight cells were randomly selected from each group for counting aggregates and six cells for autophagic vesicles. Statistical analysis was performed using SPSS (v. 19; IBM, SPSS Inc). The significance of differences between control and treated groups was analyzed with Mann-Whitney U-test. p-values <0.05 were considered significant.

4.2.12 Cytotoxicity Assay

Cytotoxicity to the AICAR and other treatments was monitored by measuring the amount of lactate dehydrogenase (LDH) enzyme from the culture medium samples. The Cyto-Tox 96 Non-Radioactive Cytotoxicity Assay kit (Promega, G1781) was used for detection according to the instructions of the manufacturer. Absorbance values after the colorimetric reaction were measured at a wavelength of 490 nm with a reference wavelength of 655 nm using a BIO-RAD Model 550 microplate reader. Statistical analysis was performed using SPSS program (v. 19; IBM SPSS Inc). The significance of differences between control and treated groups was analyzed with Mann-Whitney U-test ($n = 6$). p-values <0.05 were considered significant.

4.2.13 Assay for Cell Death Analysis

Cell death was assessed by the Annexin-V-fluorescein isothiocyanate. We used the Apoptosis Detection Kit (MBL, BV-K 101-4) according to the manufacturer's recommendations; the proportion of stained Annexin-V^+ and Annexin-V^+/Propidium $iodide^+$ cells was determined by fluorescence activated cell sorter (FACS) analysis on FACS Calibur flow cytometer (BD Biosciences Immunocytometry Systems, San Jose, CA, USA) and data were analyzed using WinMDI freeware (Joseph Trotter, La Jolla).

4.2.14 Immunohistochemistry

Patients with dry AMD rich with drusen had been diagnosed based on biomicroscopy and fundus photographs in the Department of Ophthalmology of Freiburg University Hospital. The study was approved by the Ethics Committee of the Freiburg University Hospital and the tenets of the Declaration of Helsinki were followed. Eyes from two age-matched patients without clinically diagnosed AMD were used as a control; one eye was provided by the Department of Ophthalmology of Freiburg University Hospital and the other one by the Department of Ophthalmology of University of Debrecen. In both cases, the tenets of the Declaration of Helsinki were followed. Enucleated eyes from cadaver human samples were embedded in paraffin according to a routine protocol and horizontal sections (5 μm) of four eyes were immunostained for SQSTM1/p62, ubiquitin (Ub) and ELAVL1/HuR. The extent of immunopositivity in the retinal pigment epithelial cells was evaluated microscopically (no staining or positive staining) by selecting 5 mm long areas of the foveomacular, perimacular and peripheral regions. All the horizontal sections were, based on the histological anatomy, from the corneal level. Foveomacular, perimacular and peripheric areas were analysed as a pack from the same horizontal section. The stainings were done with Thermo Scientific's UltraVision LP Detection System AP Polymer & Fast Red Chromogen (TL-015-AF) kit according to the manufacturer's instructions. The antibodies used were mouse monoclonal for SQSTM1/p62 (Santa Cruz, sc-28359), rabbit polyclonal for ubiquitin (Dako, Z0458) and the mouse monoclonal for ELAVL1/HuR (Santa Cruz, sc-5261). The dilutions were 1:500, 1:1100 and 1:500 respectively. Human brain with Alzheimer's disease was used as a method control for the stainings (data not shown). After the staining samples were analyzed as described above, using a Zeiss AX10 Imager A2 (Gottingen) light microscope and a Jenoptik ProgRes C5 (Optical Systems) digital camera mounted on to the microscope. Photographs were taken with the same camera. The statistical analysis for the results was conducted with a Mann-Whitney test in theSPSS Statistics 17.0 program (IBM SPSS Inc).

4.3 RESULTS

4.3.1 AICAR Treatment Strongly Counteracts the MG-132-induced Increase of SQSTM1/p62 Protein Levels in ARPE-19 Cells

In order to identify the optimal conditions to study the effects on SQSTM1/p62 protein levels, the ARPE-19 cells were first treated with the proteasome inhibitor MG-132 (5 μM) and/or the autophagy activator, AICAR (2 mM) over a time range (data not shown).

Western blotting analysis revealed that a statistically significant change in total SQSTM1/p62 protein levels was detectable only after 24 h treatments, so this time point was selected for further studies. In particular, as shown in Figure 9A, the proteasome inhibitor MG-132 significantly increased total SQSTM1/p62 protein levels, while concomitant treatment with MG-132 and AICAR robustly decreased SQSTM1/p62 protein levels. In contrast, no difference in SQSTM1/p62 protein levels was detected after exposure to AICAR alone (Figure 9A). Interestingly, by performing cellular fractionation, we found that in comparison to control cells, MG-132 evoked a significant increase in the SQSTM1/p62 protein levels mainly in the nuclear/perinuclear compartment and also in the cytoplasm (+1658%, $p<0.05$ and +48%, $p<0.001$, respectively; Supplemental figure 1A). Analogously to SQSTM1/p62, MG-132 also significantly increased ELAVL1/HuR protein levels in the nuclear/perinuclear compartment, in the cytoplasm (+154%, $p<0.001$ and +64%, $p<0.01$ respectively; Supplemental figure 1B) and in the total homogenate (Figure 9B). In contrast to SQSTM1/p62, the MG-132-induced increase of ELAVL1/HuR protein was not affected by the concomitant treatment with AICAR, as reported in Figure 9B, suggesting that ELAVL1/HuR protein is not degraded via autophagy.

To confirm the capability of AICAR to induce autophagy, MAP1LC3A/LC3–II protein levels were detected after 0,5 h, 3 h, 12 h and 24 h by western blotting (Figure 9C). Indeed, when co-treated with MG-132, AICAR clearly increased MAP1LC3A/ LC3-II protein levels after 0,5 h, while after 24 h treatmentMAP1LC3A/LC3 lipidation was already over (Figure 9C), in accordance with the SQSTM1/p62 levels. We also wanted to compare AICAR response with starvation, a condition that is known as autophagy inducer. As well as for AICAR, starvation-induced autophagy required the presence of the proteasome inhibitor MG-132; conversely to AICAR, starvation-induced autophagy under proteasome inhibition begun later than AICAR (3 h vs 0,5 h) in ARPE-19 cells.

4.3.2 MG-132 Treatment Triggers the Up-regulation of SQSTM1/p62 Expression through the RNA-binding ELAVL1/HuR Protein

It has been documented that SQSTM1/p62 is oxidative stress-related and ubiquitin-binding protein [Nakaso et al. 2004]. We here confirmed that 24 h MG-132 treatment induces the increase of SQSTM1/p62 mRNA expression in the total homogenate of ARPE-19 cells (Supplemental figure 2B). Then we wanted to determine whether a positive regulation of SQSTM1/p62 expression occurs also at post-transcriptional level in human ARPE-19 cells, following MG-132 treatment.

First, we analyzed the SQSTM1/p62 sequence to identify the cis-acting elements and the corresponding trans-acting factors potentially affecting SQSTM1/p62 mRNA stability and/or translation. A detailed primary sequence analysis of SQSTM1/p62 revealed the presence of ARE in the 3′-untranslated region (3′-UTR), three of which (AUUUA) represent the canonical class I sequence recognized by the RNA-binding ELAV proteins. This region was consequently selected to design a probe used in protein-RNA binding AlphaScreen assay, an in vitro technology which can be utilized to evaluate the possible binding between ELAVL1/HuR protein and SQSTM1/p62 mRNA. An ARE-bearing probe,

a portion of TNFα 3′UTR, was employed as the positive control of the experiment since it contains well characterized ELAV-target sequences [Schaljo et al. 2009].

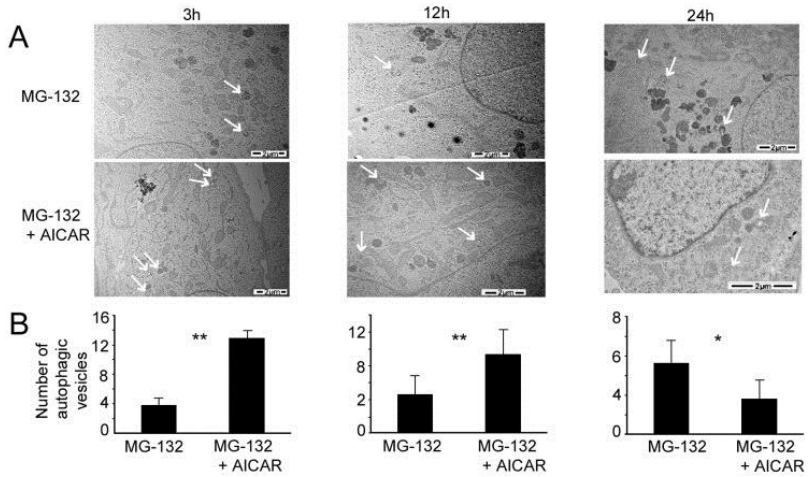

Figure 13. Transmission electron micrographs of ARPE-19 cells exposed to AICAR or/and MG-132 and autophagic vesicles quantification. (A) Representative transmission electron micrographs of ARPE-19 cells exposed to MG-132 5 μM solely and with AICAR 2 mM for 3 h, 12 h and 24 h. Autophagic vesicles are indicated by arrows. (B) Quantification of autophagic vesicles in ARPE-19 exposed to MG-132 5 μM solely and with AICAR 2 mM for 3 h, 12 h and 24 h. Six parallel samples were measured in all treatments. *p<0.05, **p<0.01, Mann–Whitney.

As shown in Figure 10A and 10B, ELAVL1/HuR protein physically interacts with the SQSTM1/p62 probe, leading to the formation of a stable protein-RNA probe complex. From saturation binding experiments we calculated the dissociation constants for the two RNA probes. The resulting binding efficiency for the SQSTM1/p62 probe was 8 times weaker than the TNFα probe, as it can be reasonably explained by the presence of four canonical AREs within the TNFα probe compared to the one present in the SQSTM1/p62 probe.

To confirm the finding obtained in the in vitro experiments and to evaluate whether the binding between ELAVL1/HuR protein and SQSTM1/p62 mRNA exists also in our cell system, we then performed immunoprecipitation coupled with RT-real-time qPCR experiments on control and MG-132 treated cells. It was found that the MG-132-induced up-regulation of SQSTM1/p62 mRNA in the cytoplasm of ARPE-19 cells (Figure 10C) was accompanied by a parallel increase of the binding between ELAVL1/HuR protein and SQSTM1/p62 mRNA in the same cellular fraction (Figure 10D), indicating that MG-132 treatment induced a positive regulation of SQSTM1/p62 expression that occurred also at the

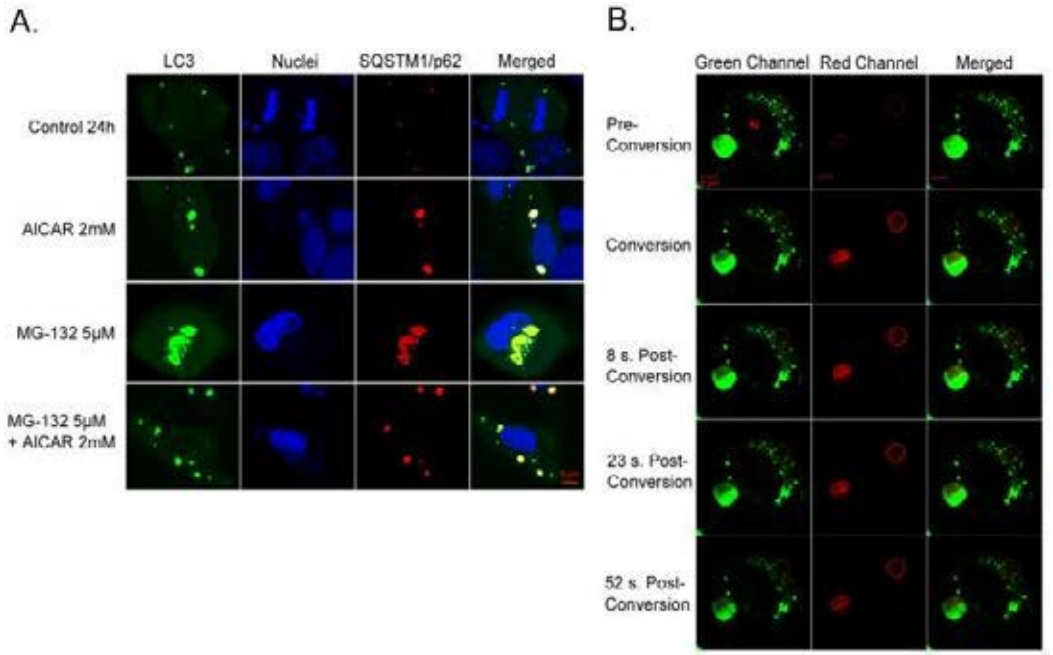

Figure 14. Colocalization of SQSTM1/p62 and MAP1LC3A/LC3 and position changes of SQSTM1/p62, revealed by confocal microscopy analysis. A light merge orange/yellow signal of colocalizing MAP1LC3A/LC3 (pDendra2-hLC3, green) and SQSTM1/p62 (pDsRed2-hp62, red) is detectable, usually near to the cell nuclei. Nuclei are stained with blue dye. The scale bar equals to 5 μm. (A): Confocal microscopy images of untreated control ARPE-19 cells and cells exposed to AICAR 2 mM or/and MG-132 5 μM for 24 h. A = Aggregates (B): Position of SQSTM1/p62 (pDendra2-hp62) in ARPE-19 cells, revealed by confocal microscopy analysis. SQSTM1/p62 in two different areas was photoconverted within approximately 7 sec (circled). Within 1 minute after photoconversion, the photoconverted SQSTM1/p62 is stationary. Cells have been exposed to 5 μM MG-132 for 24 h. N = Cell nucleus.

post-transcriptional level via ELAVL1/HuR protein. To further confirm this hypothesis, we silenced ELAVL1/HuR expression in ARPE-19 cells by siRNA technology and then exposed these cells to MG-132 for 24 h. First, we found that MG-132 treatment strongly up-regulates ELAVL1/HuR mRNA expression in ARPE-19 cells (Supplemental figure 2A). Conversely, in silenced cells, MG-132 does not affect ELAVL1/HuR mRNA total amount that is indeed comparable to control levels (Supplemental figure 2A). We then evaluated ELAVL1/HuR protein levels finding that, besides ELAVL1/HuR mRNA, ELAVL1/HuR-siRNA also counteracted MG-132-induced ELAVL1/HuR protein accumulation (Figure 11A). In parallel, we found that, in ELAVL1/HuR-silenced cells, the MG-132 exposure leads to an up-regulation of SQSTM1/p62 mRNA expression to a less extent than in MG-132-treated control cells (Supplental figure 2B). Moreover, the MG-132-induced increaseof SQSTM1/p62 protein was counteracted in ELAVL1/HuR silenced cells (Figure 11B), for the first time suggesting that the positive regulation of SQSTM1/p62 expression, during proteasomal inhibition, requires the specific presence of ELAVL1/HuRprotein.

4.3.3 AICAR Promotes the Complete Clearance of MG-132-induced Protein Aggregates, SQSTM1/MAP1LC3A (p62/LC3) Co-localization and Autophagy-related Gene Expression

As shown in Figure 9A, SQSTM1/p62 protein levels decreased following concomitant treatment with MG-132 and AICAR, subsequently we investigated in more detail the capacity of AICAR to affect protein aggregation which normally occurs under proteasome inhibition in ARPE-19 cells. The cells were thus exposed to AICAR and MG-132 and protein aggregates were examined in a transmission electron microscope. As shown in Figure 12, AICAR was able to completely abolish the MG-132-induced protein aggregation after 24 h treatment. Moreover, there was also observed obvious reduction of aggregates after 3 h and 12 h AICAR- and MG-132-co-treated cells (data not shown). Consistently with Figure 9 results, the amount of autophagic vesicles increased during first 3 and 12 hours significantly when cells were treated with AICAR together with MG-132 (Figure 13). These results show that this concomitant treatment strongly switches-on autophagy at an early time and clearance is already over after one day.

Since it is known that SQSTM1/p62 protein contains MAP1LC3A/LC3 interacting domain [Pankiv et al. 2007] we evaluated if SQSTM1/p62 protein would be co-localized with the autophagosome marker MAP1LC3A/LC3 under different stimuli in ARPE-19 cells. The cells were transfected with pDendra2-hLC3 (MAP1LC3A/LC3) and pDsRed2-hp62 (SQSTM1/p62) plasmids, exposed to AICAR and MG-132 as previously described in the text, and analyzed by live confocal microscopy. Figure 14A illustrates that MAP1LC3A/LC3 and SQSTM1/p62 proteins co-localized after all treatments and that a clear perinuclear accumulation of both proteins could be seen after MG-132-induced proteasome inhibition. In agreement with previous data, the cells treated concomitantly with MG-132 and AICAR exhibited a strong reduction of the perinuclear aggregates containing both MAP1LC3A/LC3 and SQSTM1/p62 proteins (Figure 14A). In addition, we noted that MAP1LC3A/LC3 punctas were somewhat larger in AICAR-treated cells than untreated cells. This interesting observation remains still to be studied.

4.3.4 Accumulated SQSTM1/p62 Protein is Stationary Following 24 hours' Proteasome Inhibition in ARPE-19 Cells

It has been previously shown that SQSTM1/p62 protein accumulates in perinuclear aggregates that undergo autophagy clearance [Bjørkøy et al. 2005, Viiri et al. 2010]. According to our unpublished data there are proteins that have reversible binding capacity to perinuclear aggregates. Therefore, we wanted to evaluate whether binding of SQSTM1/p62 to aggregates is reversible or irreversible prior to autophagy. In order to observe whether, under MG-132 stimulus, the increased SQSTM1/p62 protein levels were accompanied by its intracellular translocation in ARPE-19 cells, the fusion protein plasmid construct pDendra2-hp62 (SQSTM1/p62) was created and transfected to cells. Confocal microscopy was used for live cell imaging and the movement of SQSTM1/p62 protein was evaluated after photo converting pDendra2-hp62 (SQSTM1/p62) (Figure 14B). Two areas containing SQSTM1/p62 protein were photoconverted: the intensively aggregated SQSTM1/p62 and the amorphously aggregated SQSTM1/p62. We detected no position

changes of SQSTM1/p62 protein from the converted area to other parts of the cell within 1 minute, indicating that accumulated SQSTM1/p62 is stationary in ARPE-19 cells treated for 24 h.

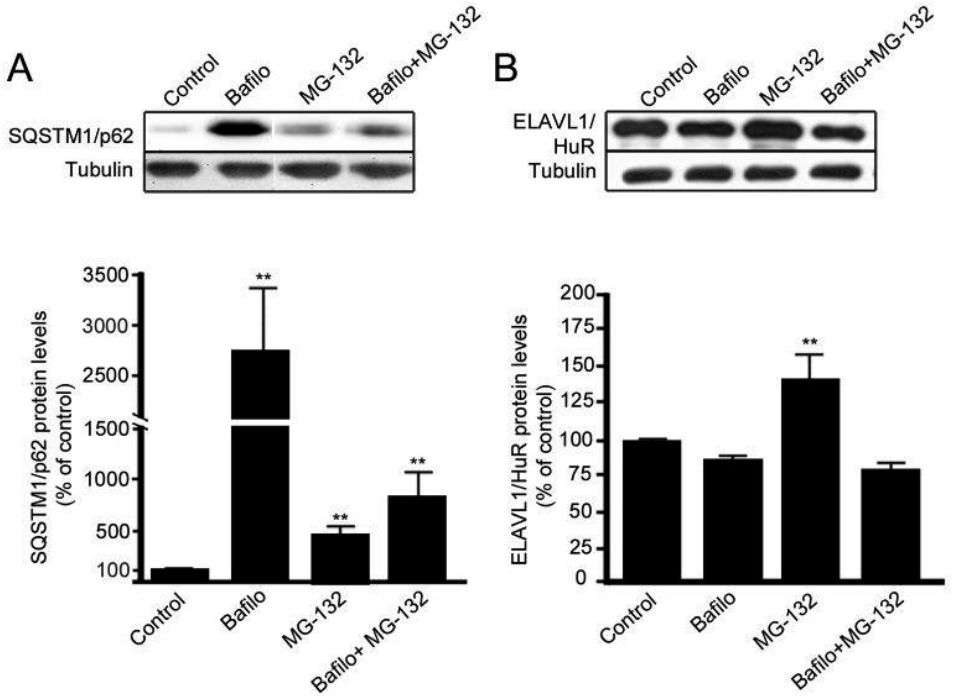

Figure 15. SQSTM1/p62 protein, but not ELAVL1/HuR protein, is degraded by autophagy in ARPE-19 cells. Representative western blotting and densitometric analysis of SQSTM1/p62 (A) and ELAVL1/HuR (B) proteins in the total homogenates of ARPE-19 cells after exposure to bafilomycin (50 nM) or/and MG-132 (5 μM) for 24 h. α-tubulin was used as a loading control. Results are expressed as means ± S.D. The data were analyzed by ANOVA, followed by Mann-Whitney; **p<0.01, untreated control cells vs. treated cells, n=7.

4.3.5 AICAR is Well-tolerated and Prevents Cell Death in MG-132 Long-exposed ARPE-19 Cells

Next we evaluated how well ARPE-19 cells could tolerate exposure to AICAR. Cellular toxicity was evaluated in two ways after 24 h exposure to AICAR on its own and/or with the proteasome inhibitor MG-132 by lactate dehydrogenase and Annexin-V assays. AICAR treatment, in the presence or absence of the proteasome inhibitor, did not increase lactate dehydrogenase release as compared to untreated control cells after 24 h (Supplemental figure 3A), evidence of the good cellular tolerability towards AICAR. Annexin-V and Propidium Iodide double staining revealed that MG-132 treatment is able to induce apoptosis after prolonged (48 and 72 h) exposure; in particular, we found that proteasome inhibition clearly induced early and late apoptosis, the latter being more pronounced after 72 h of treatment (Supplemental figure 3B). After exposure for both 48 and 72 h to MG-132, the concomitant presence of AICAR counteracted the apoptotic effects, indicating that

AICAR exerted cytoprotective properties against proteasome inhibition in ARPE-19 cells, by favoring autophagy which reduced proteasome blockade-induced toxicity.

4.3.6 SQSTM1/p62 Protein, but not ELAVL1/HuR Protein, is Degraded by Autophagy

Bafilomycin is known to be an autophagy inhibitor preventing the fusion of autophagosomes and lysosomes, although the effect may change between cell types and exposure time [Klionsky et al. 2008]. To test how bafilomycin affects SQSTM1/p62 protein expression in ARPE-19, these cells were treated with either 50 nM bafilomycin or 5 μM MG-132 or with both agents simultaneously, and total protein extracts were analyzed by western blotting. In accordance with our previous experiments, ARPE-19 cells treated with bafilomycin displayed a dramatic increase of SQSTM1/p62 protein levels (Figure 15A). In addition, when cells were exposed to both bafilomycin and MG-132, there was a statistically significant increase of the SQSTM1/p62 protein amount compared to untreated (Figure 15A), although to a lesser extent than with bafilomycin alone, implying that SQSTM1/p62 clearance was mediated via autophagy in ARPE-19 cells. Conversely, we did not observe any change in ELAVL1/HuR protein levels after bafilomycin (Figure 15B), further indicating that ELAVL1/HuR protein was being degraded via proteasome.

4.3.7 SQSTM1/p62 Protein Levels in the Foveo-macula Areas of AMD Patients

Since, it is uncertain that the compounds used to regulate autophagy in the cell culture model also mimic cellular aging and age-related disease we wanted to analyze these key proteins in human tissue samples. The SQSTM1/p62 staining in the foveomacular areas of the AMD patients was more extensive compared to the perimacular and peripheral areas ($p<0.001$), the latter representing the internal control (Figure 16; Table 1). The drusen were mostly SQSTM1/p62 negative while the nuclei of RPE cells were SQSTM1/p62 negative. A uniform staining of ubiquitin in RPE cells and Bruch's membrane was observed in all these regions (Figure 17). There were no differences in the extent of ubiquitin staining between these regions in all groups ($p>0.1$) (Table 1). Most of the nuclei of RPE cells were ubiquitin negative and most of the drusen were strongly ubiquitin positive. The foveomacular nuclei showed less extensive immunopositivity for ELAVL1/HuR protein than the perimacular and peripheral regions (Figure 18). However this difference was not statistically significant in any of the groups studied ($p>0.1$) (Table 1). The cytoplasms of RPE cells were ELAVL1/HuR negative while the drusen were mostly ELAVL1/HuR negative. We also performed the same immunohistochemistry experiments in age-matched control samples. We found that they were mostly SQSTM1/p62 negative, especially in the macular region (Figure 19A); all the nuclei of RPE cells were negative, and there were only a few SQSTM1/p62 immunopositive cytoplasms randomly distributed through-out the RPE cell layer. In the control patient samples Bruch's membrane was mostly immunonegative for ubiquitin; occasionally through-out the RPE cell layer, few cytoplasms were weakly ubiquitin positive, while all of the nuclei were negative in all the regions studied (Figure 19B). In these control sections, half of the nuclei showed weak immunopositivity for ELAVL1/HuR while the cytoplasms of RPE cells were negative through-out the RPE cell layer (Figure 19C).

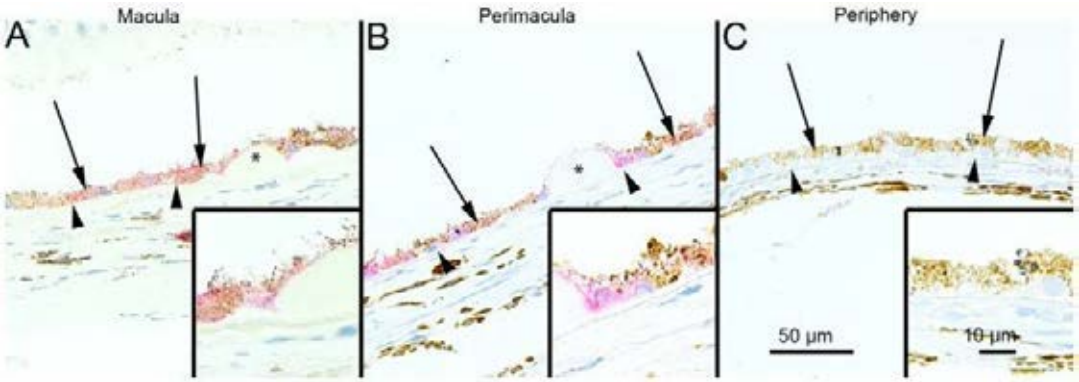

Figure 16. Sections of eyes with clinically diagnosed AMD immunostained for SQSTM1/p62. The extent of cytoplasmic immunopositivity in the retinal pigment epithelial cells (RPE, shown by arrows) and in the drusen was evaluated microscopically (no staining or positive staining) by selecting 5 mm long areas of foveomacular (A), perimacular (B) and peripheral (C) regions. The SQSTM1/p62 staining in the foveomacular areas was more extensive as compared to the perimacular and peripheral areas (B and C, respectively). The drusen (shown by asterisks) were mostly SQSTM1/p62 negative. The nuclei of RPE cells were SQSTM1/p62 negative. (Original magnifications of x 200 and in insets x 400; Bruch's membrane shown by arrow heads).

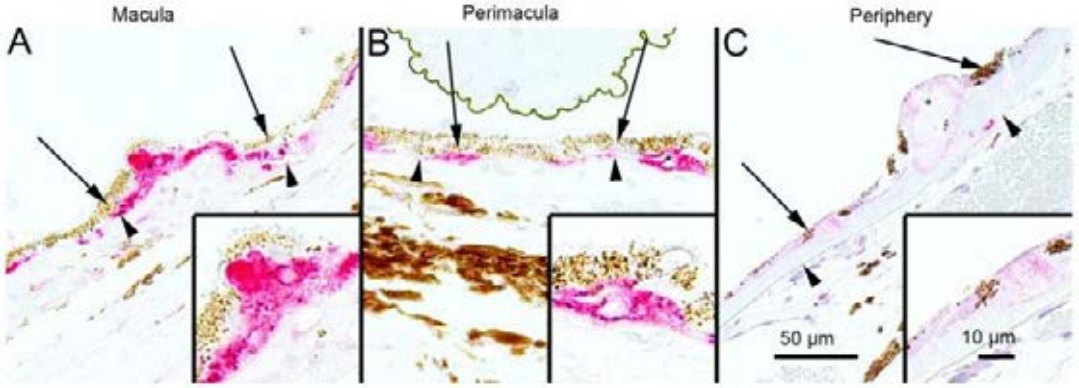

Figure 17. Sections of eyes with clinically diagnosed AMD immunostained for ubiquitin. The extent of Bruch's membrane immunopositivity of the retinal pigment epithelial cells (RPE, shown by arrows) and in the drusen (asterisks) was evaluated microscopically (no staining or positive staining) by selecting 5 mm long areas of foveomacular (A), perimacular (B) and peripheral (C) regions. The uniform staining of ubiquitin in RPE cells Bruch's membrane was observed in all these regions (arrows). There were no differences in the extent of staining between these regions in each group. The nuclei of RPE cells were mostly ubiquitin negative. Most of the drusen were strongly ubiquitin-positive (asterisks). (Original magnifications of x 200 and in insets x 400; Bruch's membrane shown by arrow heads).

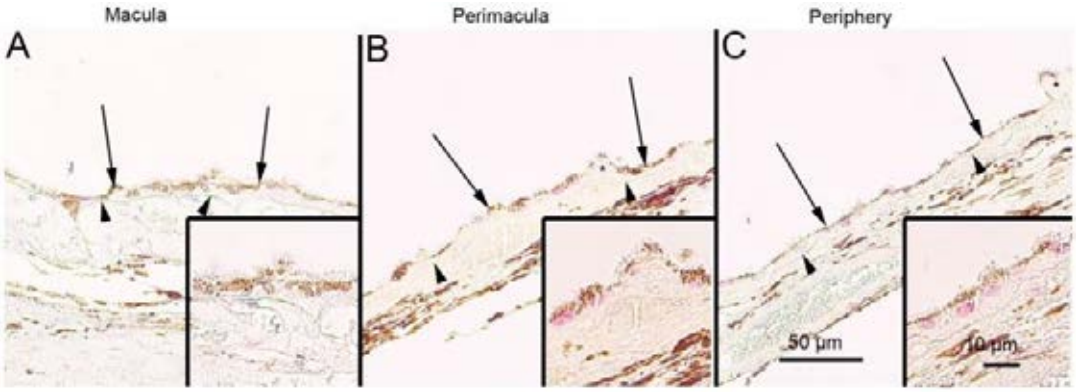

Figure 18. Sections of eyes with clinically diagnosed AMD immunostained for ELAVL1/HuR. The immunopositivity of the nuclei of RPE cells (shown by arrows) and the extent of immunopositivity in the drusen (asterisks) was evaluated microscopically (no staining or positive staining) by selecting 5 mm long areas of foveomacular (A), perimacular (B) and peripheral (C) regions. The foveomacular nuclei showed less extensive immunopositivity for ELAVL1/HuR than the perimacular and peripheral regions. However this difference was not statistically significant in any of the groups studied ($p>0.1$). The cytoplasms of RPE cells were ELAVL1/HuR negative. Most of the drusen were ELAVL1/HuR-negative. (Original magnifications of x 200 and in insets x 400; Bruch's membrane shown by arrow heads).

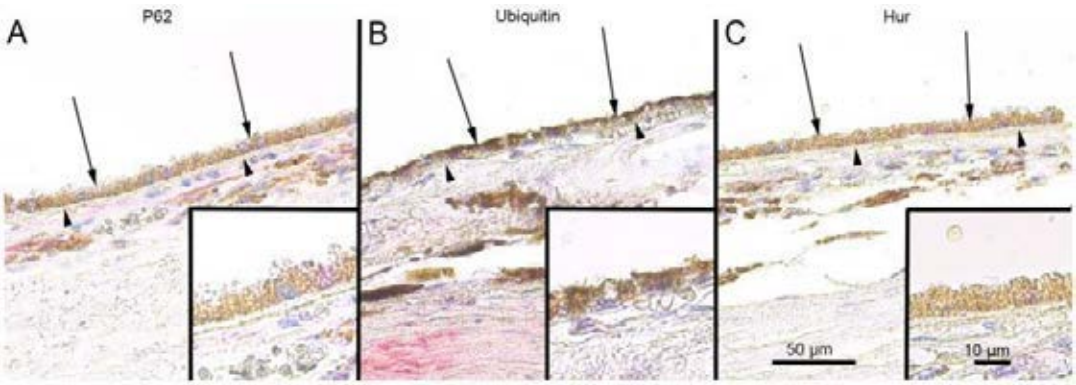

Figure 19. Sections of foveomacular areas of age-matched control eyes for SQSTM1/p62, ubiquitin and ELAVL1/HuR. The extent of cytoplasmic immunopositivity for SQSTM1/p62, Bruch's membrane immunopositivity for ubiquitin and the immunopositivity of nuclei of RPE cells for ELAVL1/HuR (foveomacular areas shown; A, B and C respectively) in the RPE cells (shown by arrows) was evaluated microscopically (no staining or positive staining). For SQSTM1/p62 there were only a few immunopositive cytoplasm's randomly distributed through-out the RPE cell layer and the nuclei were negative. Bruch's membrane (shown by arrowheads) was immunopositive for ubiquitin occasionally through-out the RPE cell layer in very small amounts while all of the nuclei were negative. Half of the nuclei showed minor immunopositivity for ELAVL1/HuR while the cytoplasm's of RPE cells were negative. The foveomacular areas showed no difference in immunohistochemical stainings when compared to areas of perimacular and peripheral retina in all of the proteins studied. (Original magnifications of x 200 and in insets x 400).

4.4 DISCUSSION

In this study, we show for the first time that in ARPE-19 cells proteasome inhibition leads to increased ELAVL1/HuR expression by acting in a dual manner: on one side inducing ELAVL1/HuR transcription and, on the other side, decreasing its protein degradation; during proteasomal inhibition ELAVL1/HuR protein binds to SQSTM1/p62 mRNA to potentiate post-transcriptionally SQSTM1/p62 expression levels in ARPE-19 cells. SQSTM1/p62 protein is cleansed by autophagy after its stationary binding to perinuclear protein aggregates during proteasome inhibition. The cleansing can be accelerated by exposure to the AMPK activator AICAR, which counteracts the MG-132 - mediated damaging effects and improves survival in RPE. Interestingly, SQSTM1/p62 rather than ELAVL1/HuR protein accumulates strongly in the drusen rich macular area in human cadaver dry AMD samples - an evidence for impaired autophagy in the pathology of AMD. These major findings are schematically summarized in Figure 20.

Many previous studies have focused on to the transcriptional-dependent events that affect SQSTM1/p62 expression, whereas little data is available on SQSTM1/p62 post-transcriptional control. Our findings indicate that, in response to MG-132 stimulus, the elevation in SQSTM1/p62 mRNA levels is due to the activation of specific intracellular molecular cascades that are not simply at the transcriptional level, but also involve the downstream fate of SQSTM1/p62 transcript through the RNA-binding ELAVL1/HuR protein. Indeed, we first identified within SQSTM1/p62 3′-UTR primary sequence the presence of ARE, that are putative ELAV-binding sites. The in vitro experiment seems to confirm our prediction, demonstrating that the recombinant HuR protein binds specifically to the ARE-bearing RNA probe of SQSTM1/p62. The ELAVL1/HuR protein capability to bind to SQSTM1/p62 mRNA was further validated in vitro by immunoprecipitation and real time qPCR experiments. In particular, the isolation of the transcripts co-immunoprecipitated with endogenous ELAVL1/HuR protein showed that this RNA binding protein had associated with SQSTM1/p62 mRNA more prominently after proteasome inhibition in ARPE-19 cells. Proteasome inhibition caused ELAVL1/HuR protein accumulation, an increase in the amount of SQSTM1/p62 protein and mRNA and an increase of the formation of the ELAVL1/HuR protein-SQSTM1/p62 mRNA complex. Therefore the binding of ELAVL1/HuR to a low affinity mRNA sequence, such as SQSTM1/p62, can best be explained by an alteration in the stoichiometric parameters regulating the mass action law. The increase of ELAVL1/HuR at both mRNA and protein levels in MG-132-treated cells suggests that the ELAVL1/HuR protein up-regulation may be due not only to proteasome inhibition but also to an effect on new ELAVL1/HuR protein synthesis.

In confirmation of the specific involvement of ELAVL1/HuR protein in SQSTM1/p62 post-transcriptional expression regulation, we observed that the MG-132-induced increase of SQSTM1/p62 protein was blunted in ELAVL1/HuR silenced RPE cells. Accordingly, we found that, in ELAVL1/HuR-silenced cells, the MG-132 exposure leads to an up-regulation of SQSTM1/p62 mRNA expression in a less extent than in MG-132-treated control cells, suggesting that physiologically the MG-132-mediated SQSTM1/p62 increase occurs at both

transcriptional and post-transcriptional level, the latter one via ELAVL1/HuR protein. These findings are particularly striking since post-transcriptional mechanisms are emerging as fundamental, precise regulators of gene expression in many stress-related

Table 1. Cytoplasmic SQSTM1/p62, ubiquitin and ELAVL1/HuR proteins in foveomacular, perimacular and peripheral RPE cells. Eight 5 mm long regions from macular, perimacular and peripheral retina were selected from eyes with clinically diagnosed AMD. If the optical nerve was visible, the macular area was selected next to it; if not, a region which contained most drusen was selected. Peripheral regions were selected close to the ora serrata so that it would have as few as possible drusen. The perimacular region was selected between these two so that it would contain few drusen. The extent of cytoplasmic immunopositivity was measured and its percentage in relation to the whole measurement was calculated. P-value for SQSTM1/p62 between macular-perimacular and macular-peripheral retina groups is $p<0.001$. The differences among the three groups for ubiquitin and ELAVL1/HuR are not statistically significant ($p>0.1$) The statistical analysis for the results was conducted with a Mann-Whitney test. MA = mean value,SD = standard deviation.

SQSTM1/p62	**Macula**	**Perimacula**	**Peripheral retina**
Sample		**Percentage (%)**	
1	100	48	0
2	100	64	0
3	92	16	12
4	100	26	36
5	90	7	36
6	100	48	0
7	100	38	24
8	100	22	18
MA; SD (%)	**97,8; 4,2**	**33,6; 19,2**	**15,8; 15,4**
Ubiquitin	**Macula**	**Perimacula**	**Peripheral retina**
Sample		**Percentage (%)**	
1	15	30	0
2	14	44	9,6
3	64	66	40
4	70	56	26
5	70	26	32
6	64	32	30
7	20	9	7,4
8	16,4	16,8	4
MA; SD (%)	**41,7; 27,2**	**35; 19,3**	**18,6; 15,1**
ELAVL1/HuR	**Macula**	**Perimacula**	**Peripheral retina**
Sample		**Percentage (%)**	
1	6,7	8,7	0
2	32,6	0	66,7
3	56,4	100	61,5
4	5,6	36,4	56,2
5	30,4	50	42,5
6	38,3	35,4	27,1
7	0	0	0
8	0	0	0
MA; SD (%)	**21,3; 21,1**	**28,8; 34,9**	**31,8; 28,9**

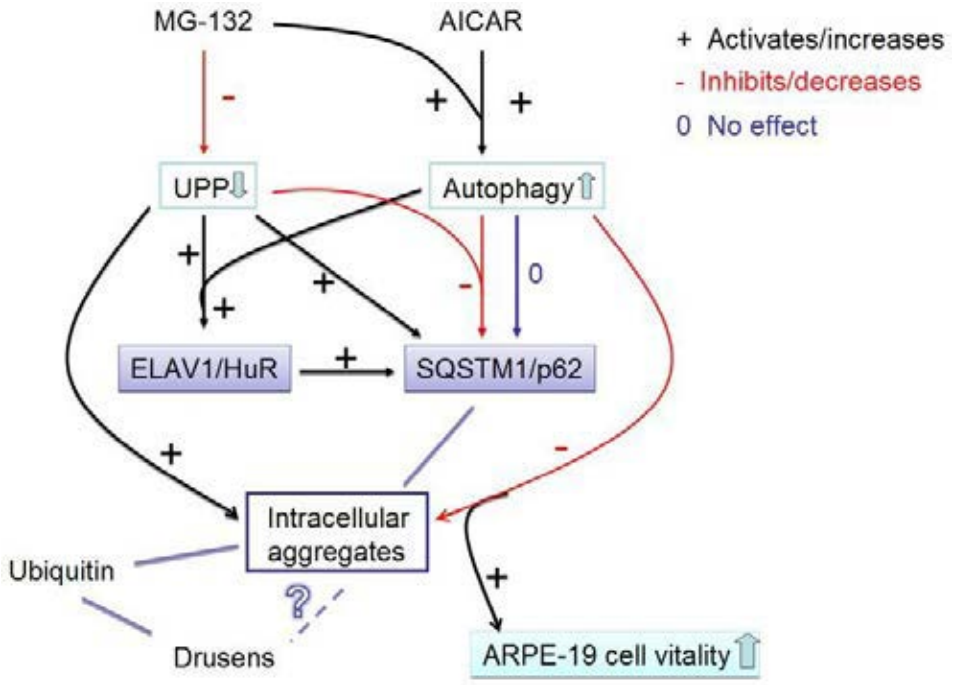

Figure 20. Summary of the results. The proteasome inhibitor MG-132 down-regulates (−) the ubiquitin-proteasome pathway (UPP). AMPK-activator AICAR and proteasome inhibitor MG-132 co-treatment activates (+) the autophagy. UPP inhibition significantly increases (+) SQSTM1/p62 protein levels, while autophagy induction during UPP inhibition robustly decreases (−) SQSTM1/p62 protein levels. Since SQSTM1/p62 localizes to aggregates, the decreasing of SQSTM1/p62 reveals its autophagy clearance. In addition, proteasome inhibition significantly increases ELAVL1/HuR protein levels by itself and during the autophagy induction (+). Proteasome inhibition induces a positive regulation of *SQSTM1/p62* expression that occurs also at post-transcriptional level via ELAVL1/HuR protein (+). Activated autophagy is able to completely abolish the MG-132-induced protein aggregation (−), which, in turn improves the cell vitality. Ubiquitin is also found in intracellular aggregates in ARPE-19 cells as well as from drusens. In contrast, SQSTM1/p62 is found only in the intracellular aggregates in ARPE-19 cells, but not in drusens. However, SQSTM1/p62 levels were high in macular area of RPE cells revealing impaired autophagy. What is the relation between drusen and intracellular aggregates remains still unknown. Red lines with minus symbol represent inhibiting and decreasing events in ARPE-19 cells. Black lines and plus symbol represent activating and increasing events in the ARPE-19 cell. Zero (0) and dark blue line indicate neutral effects in the ARPE-19 cell. UPP: ubiquitin-proteasome pathway.

conditions [Abdelmohsen et al. 2008, Amadio et al. 2008]. Moreover, our results are in line with a report showing that, in human fibroblasts, MG-132 induces ELAVL1/HuR export to the cytoplasm, where it promotes the stabilization/translation of target mRNAs [Bonelli et al. 2004].

For the first time we show that, when co-treated with proteasome inhibitor MG-132, AICAR triggered autophagy in ARPE-19 cells, as indicated by the increase of both LC3 lipidation and autophagosome vesicles formation. As well as for AICAR, we found that also starvation alone cannot induce autophagy in ARPE-19 cells: indeed, both AICAR and starvation require the presence of MG-132 to trigger autophagic process. Notably, LC3II increase was detectable, respectively, after 0,5 h treatment with AICAR+MG-132, and 3 h treatment with starvation+MG-132, suggesting a different time course for autophagy activation by the two co-stimuli.

In ARPE-19 cells the MG-132–mediated increase of SQSTM1/p62 protein levels was robustly counteracted by the autophagy inducer AICAR. In contrast to SQSTM1/p62, the MG-132-triggered accumulation of ELAVL1/HuR protein was not affected by AICAR treatment, pointing to different proteolytic mechanisms between SQSTM1/p62 and ELAVL1/HuR: one being decreased in autophagy and the other involving the proteasomal pathway, respectively. Accordingly, a previous observation in another human cellular model reported that HuR could undergo proteasome mediated proteolysis [Abdelmohsen et al. 2009].

Moreover, by using pDendra2-hLC3 (MAP1LC3A/LC3) and pDendra2-hp62 (SQSTM1/p62) plasmids, with which the position of the protein in the cell can be detected from a desired time point, we analyzed protein trafficking in cells [Klionsky et al. 2012], showing that both molecules involved in autophagy simultaneously disappeared via induction of autophagy in response to MG-132 and AICAR co-treatment. As far as we are aware, this is the first time that the binding of SQSTM1/p62 protein to perinuclear aggregates has been revealed as an irreversible process. We recently documented that when SQSTM1/p62 mRNA was silenced, ubiquitin localization in perinuclear aggregates and autophagosome formation were disturbed in ARPE-19 cells; here we show that AICAR treatment alone does not decrease SQSTM1/p62 protein levels, indicating that selective SQSTM1/p62 degradation in autophagy is favoured when ubiquitinated aggregates are present, as previously documented [Korolchuk et al. 2009a, Viiri et al. 2010]. It is noteworthy, that AICAR significantly decreased protein aggregates and improved survival in MG-132-treated RPE cells, providing clear evidence for an AICAR-mediated protective effect in this stressful condition. AICAR is a well-known autophagy inducer which acts via AMPK signalling, although it may well have other effects in different experimental models [Samari and Seglen 1998, Meley et al. 2006, Matsui et al. 2007, Liang et al. 2007, Viana et al. 2008, Salminen and Kaarniranta 2012].

Interestingly, it has been demonstrated that in human AMD donor samples both accumulations of autophagic markers and decreased lysosomal activity can be observed [Wang et al. 2009c]. Furthermore, an effective autophagic clearance system has been recently documented in human RPE cells [Ryhänen et al. 2009, Wang et al. 2009a, Kurz et al. 2009, Viiri et al. 2010]. During aging, lipofuscin accumulates in lysosomes – this is evidence for a declining cellular capability to degrade proteins [Krohne et al. 2010a]. In addition, lipofuscin promotes the misfolding of intracellular proteins, which exerts an additional oxidative stress in the RPE cells [Shamsi and Boulton 2001, Kaarniranta et al. 2010].

As recently suggested by our group [Viiri et al. 2010] and here confirmed in detail, the SQSTM1/p62 clearance via autophagy can be prevented by the lysosome inhibitor bafilomycin. Under bafilomycin treatment, an intense autophagosome formation, in parallel with SQSTM1/p62 accumulation, can be observed, further confirming SQSTM1/p62 as a good marker for impaired autophagy.

Our human AMD samples here studied show a significant elevation of SQSTM1/p62 protein levels in the macula, strongly indicating that SQSTM1/p62 accumulation may be an index of impaired autophagy. In addition, most of the drusen of AMD patients were strongly ubiquitin positive, but staining for SQSTM1/p62 was observed only intracellularly. This might imply that SQSTM1/p62 is mostly degraded by the autophagic pathway and, unlike ubiquitin, SQSTM1/p62 is not exocytosed to the extracellular space of the RPE cells [Liang et al. 2007, Kaarniranta et al. 2009, Krohne et al. 2010b]. Recently published papers have reported that ubiquitin and SQSTM1/p62 are strongly co-localized in the perinuclear aggregates [Korolchuk et al. 2009b, Viirit et al. 2010], but here we could detect only ubiquitin in the extracellular drusen of AMD samples. ELAVL1/HuR protein level staining in human dry AMD macula was rather reduced, although not significantly. Since ELAVL1/HuR is degraded in proteasomes, our findings provide evidence that proteasomes are active in these AMD cases, even though proteasomal activity may decrease during aging in the RPE cells [Mullins et al. 2000, Shamsi and Boulton 2001, Li et al. 2008]. As a confirmation of our hypothesis, the foveomacular areas from control no-AMD patients showed weak staining for SQSTM1/p62, ELAVL1/HuR, ubiquitin proteins, comparable to those observed in perimacular and peripheral retina of AMD patients.

Besides many recent advances in the understanding of autophagy mechanisms, it is now widely accepted that dysfunctions in these processes have a key role in many neurodegenerative diseases, including AMD. Moreover, autophagy is increasingly emerging as a novel target of therapies aimed to counteract protein aggregation and improve cell viability; within this context, preservation of autophagy may protect RPE cell from degeneration and thus represents a potential tool to slow or even prevent the development of AMD [Kaarniranta et al. 2013].

4.5 ACKNOWLEDGEMENTS

The authors thank Anne Seppänen, Tuomas Ryhänen, Tuomas Paimela, Anne-Mari Haapaniemi and Tapio Nuutinen for technical assistance and Dr. Ewen MacDonald for checking the language.

5 Hsp70 Binds Reversibly to Proteasome Inhibitor-induced Protein Aggregates and Evades Autophagic Clearance in ARPE-19 Cells

ABSTRACT

Age-related macular degeneration (AMD) is characterized primarily by degeneration of the macular retinal pigment epithelium (RPE) that secondarily leads to cell death of photoreceptors and impaired central vision. Hallmarks of AMD are accumulation of lysosomal lipofuscin and extracellular drusen, which indicate impaired proteolysis in RPE cells. Cellular proteostasis is strongly regulated by molecular chaperones such as Hsp70 and proteasomal and autophagic clearance systems. We have recently shown that autophagy receptor SQSTM1/p62 binds irreversibly to proteasome inhibitor–induced perinuclear protein aggregates and undergoes autophagic clearance in RPE cell cultures. Revealing decreased autophagy, SQSTM1/p62 accumulates in macular area of donor AMD patient samples. In this study, we show that Hsp70 binds reversibly to proteasome inhibitor–induced perinuclear protein aggregates and does not become degraded by autophagy in ARPE-19 cells. Our observation reveals new opportunities to use a cytoprotective Hsp70 as a therapy target in the prevention of RPE cell degeneration and development of AMD.

5.1 INTRODUCTION

Age-related macular degeneration (AMD), the leading cause of irreversible blindness in the Western world, is characterized primarily by degeneration of the macular retinal pigment epithelium (RPE) [Kaarniranta et al. 2011]. RPE damage leads secondarily to cell death of photoreceptors (rods and cones) and impaired vision. The cells of RPE are exposed to chronic oxidative stress originated mainly from three sources: (i) high levels of oxygen consumption, (ii) exposure to lipid peroxidation products derived from the ingestion of photoreceptor outer segments, and (iii) exposure to constant light stimuli. Chronic oxidative stress may evoke misfolding and aggregation of proteins especially during aging. Heat shock proteins (Hsps) attempt to repair the misfolding damage. If this fails, soluble proteins become ubiquitinated and targeted into proteasomes for degradation [Jung et al. 2009, Kaarniranta et al. 2013]. Increased levels of Hsps have been observed in RPE cells with accumulated lipofuscin and in retina samples of AMD patients [Schutt et al. 2002, Decanini et al. 2007]. Moreover, proteasomal activity declines during aging, which leads to aggregation of oxidized and ubiquitinated proteins, as has been documented to happen in RPE [Li et al. 2008, Viiri et al. 2013]. Impaired proteasomal clearance in RPE cells induces selective macroautophagy (referred to as autophagy) [Viiri et al. 2010, Viiri et al. 2013], which is the most prevalent form of autophagy. It involves

formation of a double-membrane structure (autophagosome) and engulfment of cytoplasmic proteins, lipids and damaged organelles [Klionsky et al. 2012]. Thereafter, autophagosomes fuse with primary lysosomes, and their contents become degraded by lysosomal enzymes [Kaarniranta et al. 2013].

Cellular homeostasis is largely dependent on the quality control of proteins, which is called proteostasis [Tokarz et al. 2013]. Hsp70 is one of the key chaperone proteins in the regulation of proteostasis together with proteasomal and autophagic clearance [Tokarz et al. 2013]. SQSTM1/p62 (Sequestosome 1) is the best-characterized and most ubiquitously expressed autophagy adaptor that connects proteasomal clearance with autophagy [Bjørkøy et al. 2005, Komatsu et al. 2007, Kaarniranta et al. 2009, Pankiv et al. 2010, Viiri et al. 2010, Viiri et al. 2013]. We have previously shown that SQSTM1/p62 binds irreversibly to perinuclear protein aggregates and undergoes autophagic clearance [Viiri et al. 2013]. On the other hand, alleviation of autophagy is usually accompanied by accumulation of SQSTM1/p62, especially on areas that are rich of ubiquitin-stained protein aggregates, as recently reported in AMD patients [Viiri et al. 2010, Viiri et al. 2013].

When proteasomal clearance becomes inhibited in RPE cells, Hsp70 accumulates in same protein aggregates with SQSTM1/p62 [Ryhänen et al. 2009, Viiri et al. 2013]. SQSTM1/p62 rather than Hsp70 is considered to be a marker for autophagic activity [Viiri et al. 2010, Viiri et al. 2013]. In this study, we show that Hsp70 binds in a reversible manner to proteasome inhibitor–induced perinuclear protein aggregates and does not become degraded by autophagy in ARPE-19 cells.

5.2 MATERIALS AND METHODS

ARPE-19 cells originated from human retinal pigment epithelium were obtained from the American Type Culture Collection (ATCC). The cells were grown to confluence in a humidified 10% CO2 atmosphere at 37°C in Dulbecco's MEM/Nut MIX F-12 (1:1) medium (Life Technologies, 21331) containing 10% inactivated fetal bovine serum (Hyclone, SV30160-03), 100 units/ml penicillin, 100 μg/ml streptomycin (Lonza, DE17-602E), and 2 mM L-glutamine (Lonza, BE17-605E). In order to induce protein aggregates, the cells were exposed to 5 μM of MG-132 proteasome inhibitor (Calbiochem, 474790). Lysosomal function was disturbed by 50 nM of bafilomycin A1 (Sigma, B1793). Autophagy was activated with the AMPK (AMP-activated protein kinase) activator AICAR (5-Aminoimidazole-4-carboxyamide ribonucleoside, Toronto Research Chemical, A611700) at 2 mM concentration or induced by starving the cells in serum-free medium. All exposures lasted for 24 hours.

5.2.1 Transmission Electron Microscopy

Cell culture samples were prefixed with 2.5% glutaraldehyde in 0.1 M phosphate buffer (pH 7.4) for 2 hours at room temperature. After 15 minutes washing with 0.1 M phosphate buffer, the cells were post-fixed in 1% osmium tetraoxide and 0.1 M phosphate buffer for 1 hour, and washed with phosphate buffer for 15 minutes prior to standard ethanol dehydration. Subsequently, the samples were infiltrated and embedded in LX-112 resin. Polymerization was carried out at 37°C for 24 h and at 60°C for 48 hours.

The sections were examined with a JEM-2100F transmission electron microscope (Jeol) at 200 kV.

5.2.2 Western Blotting

For Western blotting, whole cell extracts containing 20 μg of protein were run in 10% SDS-PAGE gels and then transferred to nitrocellulose membranes (Amersham Biosciences) using a semi-dry transfer apparatus (Bio-Rad Laboratories). Successful transferof proteins from gels to membranes was monitored by Ponceau S staining (Sigma). The membranes were blocked in 0.3% Tween 20/PBS (phosphate-buffered saline) containing 3% fat-free dry milk for 1.5 hours at room temperature (RT). Subsequently, the membranes were incubated overnight at 4°C with a mouse monoclonal Hsp70 antibody (StressGen) or with a mouse monoclonal anti-α-tubulin (Sigma). Primary antibodies were diluted 1:5000 and 1:8000, respectively, in 0.3% Tween 20/PBS containing 0.5% bovine serum albumin. After three 10-minute washes with 0.3% Tween 20/PBS, the membranes were incubated for 2 hours at RT with horseradish peroxidase-conjugated secondary antibodies (Amersham Biosciences). Secondary antibodies were diluted 1:20 000 for Hsp70 and 1:10 000 for α-tubulin in 0.3% Tween 20/PBS containing 3% fat-free dry milk. Before detection, all membranes were washed as mentioned above. Protein-antibody complexes were detected with an enhanced chemiluminescence method (Millipore).

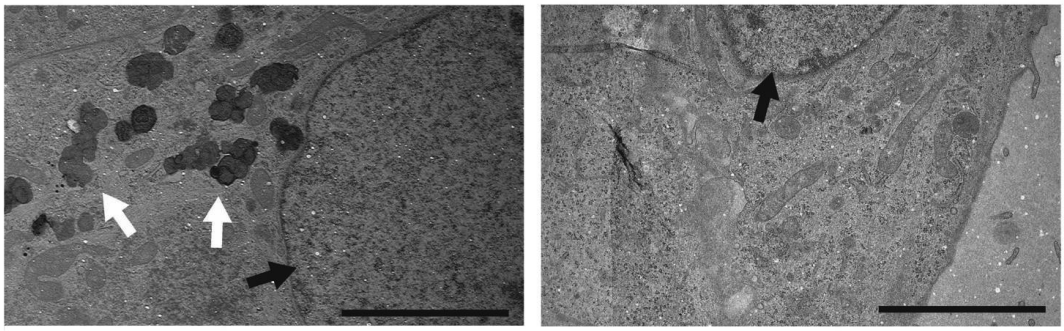

Figure 21. Representative transmission electron micrographs on untreated control ARPE-19 cells (left) and cells exposed to 5 μM MG-132 for 24 h. Aggregates are indicated by white and nuclei by black arrows. Scale bar = 3 μm.

5.2.3 pDendra2-Hsp70 Fusion Plasmid Construction

The functional open reading frame (ORF) of human Hsp70 A1A gene (NCBI Nucleotide accession no. NM_005345) was amplified from DNase-treated (DNase I, Roche) total RNA, which was extracted using the Eurozol reagent (Euroclone) from human ARPE-19 cells. RNA was reverse-transcribed by MultiScribe reverse transcriptase (Applied Biosystems), and Hsp70 cDNA was amplified with Phusion Hot start DNA polymerase (Finnzymes). Primers were 5'-ATA *CTC GAG* at**A TG**G CCA AAG CCG C (forward) and 5'-AAT *AAG CTT* g**CT A**AT CTA CCT CCT CAA TGG TG (reverse), containing target sites for restriction endonucleases *Xho*I and *Hin*dIII (italics) and stuffers (minuscules) for in-frame ligation. Sites for the initiation and termination of translation are in boldface.

Sticky ends for the amplified Hsp70 ORF as well as for the multiple cloning site of the vector pDendra2-C (Evrogen) [Gurskaja et al. 2006] were produced with the above-mentioned restriction endonucleases (MBI Fermentas). Ligated (T4 DNA Ligase, Roche) DNA containing a fusion gene of Dendra2 and Hsp70 was transfected into competent DH5α E. coli cells, which were prepared using the protocol described by Inoue et al. [Inoue et al. 1990] Following the bacterial growth, plasmids were purified as previously described [Sambrook et al. 1990]. Integrity of the construct, named pDendra2-hHsp70, was determined initially by the restriction endonuclease digestion analysis and finally by sequencing the junction sites and the entire inserted Hsp70 ORF.

The plasmid pDendra2-hp62 producing a fusion protein containing Dendra2 and human SQSTM1/p62, analogous to pDendra2-hHsp70 described above, was prepared as previously described [Viiri et al. 2013]. Preliminarily, the structure and functionality of the fusion proteins were initially monitored using RT-PCR amplification of a 365-bp fragment flanking one junction and by Western hybridization with a Hsp70 antibody (StressGen) detecting the fusion protein (not shown).

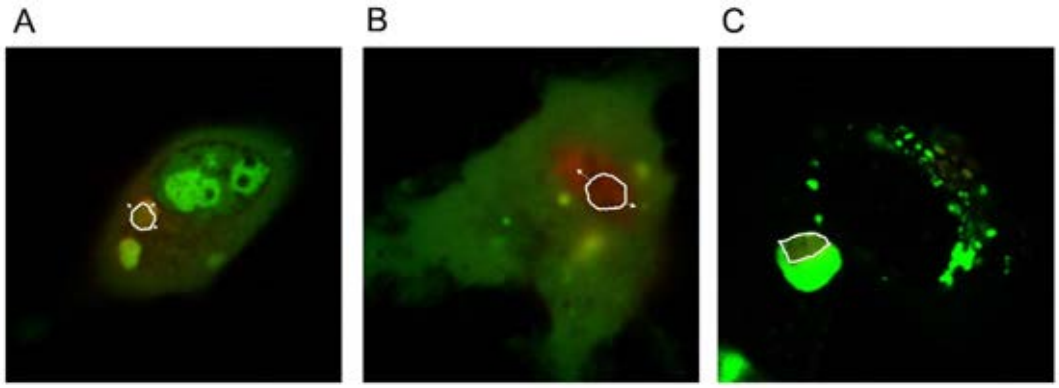

Figure 22. Transfections of ARPE-19 cells with pDendra2-hHsp70 (A and B) and with pDendra2-hp62 (C) constructs. After 24-hour transfections, cells were treated for 24 hours with bafilomycin (50 nM) and MG-132 (5 μM) (panel A) or with MG-132 alone (B andC). The pictures were taken at the moment of UV exposure within the zones drawn with a white line. White arrows indicate the spreading of red colour outside of the exposed spot. Zone diameter = 1μm.

5.2.4 Plasmid Transfection and Confocal Microscopy

The pDendra2 fusion plasmids were transfected into subconfluent cultures of ARPE-19 cells using the ExGen500 in vitro transfection reagent (MBI Fermentas) following manufacturer's instructions. In all transfection experiments for confocal microscopy, ExGen 500 in vitro Transfection Reagent (MBI Fermentas) was used according to the manufacturer's protocol. ARPE-19 cells were cultured in 8-well plates (μ-Slide, ibiTreat, tissue culture treated, Ibidi) to subconfluent density. Thereafter, the pDendra2 fusion plasmids containing 1 μg DNA per well were added, and the cells were incubated for 24 hours. Subsequently, the culture medium was changed and MG-132 (5 μM) and bafilomycin (50 nM) were added for 24 hours. Transfected cells were exposed to UV

radiation (405 nm), which changed the photo-switchable colour of Dendra2 from green to red. Fluorescent images were obtained with a Zeiss Axio Observer inverted microscope (40 × NA 1.3 or 63 × NA 1.4 oil objectives) equipped with the Zeiss LSM 700 confocal module (Carl Zeiss). For live cell imaging, Zeiss XL-LSM S1 incubator with temperature and CO2 controls was utilized. ZEN 2009 software (Carl Zeiss) was used for image processing.

5.3 RESULTS

We recently documented that SQSTM1/p62, a shuttle protein between proteasomal and autophagic clearance, binds permanently in perinuclear aggregates and subsequently undergoes autophagic clearance [Viiri et al. 2013]. Since Hsp70 binds to the same aggregates [16], we wanted to evaluate whether the binding of Hsp70 is a reversible or an irreversible process. First, ARPE-19 cells were exposed to 5 μM concentration of MG-132 for 24 hours, which evoked strong formation of perinuclear protein aggregates (Figure 21) [Ryhänen et al. 2009]. Then pDendra2-hHsp70 fusion plasmid constructwas transfected to the cells and confocal microscopy was used for live cell imaging. The movement of pDendra2-hHsp70 fusion protein was evaluated after photo conversion (Figure 22). We detected that Hsp70 protein moved from the converted area to other parts of the cell, which suggests that the binding of Hsp70 to protein aggregates is reversible. As a comparison, pDendra2-hp62 did not leave the exposed area (Figure 22, panel C) [Viiri et al. 2013].

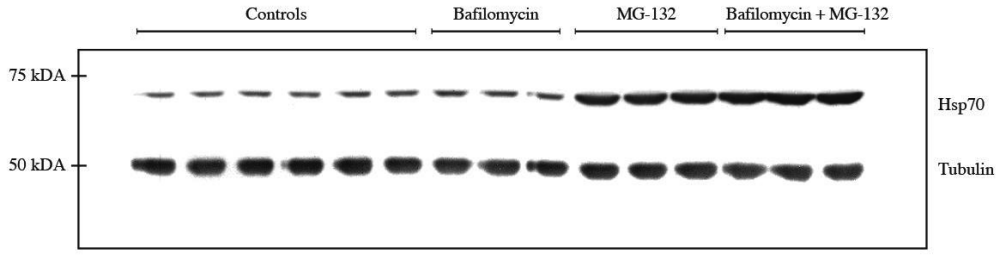

Figure 23. Image from a representative western blot showing the expression of Hsp70 in control ARPE-19 cells and in cells exposed to 5 μM of MG-132 and 50 of nM bafilomycin, together or alone for 24 hours. α-tubulin was used as a loading control.

Bafilomycin is known to inhibit autophagy by preventing the fusion of autophagosomes with lysosomes [Klionsky et al. 2012]. To examine how bafilomycin affects the expression of Hsp70 protein in ARPE-19, the cells were treated either with 50 nM of bafilomycin, 5 μM of MG-132 or both. Thereafter, total protein extracts were analysed for the expression of Hsp70 using the western blotting technique. In contrast to our previous observations with SQSTM1/p62 [Viiri et al. 2013], ARPE-19 cells treated with bafilomycin displayed no changes in Hsp70 protein levels (Figure 23). When the cells were exposed simultaneously to both bafilomycin and MG-132, there was a significant increase in the amount of Hsp70 protein. A similar increase in the levels of Hsp70 was seen in cells treated with MG-132 alone. This suggested that Hsp70 is not degraded by autophagy.

In order to confirm this hypothesis, possible effects of AICAR and serum starvation on the Hsp70 expression under MG-132 stimulation were studied. Induction of autophagy by either way did not change the Hsp70 protein levels (Figure 24). These results support the idea that Hsp70, in contrast to SQSTM1/p62, does not bind permanently to proteasome inhibitor–induced protein aggregates and does not undergo the autophagic clearance.

5.4 DISCUSSION

In the present study, we have shown that the best-known molecular chaperone Hsp70 binds to perinuclear protein aggregates by a reversible mechanism under proteasome inhibition in human retinal ARPE-19 cells. We have recently shown using pDendra2-hLC3 (MAP1LC3A/LC3) and pDendra2-hp62 (SQSTM1/p62) plasmids, with which localisation of the proteins in a cell can be detected at a desired time point, that both LC3 and SQSTM1/p62 disappeared via autophagic clearance in response to the inhibition of proteasomes and the induction of autophagy. The binding of SQSTM1/p62 protein to perinuclear aggregates was observed to be an irreversible process [Klionsky et al. 2012, Viiri et al. 2013]. In contrast to our previous results, we show here by pDendra2-hHsp70 fusion plasmid construction analyses that Hsp70 moves from protein aggregates during proteasome inhibition, indicating reversible binding of Hsp70 to protein aggregates.

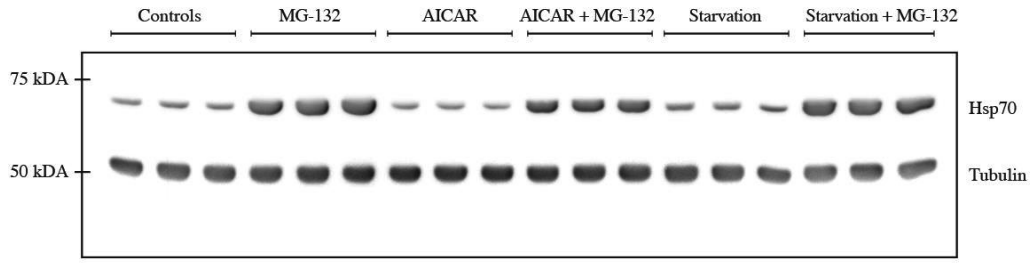

Figure 24. Image from a representative western blot showing the expression of Hsp70 protein in control ARPE-19 cells and in cells exposed to 5 μM of MG-132, 2 mM of AICAR, starvation or simultaneously to 5 μM of MG-132 and 2 mM of AICAR or starvation for 24 hours. α-tubulin was used as a loading control.

Blocking the expression of SQSTM1/p62 rather than Hsp70 using mRNA silencing results in decreased autophagosome formation in ARPE-19 cells [Viiri et al. 2013]. However, both of them had similar cytoprotective capacity under proteasome inhibition. Cytoprotection was obviously involved in the repairing chaperone function of Hsp70, while SQSTM1/p62 regulated the induction of autophagic clearance. Once autophagy was induced during proteasome inhibition, SQSTM1/p62 degradation also became accelerated. In this study, we have shown that the induction of autophagy by AICAR or by starvation, or the inhibition of autophagy by bafilomycin, did not change Hsp70 levels under proteasome inhibition. This indicates that Hsp70 is protected from autophagic clearance.

Hsp70 consists of two major functional domains; the amino-terminal domain that possesses the ATP/ADP binding site as well as the ATPase activity, and the carboxy-

terminal domain, which contains the binding site for substrate peptides [da Silva and Borges 2011]. In the ATP-bound state, substrates can easily bind to and dissociate from Hsp70. When ATP is hydrolysed to ADP, the affinity of a substrate to Hsp70 becomes increased [Bukau and Horwich 1998]. An important feature in the Hsp70's cycle is that chaperone proteins have several co-chaperones that modulate substrate interactions. We found that Hsp70 binds in a reversible manner to proteasome inhibitor–induced protein aggregates. This process might be controlled by the ATP/ADP regulation cycle. Post-translational modifications of Hsp70 such as SUMOylation, ubiquitination or glycosylation may also control the binding activity of Hsp70 to the client proteins in aggresomes and prevent its autophagic clearance [Guinez et al. 2008, Mishra et al. 2009, Janer et al. 2010, Lee et al. 2012, Wang et al. 2013, Yang et al. 2013]. There is evidence that in contrast to SQSTM1/p62, Hsp70 favours proteasomal clearance in certain stress conditions [Lee et al. 2012].

Damage in cellular macromolecules accumulates during aging and tissue degeneration in postmitotic cells, such as RPE cells [Kaarniranta et al. 2013]. It has recently been proposed that declining heat shock response, reduced levels of Hsps, and the resultant loss of protein quality control may exacerbate protein damage during aging [Galderwood et al. 2009, Rodgers et al. 2009, Kinnunen et al. 2012, Klettner et al. 2013]. Molecular Hsp70 chaperone therapy might be a new formulation strategy in the treatment of retinal pigment epithelium and AMD [Klettner 2004]. RPE cells are phagocytic and they can internalise extracellular material as occurs e.g. with photoreceptor outer segments during normal visual cycle. The shed photoreceptor outer segment particles are taken up by RPE via endocytic and phagocytic processes and degraded in lysosomes [Kaarniranta et al. 2013]. In aged RPE cells, however, lysosomal enzyme activity is decreased, which leads to harmful lipofuscin accumulation and reflects the severity of AMD [Krohne et al. 2010a]. In the Hsp70-based therapy, proteins should be targeted to lysosomes due to phagocytic process [Yu et al. 2001]. Interestingly, Hsp70 has been found in lysosomal fractions of RPE cells [Schutt et al. 2002, Ryhänen et al. 2009]. It might be hypothesized that Hsp70 as a molecular chaperone keeps lysosomal enzymes functionally active, prevents lipofuscin accumulation in RPE cells and thereby suppresses the development of AMD [Karlsson et al. 2013]. Hsp70 has also anti-inflammatory capacity [Paimela et al. 2011]. Inflammation is a central hallmark in the pathogenesis of AMD. Therefore, Hsp70 might also prevent inflammatory signalling in RPE cells. The present data importantly show that Hsp70 is protected from lysosomal clearance system and thus provide opportunity to develop its use in protein, drug or laser therapy for the prevention of AMD.

5.5 ACKNOWLEDGEMENTS

Authors thank Mrs Anne Seppänen, Tuomas Paimela MD, medical student Matti Onnela and Henna Paterno, LLB, BA, for technical assistance. This work was supported by the EVO grants of Kuopio University Hospital, the Finnish Cultural Foundation and its North Savo Fund, the Finnish Eye Foundation, the Finnish Funding Agency for

Technology and Innovation, Health Research Council of the Academy of Finland and the Päivikki and Sakari Sohlberg Foundation.

6 Bevacizumab Does not Affect Autophagy Clearance During Proteasomal Inhibition in Human Retinal Pigment Epithelial Cells

ABSTRACT

The most common reason for blindness in developed countries is age-related macular degeneration (AMD) that can be classified into two main categories: the atrophic, or dry form and the exudative, or wet form. The diagnostic difference between dry and wet AMD is the development of choroidal neovascularization in wet AMD. A master regulator in the development of neovascularization is Vascular Endothelial Growth Factor (VEGF) A, which is therapeutically inhibited to treat wet AMD. Current VEGF-antagonists are the Fab-Fragment ranibizumab (Lucentis), the fusion protein aflibercept (Eylea) and the off-label used antibody bevacizumab (Avastin). Due to its low costs, Avastin is largely used worldwide in clinics. Recent findings reveal that proteasomal and lysosomal clearance systems including autophagy have been disturbed in AMD. Failure of autophagy in aged postmitotic cells, including retinal pigment epithelial (RPE) cells, can result in accumulation of aggregate-prone proteins, cellular degeneration and finally, cell death that secondarily lead to photoreceptor damage and visual loss. In this study, we show that bevacizumab does not affect autophagy clearance in ARPE-19 cell during proteasome inhibition and protein aggregation.

6.1 INTRODUCTION

Age-related macular degeneration (AMD) is the most common reason for legal blindness in the developed countries. Phenotypically, AMD can be divided into two main groups: dry (atrophic) and wet (exudative) type and further subdivided into early and late stage disease [Kaarniranta et al. 2013]. The early stage of dry AMD is asymptomatic, although pigment mottling, accumulation of intracellular lysosomal lipofuscin, and extracellular drusen deposits can be detected in ophthalmological examinations. The late stage of dry AMD, also known as geographic atrophy, is characterized by discrete areas of RPE loss and impairment of the overlying retinal photoreceptor cells and severe visual loss [Kinnunen et al. 2012, Klettner et al. 2013]. Today there is no effective treatment for dry AMD, although omega-fatty acid and antioxidants are usually recommended for high risk AMD patients [Kaarniranta and Salminen 2009, Chew et al. 2013]. In wet AMD, aberrant blood vessels sprout from the choroidal capillaries and penetrate through the Bruch's membrane leading to subretinal membranes, hemorrhage, retinal edema and damage to retinal cells. This proliferative process is called choroidal neovascularisation (CNV). Wet AMD results in a rapid loss of vision if not treated. A major factor in the development of

neovascularization is Vascular Endothelial Growth Factor (VEGF) A, which is therapeutically inhibited to treat wet AMD [Klettner 2014]. In addition to its pathological effects, VEGF-A has important physiological functions both systemically and in the retina. Current VEGF-antagonists are the Fab-Fragment ranibizumab (Lucentis), the fusion protein aflibercept (Eylea) and the off-label used antibody bevacizumab (Avastin). In addition, the aptamer pegaptanib (Macugen) is approved for the treatment of AMD, but rarely used. These molecules differ in molecular size and structure which impacts on their pharmacological behavior such as their effects on retinal cells, ocular and systemic clearance, or systemic VEGF-A inhibition. Although all these drugs have been shown to be equally effective in the treatment of wet AMD, the respective therapeutic molecule may have different systemic and/or retinal effects especially after prolonged usage [The CATT Research group 2011, IVAN Study Investigators 2012, Schmidt-Erfurth et al. 2014].

Bevacizumab is a recombinant full-length humanized antibody with a molecular weight of 149-kDa, binding to all VEGF-A isoforms and reducing angiogenesis and vascular permeability. It was originally developed to target pathologic angiogenesis in malignant tumors and approved by the authorities for the treatment of metastatic colorectal cancer [Klettner 2014]. However, mostly because of economic reasons, bevacizumab is widely used intravitreally as an off-label treatment for proliferative eye diseases, such as CNV related to AMD, diabetic macular edema and macular edema caused by retinal vein occlusion. The intravitreal injection of 1.25 mg of bevacizumab has been shown to be comparable in efficacy to the officially approved treatment with ranibizumab. The CATT Study (The Comparison of Age-Related Macular Degeneration Treatment Trials) and IVAN Study (Inhibit VEGF in Age Related Choroidal Neovascularization) compared the relative safety and effectiveness of bevacizumab and ranibizumab in treatment [The CATT Research group 2011, IVAN Study Investigators 2012]. Patients with newly diagnosed exudative AMD were followed up for 2 years, and the results showed similar outcomes using either drug, with bevacizumab showing non-inferiority to ranibizumab.

The half-life in vitreous humour is similar with both compounds - 7 days for bevacizumab and 9 days for ranibizumab, resulting in similar treatment intervals [Drolet et al. 2000, Zhu et al. 2008]. However, the systemic half-life is different, i.e. 20 days for bevacizumab vs. 6 hours for ranibizumab, and the maximum systemic exposure with 1.25mg bevacizumab is 20-690 ng/ml and with 0.5mg ranibizumab 0.8-2.9 ng/ml [Xu et al. 2013]. Since the systemic exposure is lower with ranibizumab, it may be associated with lower systemic toxicity [Schmidt-Erfurth and Pruente 2007]. In fact, it has been shown that intravitreal injections of bevacizumab decrease VEGF levels in blood by up to 117-fold within 1 day and by 4-fold up to 1 month later. This decrease is similar to that achieved with intravenous therapy, and it is possible that intravitreal bevacizumab may suppress baseline physiologic VEGF activity [Matsuyama et al. 2010, Qian et al. 2011]. Furthermore, bevacizumab has been detected and associated with regression of contralateral

proliferative diabetic retinopathy and iris neovascularization in rabbits after intravitreal injection in contralateral eyes [Avery et al. 2006].

In preclinical safety studies with bevacizumab, the compound was shown to be safe in general. In several studies bevacizumab showed no direct cytotoxicity in various cultured ocular cell lines or in cultured retinas [Luthra et al. 2006, Lüke et al. 2007]. Similarly, in short-term in vivo rabbit models, intravitreal bevacizumab did not cause any serious ocular toxicity [Bakri et al. 2006, Shahar et al. 2006]. However, in one study mitochondrial disruption was observed in the photoreceptor inner segments, and proteins associated with apoptosis were detected in the outer plexiform, outer nuclear, and photoreceptor layers [Inan et al. 2007]. In addition, bevacizumab, but not ranibizumab, has been shown to accumulate in the RPE cells, which may reduce heterophagic ability in these cells [Klettner et al. 2009, Klettener et al. 2010].

AMD is a neurodegenerative aggregation disease that shares its cellular pathology with Alzheimer´s disease [Kaarniranta et al. 2011]. Recently, it has been observed that one crucial mechanism behind AMD is impaired proteasomal and lysosomal proteolysis that associates with the accumulation of lipofuscin and drusen [Kaarniranta et al. 2010, Kaarniranta et al. 2013, Viiri et al. 2013]. Autophagy is a basic lysosomal catabolic mechanism which ''self eats'' cellular components which are unnecessary or dysfunctional for the cell [Kaarniranta et al. 2013, Viiri et al. 2013, Kivinen et al. 2014]. Autophagy comprises three intracellular pathways in eukaryotic cells, which are macroautophagy (hereafter referred to as autophagy), microautophagy, and chaperone-mediated autophagy. Autophagy has a key role in normal cellular homeostasis, but it is also triggered as an adaptive response during AMD associated stress conditions [Kaarniranta and Salminen 2009, Klettner et al. 2013]. Autophagy process begins with the formation of isolation membranes called phagophores; these later then become elongated and surround portions of cytoplasm containing oligomeric protein complexes and organelles to form mature double membrane autophagosomes. The autophagosomes fuse with lysosomes and their content is then degraded by lysosomal enzymes. Failure of autophagy in aged postmitotic cells, including RPE cells, can result in accumulation of aggregate-prone proteins, cellular degeneration and finally cell death that secondarily leads to photoreceptor damage and visual loss [Viiri et al. 2010, Viiri et al. 2013]. SQSTM1/p62 (Sequestosome 1) is the best-characterized and ubiquitously expressed autophagy receptor that connects proteasomal clearance with lysosomes [Bjørkøy et al. 2005, Komatsu et al. 2007, Korolchuk et al. 2009b, Viiri et al. 2010, Pankiv et al. 2010]. Alleviation of autophagy is usually accompanied by an accumulation of SQSTM1/p62 mostly in large perinuclear aggregates or inclusion bodies which are also positive for ubiquitin. In this study, we show that bevacizumab does not affect autophagy clearance in ARPE-19 cell during proteasome inhibition and protein aggregation.

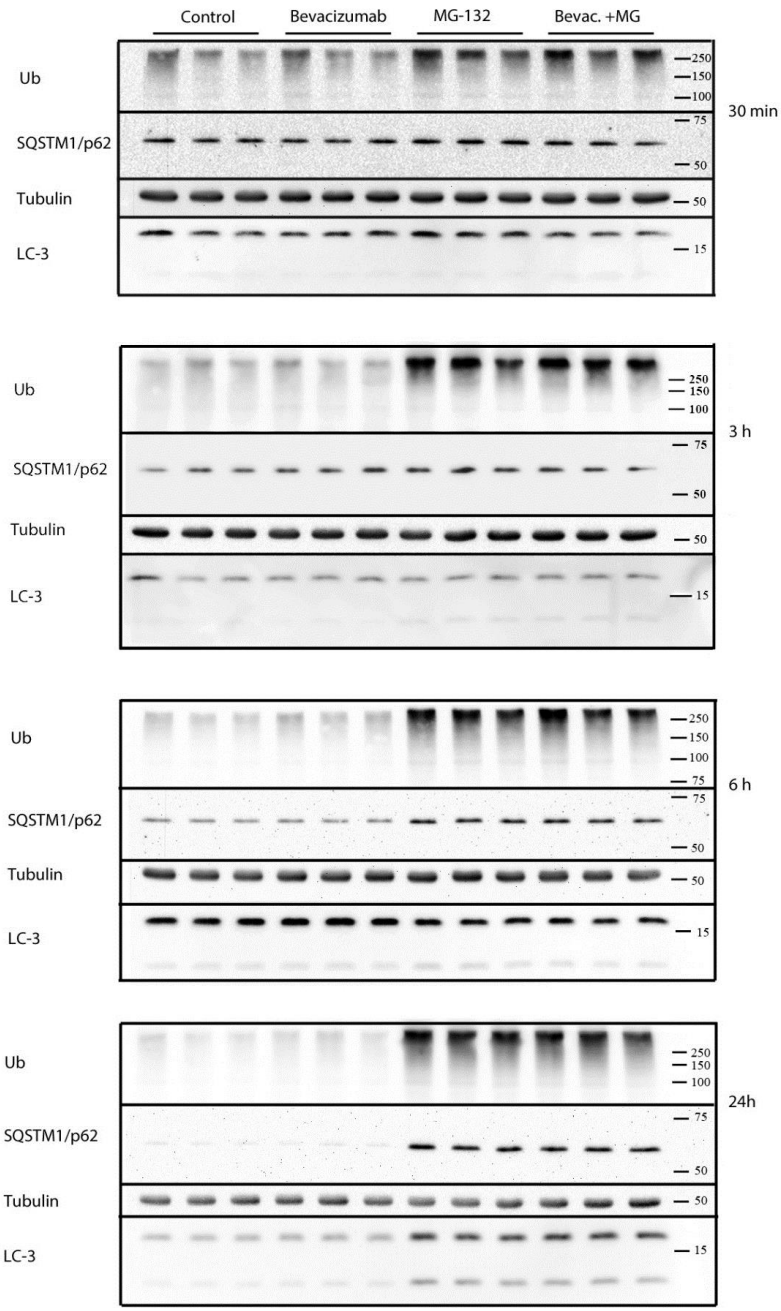

Figure 25. Western blotting from the ARPE-19 cells exposed solely to 0.25 mg/ml bevazicumab or 1 μM MG-132 proteasome inhibitor or combination of bevacizumab and MG-132 for 0.5 hours, 3 hours, 12 hours and 24 hours. α -tubulin was used as a loading control.

6.2 MATERIALS AND METHODS

6.2.1 Cell Culture

ARPE-19 human RPE cells were obtained from the American Type Culture Collection (ATCC). The cells were grown to confluence in a humidified 10% CO2 atmosphere at 37°C in Dulbecco's MEM/Nut MIX F-12 (1:1) medium (Life Technologies, 21331) containing 10% inactivated fetal bovine serum (Hyclone, SV30160-03), 100 units/ml penicillin and 100 mg/ml streptomycin (Lonza, DE17-602E) and 2 mM L-glutamine (Lonza, BE17-605E). The cells were exposed solely to 0.25 mg/ml bevazicumab (Pharmacy of Kuopio University Hospital) or 1 µM MG-132 proteasome inhibitor (Calbiochem, 474790) or combination of bevacizumab and MG-132 for 0.5 hours, 3 hours, 12 hours and 24 hours. Moreover, the cells were exposed solely to 0.25 mg/ml bevazicumab for 1 hour, 4 hours, 1 day, 3 days or 7 days. To prevent autophagy flux, 50 nM bafilomycin A1 (Sigma, B1793) for 1 hour and 4 hours was used.

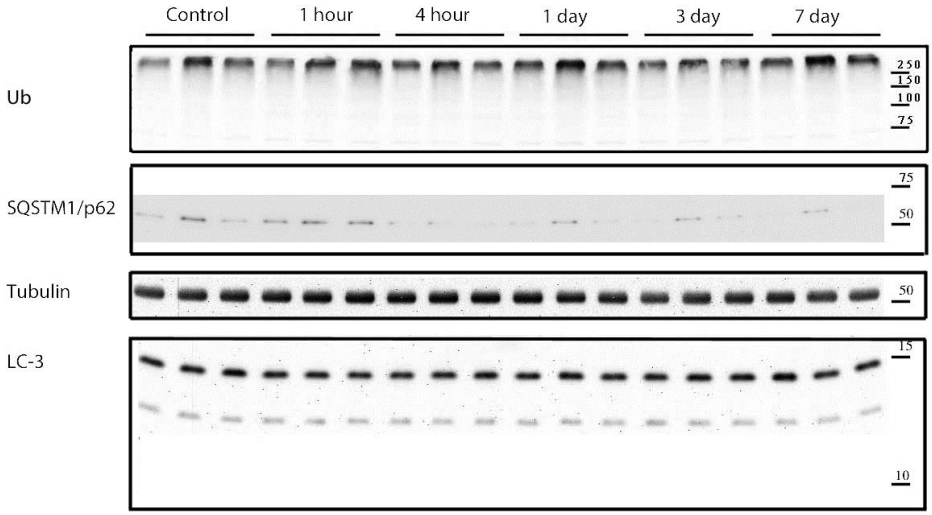

Figure 26. Western blotting from the ARPE-19 cells exposed solely to 0.25 mg/ml bevazicumab or 1 µM MG-132 proteasome inhibitor or combination of bevacizumab and MG-132 for 1 hour, 4 hours, 1 day, 3 days or 7 days. α -tubulin was used as a loading control.

6.2.2 Western Blotting

The whole cell extracts were prepared in M-PER (Mammalian Protein Extraction Reagent, Thermo Scientific, 78501) according to the manufacturer's protocol. Proteins were diluted in 3X sodium dodecyl sulphate (SDS) protein gel loading solution, boiled for 5 minutes, separated on 15% SDS-polyacrylamide gel electrophoresis (SDS-PAGE) and processed following standard procedures. The rabbit polyclonal ubiquitin antibody (DakoCytomation, Z0458) was diluted in 3% milk powder, 0.3% Tween 20/PBS at 1:500. Secondary antibody was diluted in 3% milk powder, 0.3% Tween 20/PBS at 1:20 000. The

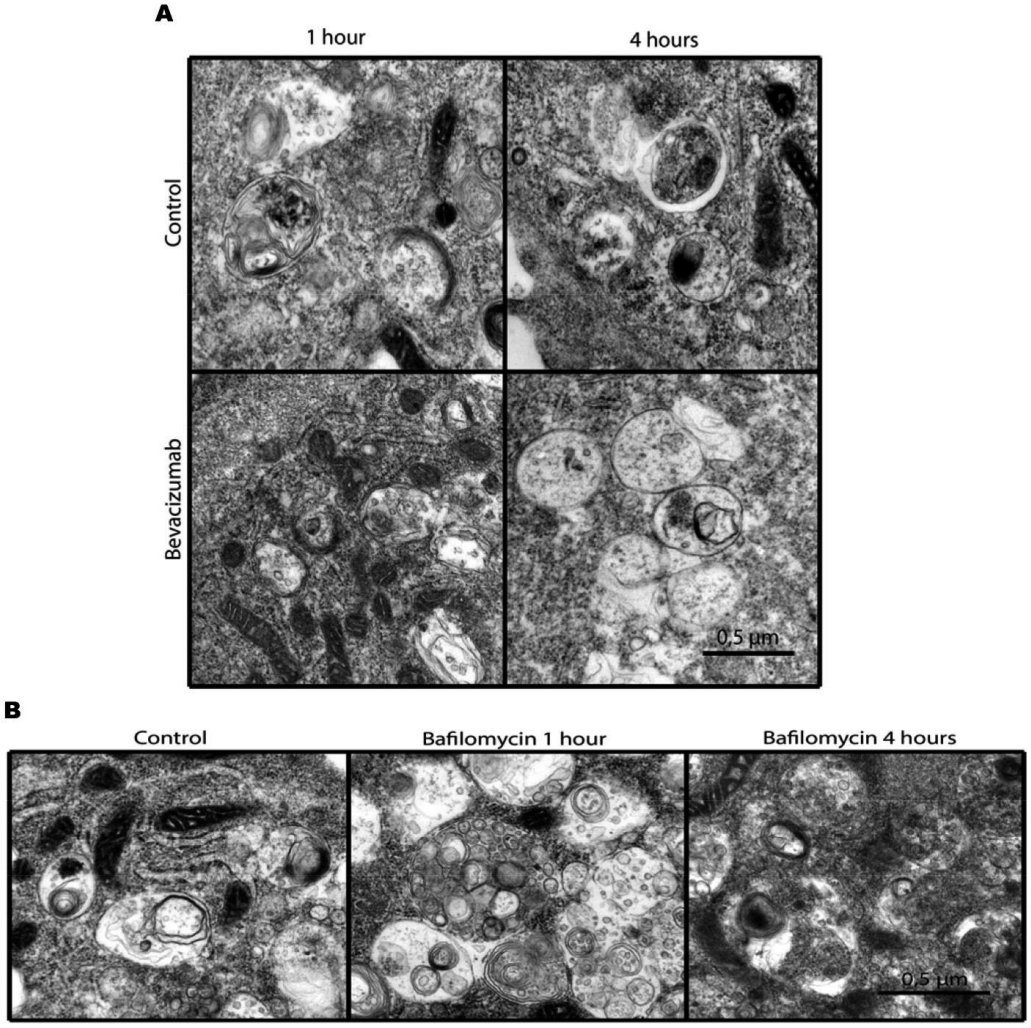

Figure 27. AB Transmission electron microscope pictures from RPE cells predisposed to 0.25 mg/ml bevazicumab for 1 and 4 hours. (A). RPE cells cultured in normal medium were used as a control. To provide a positive control the cells were either non-stressed or exposed to 50 nM bafilomycin for 1 hour or 4 hours (B).

mouse monoclonal anti-SQSTM1/p62 (Santa Cruz Biotech, sc-28359) was diluted in 0.5% bovine serum albumin, 0.3% Tween 20/PBS at 1:1000. Secondary antibody was diluted in 3% milk powder, 0.3% Tween 20/PBS at 1:20 000. The mouse monoclonal anti-α-tubulin (Sigma, T5168) was diluted in 1% milk powder, 0.05% Tween 20/PBS at 1:8000. Secondary antibody was diluted in 1% milk powder, 0.05% Tween 20/PBS at 1:10 000. The rabbit monoclonal anti-MAP1LC3A/LC3 (anti-LC3, microtubule-associated protein light chain 3A) (Cell Signaling, 3868) was diluted in 5% bovine serum albumin, 0.1% Tween 20/PBS at 1:1000. Secondary antibody was diluted in 3% milk powder, 0.1% Tween 20/PBS at 1:2000. The nitrocellulose membranes signals were detected by chemiluminescence. Experiments

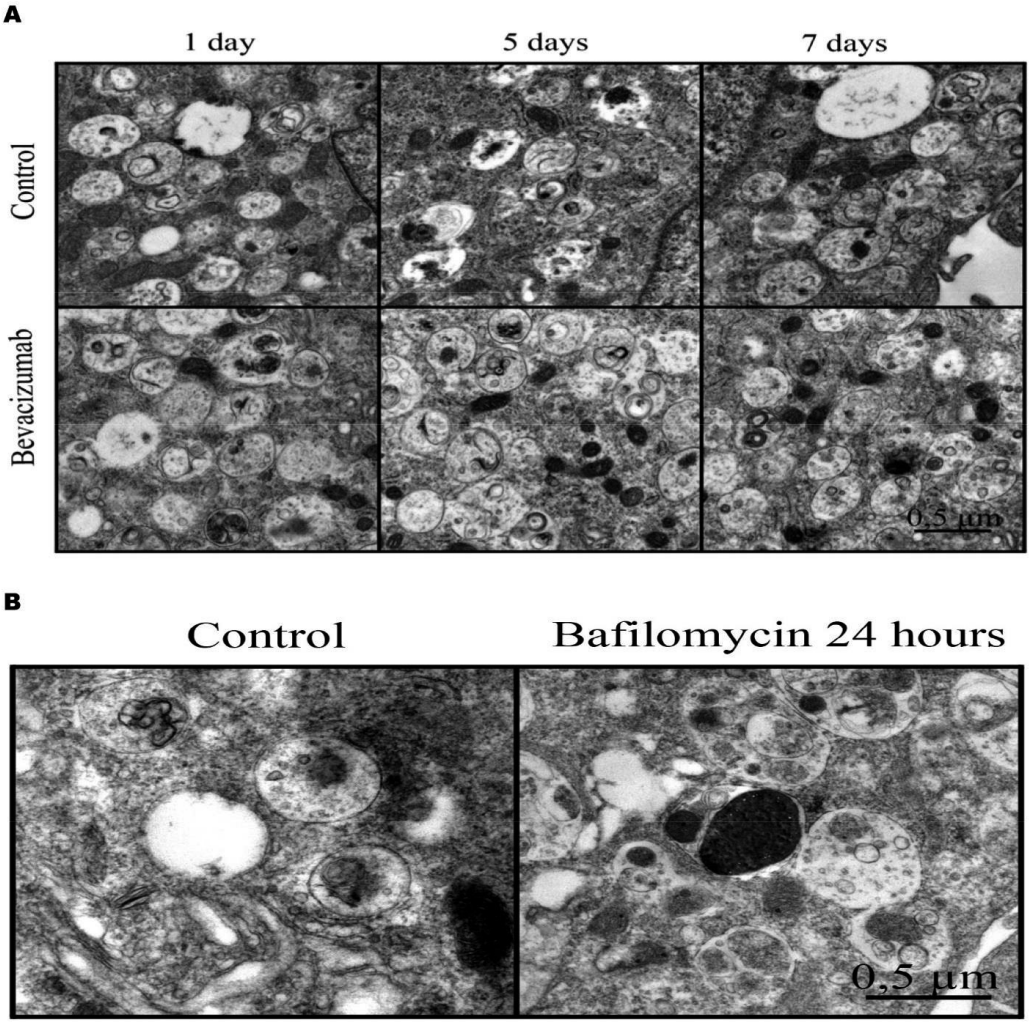

Figure 28. AB Transmission electron microscope pictures from RPE cells predisposed to 0.25 mg/ml bevazicumab for 1, 5 and 7 days. RPE cells cultured in normal medium were used as a control. To provide a positive control the cells were either non-stressed or exposed to 50 nM bafilomycin for 24 hours (B).

were performed in duplicate for each cell preparation and α-tubulin was used to normalize the data. Statistical analysis of western blot data was performed on the densitometric values obtained with the NIH image software 1.61 (downloadable at http://rsb.info.nih.gov/nihimage) and Quantity OneH software.

6.2.3 Transmission Electron Microscopy

ARPE-19 cell culture samples were prefixed with 3% glutaraldehyde in PBS at 4°C overnight. After 3x10 min washing in PBS, the samples were post-fixed in 2 % osmium tetroxide for 60 min, washed with phosphate buffer for 15 min prior to standard ethanol

dehydration, and embedded in Araldite®. Ultrathin (60 nm) sections were cut and examined with a Zeiss 902 electron microscope. Autophagic vesicles were manually counted. Eight cells were randomly selected from each group for counting autophagic vesicles. Statistical analysis was performed using SPSS (v. 19; IBM, SPSS Inc). The significance of differences between control and treated groups was analyzedwith Mann-Whitney U-test. A p-valus of 0.05 or less was considered significant.

6.3 RESULTS

First, the effect of proteasome inhibition on expression of ubiquitin protein conjugates, SQSTM1/p62 and MAP1LC3A/LC3 were studied in human ARPE-19 RPE cells. The cells were either non-stressed or exposed to bevacizumb 0.25mg/ml or 1 μM MG-132, or simultaneously exposed to both of the drugs for 30 min, 3 hours, 6 hours and 24 hours and analyzed by western blotting. A robust increase in the ubiquitin protein conjugates were observed in all the studied time points during proteasome inhibition (Figure 25). Increased SQSTM1/p62 levels were seen at the 6 and 24 hours time points in response to proteasome inhibition. Increased lipidation of the MAP1LC3A/LC3 was detected at the 24 hours time point during proteasome inhibition revealing autophagy activation. No changes of protein levels were found in samples treated solely with bevacizumab which indicates a good tolerability.

To study the long-term effect of bevacizumab (0.25 mg/ml) on the expression of ubiquitin protein conjugates, SQSTM1/p62 and MAP1LC3A/LC3, the cells were either non-stressed or exposed to bevacizumab for 1 hour, 4 hours, 1 day and 7 days and analyzed by western blotting. Bevacizumab did not change the expression levels of any of the proteins studied (Figure 26).

The ultrastructure and amount of autophagosomes were examined using transmission electron microscopy. Neither in control or in 0.25 mg/ml bevacizumab cells treated for 1 hour or 4 hours, cellular abnormalities or changes in autophagosomes were observed (Figure 27A, Table 2). Bafilomycin is known to be an autophagy inhibitor preventing the fusion of autophagosomes and lysosomes, but robustly increasing the amount of autophagosomes [Klionsky et al. 2012, Viiri et al. 2013]. To provide a positive control, the cells were either non-stressed or exposed to 50 nM bafilomycin for 1 hour or 4 hours. As expected, there was a clear statistically significant difference between control and bafilomycin groups studied; $p>0.01$ (Figure 27B, Table 3). We did not observe cellular abnormalities or changes in autophagosomes for a long time exposure up to seven days with bevacizumab (Figure 28A, Table 4). However, when cells were exposed to 50 nM bafilomycin, already at 24 hours a clear statistically significant difference between control and bafilomycin groups studied could be observed; $p>0.001$ (Figure 28B, Table 5).

Table 2. Bevacizumab exposure, short. Autophagosomes in ARPE-19 cells exposed to bevacizumab 0.25 mg/ml for 1 and 4 hours. Control cells were cultured in normal medium. Autophagosomes were calculated from pictures taken with a transmission electron microscope. There was no statistically significant difference between any of the groups studied ($p>0.1$). MA = mean value, SD = standard deviation, N = samples analyzed.

	N	**MA**	**SD**
Control	12	3,33	2,06
1 hour	17	4,35	2,35
4 hours	10	3,60	1,07

Table 3. Bafilomycin exposure, short. Autophagosomes in ARPE-19 cells exposed to bafilomycin 50 mM for 1 hour and 4 hours. Control cells were cultured in normal medium. Autophagosomes were calculated from pictures taken with a transmission electron microscope. There was a clear statistically significant difference between control and bafilomycin groups studied ($p<0.001$). MA = mean value, SD = standard deviation, N = samples analyzed.

	N	**MA**	**SD**
Control	12	3,33	2,06
1 hour	11	7,36	2,29
4 hours	9	8,00	2,06

Table 4. Bevacizumab exposure, long. Autophagosomes in ARPE-19 cells exposed to bevacizumab 0.25 mg/ml for 1 day, 5 days and 7 days. Control cells were cultured in normal medium. Autophagosomes were calculated from pictures taken with a transmission electron microscope. There was no statistically significant difference between any of the groups studied ($p>0.1$). MA = mean value, SD = standard deviation, N = samples analyzed.

	N	**MA**	**SD**
Control	41	6,34	3,47
1 day	42	5,90	2,83
3 days	42	7,00	3,15
7 days	50	6,46	2,83

Table 5. Bafilomycin exposure, long. Autophagosomes in ARPE-19 cells exposed to bafilomycin 50 mM for 24 hours. Control cells were cultured in normal medium. Autophagosomes were calculated from pictures taken with a transmission electron microscope. There was a high statistically significant difference between the groups studied ($p<0.0001$). MA = mean value, SD = standard deviation, N = samples analyzed.

	N	**MA**	**SD**
Control	41	6,34	3,47
Bafilomycin	28	18,29	7,29

6.4 DISCUSSION

We show that bevacizumab does not affect autophagy clearance in ARPE-19 cells during accumulation of intracellular protein aggregates and proteasome inhibition. Moreover, in contrast to bafilomycin, bevacizumab does not affect autophagy during short or long time exposures. Our observations reveal that bevacizumab is well tolerated by RPE cells and does not disturb the crucial autophagy clearance system.

In human AMD donor samples both accumulations of autophagic markers and decreased lysosomal activity can be observed [Wang et al. 2009c]. Furthermore, an effective autophagic clearance system has recently been documented in human RPE cells [Ryhänen et al. 2009, Wang et al. 2009b, Kurz et al. 2009, Viiri et al. 2010, Viiri et al. 2013]. Indicating a declined proteolysis in RPE cells during aging, lipofuscin accumulates in lysosomes and drusen between Bruch´s membrane and RPE cell layer [Krohne et al. 2010a, Kaarniranta et al. 2013]. Lipofuscin is a toxic compound in RPE cells which promotes the damage of mitochondria and misfolding of intracellular proteins, creating an additional oxidative stress in the RPE cells [Shamsi and Boulton 2001, Kaarniranta et al. 2010]. When autophagy flux is inhibited by lysosome inhibitors, such as bafilomycin, it induces autophagosome formation but does not increase lysosomal proteolysis due to the decreased lysosomal enzyme activity. With both short and long term exposure, bafilomycin evoked an intense autophagosome formation, in parallel with autophagy receptor SQSTM1/p62 accumulation [Viiri et al. 2013]. Bevacizumab did not change SQSTM1/p62 expression levels confirming that there is no detrimental effect on autophagy clearance.

Ranibizumab, aflibercept and bevacizumab have been shown to be well-tolerated and they have equal efficacy in the treatment outcomes for wet AMD [Klettner and Roider 2008, The CATT Research Group 2011, IVAN Study Investigators 2012, Schmidt-Erfurth et al. 2014]. These molecules differ in molecular size, structure, binding activity and binding targets which may result in different effects at the cellular level [Klettner 2014]. At concentrations used in clinical practice, there are no toxic effects on retinal pigment epithelial cells, neural retina, or endothelial cells in vitro [Luthra et al. 2006, Spitzer et al. 2007, Miguel et al. 2012, Luthra et al. 2013, Schnichels et al. 2013]. However, bevacizumab exposure has been documented to decrease in mitochondrial activity in both the proliferating and non-proliferating endothelial cells in vitro [Luthra et al. 2013]. This suggests a selective action of bevacizumab on endothelial cells. Moreover, bevacizumab may accumulate in RPE cells, decrease heterophagy and exert pro-fibrotic effects on human RPE cells [Klettner e al. 2009, Klettner et al. 2010, Chen et al. 2012, Kaarniranta et al. 2013]. These effects of bevacizumab can be considered as complications that may affect long-term bevacizumab treatment results. All those detrimental effects may be anticipated to affect autophagy, a key proteostasis regulator, in normal cellular homeostasis, but also an adaptive response during AMD associated stress conditions [Kaarniranta and Salminen

2009, Klettner et al. 2013]. In our study, we were not able to show any effects of bevacizumab on autophagy regulation. In that aspect, bevacizumab might be considered as a safe drug in the regulation of cellular proteostasis. Comparable studies with ranibizumab and aflibercept on autophagy regulation would be interesting to carry out.

6.5 ACKNOWLEDGEMENTS

This study was supported by VTR grants of Kuopio University Hospital, the Finnish Cultural Foundation and its North Savo Fund, the Finnish Eye Foundation, the Finnish Funding Agency for Technology and Innovation, Health Research Council of the Academy of Finland, Päivikki and Sakari Sohlberg Foundation, the John von Neumann Fellowship, the University of Debrecen (RH/885/2013) and the Deutsche Forschungsgemeinschaft (KL 2425/2-1). We thank Mrs Anne Seppänen, Marion Kölln and Katrin Neblung-Masuhr for technical assistance.

8 General Discussion

8.1 SUMMARY

In the developed countries, common vision-threatening conditions such as cataracts, glaucomas and refractive errors can be nowadays efficiently treated. Thus, age-related macular degeneration is the leading cause of irreversible blindness. Pathophysiologically, AMD is associated with oxidative stress and chronic inflammation [Jarret and Boulton 2012, Ambati et al. 2013, Piippo et al. 2014]. However, there is increasing evidence suggesting that dysfunctional cellular proteostasis ultimately leads to protein aggregation and contributes to the development of AMD. The dysregulation of autophagy has a crucial role in this process as it predisposes the RPE to protein aggregation [Mitter et al. 2014].

RPE cells have an efficient autophagic protein clearance system [Ryhänen et al. 2009]. When treated with a lysosomal inhibitor, bafilomycin, autophagosome formation and SQSTM1/p62 accumulation are observed indicating the presence of dysfunctional autophagy [Viiri et al. 2010]. As we demonstrated, this accumulation of SQSTM1/p62 is not detected when the post-trancriptional factor ELAVL1/HuR is removed. Further, if there is proteasome inhibition, then the administration of AICAR (*5-aminoimidazole-4-carboxamide ribonucleotide*) activated autophagy clearance and a decrease of SQSTM1/p62 levels was observed. In addition, in this experiment SQSTM1/p62 was localized within perinuclear aggregates, indicating that SQSTM1/p62 is cleared by autophagocytosis. Thus it is proposed SQSTM1/p62 can be used as a marker for impaired autophagy [Publication I].

We observed increased levels of SQSTM1/p62 in macular regions of human cadaver samples. Perimacular and peripheral areas of cadaver samples (the internal control) and age-matched controls did not show any signs of an increase in SQSTM1/p62 levels. We did detect age-related changes (e.g. drusen) in the perimacular and peripheral areas. Interestingly, ubiquitin upregulation was observed in those areas as well as in macular areas and no differences between these groups were noted. This indicates that these regions still have an active and normally functioning UPP (*Ubiquitin-proteasome pathway*) system. Macular regions are subjected to light induced damage and are more metabolically active compared to the peripheral regions due to their higher concentration of light receptor cells. Thus, a dysregulation of autophagy may primarily affect these regions, especially in conditions when other systems controlling cellular proteostasis, such as the functions of Hsps, are unable to cope with the amounts of damaged proteins. Our findings suggest that impaired autophagy may have a substantial role in the pathogenesis of AMD [Publication I].

Molecular chaperones are the first line of defence against the harmful proteins generated by cellular stress. We studied the relationship of the chaperone Hsp70 and autophagocytosis *in vitro*. Using the same methods as applied in Publication I, we demonstrated that Hsp70 did not undergo autophagic clearance during UPP inhibition

and that its levels in cells were not affected by proteasome inhibition or inhibition of autophagy. Thus, it is concluded that Hsp70 is protected from autophagic clearance and exerts a cytoprotective role that is not connected to UPP or LPP. As Hsps are known to mediate autophagy and regulate inflammatory responses (e.g. by participating in cytokine signal transduction) [Moseley 1998, Kaarniranta et al. 2009b, Yang et al. 2009], it is possible that they could be a therapeutic target in AMD and perhaps also in similar neurodegenerative diseases, such as AD [Klettner 2004]. Upregulation of Hsp70 either by gene, drug or laser therapy may activate autophagy of RPE cells, maintain lysosomal enzymes functional and thus prevent protein aggregation [Karlsson et al. 2013, Publication II].

In Publication III, we evaluated the effect of the current standard-of-care for wet AMD i.e. aVEGF-therapy agent, bevacizumab [Käypä hoito: Kostea silmänpohjan ikärappeuma 2016 (Finnish Current Care Guideline: Wet AMD 2016)] on the autophagy activity of RPE cells. It was noted that bevacizumab did not exert any effect on autophagy clearance during UPP inhibition or accumulation of protein aggregates indicating that this agent was not altering the autophagic activity of RPE cells. We also compared a lysosomal inhibitor, bafilomycin, and bevacizumab with both short and long-term exposures. Our data suggests that bevacizumab does not disturb autophagic clearance of RPE cells, which supports bevacizumab´s safe use in AMD at the cellular level [Publication III].

To date several potential animal models for AMD have been introduced [Pennesi et al. 2012]. The problem is that their phenotype usually only encompasses a part of the features found in AMD, e.g. excess oxidative stress. We studied the presence of a proteasome marker ubiquitin and two autophagy markers SQSTM1/p62 and Beclin-1 in the eyes of collagen 18 knock-out mice. We observed that these mice showed evidence of dysfunctional autophagic flux, indicating thath these animals may represent a novel model for AMD. Interestingly, we made a novel finding, the detection of SQSTM1/p62 immunostaining in the extracellular space of RPE cells. It is possible that the massive protein aggregation observed with decreased autophagy activity leads to the export of proteins in to the extracellular space by exosomal transportation as a final attempt to maintain cellular homeostasis [Publication IV]. Alternatively, this may due to apoptosis or it may be a novel and still unknown route of cell signalling between individual RPE cells. Further studies will be necessary to clarify these cellular events.

8.2 LIMITATIONS OF THE STUDY

We mostly used RPE cell cultures and animal models in these studies. AMD in humans takes years, even decades, to develop whereas cell cultures might only live for days or weeks. In addition, the most widely used experimental animals do not have a macula. While experiments conducted in cells or experimental animals can provide insights into the mechanisms behind different pathological conditions in controlled environments, it is obvious that these results obtained cannot be unconditionally extrapolated to physiology of human vision or to the pathophysiology of AMD. Due to this fact, there is no consensus of the fundamental pathological feature behind AMD.

Since other aVEGF agents are also on the market (ranibizumab and aflibercept), it would have been interesting to incorporate these compounds into the study design. A similar study which utilized fibroblasts present in CNV found that four aVEGF therapeutic agents (ranibizumab, bevacizumab, pegaptanib, and aflibercept) could inhibit cellular proliferation but showed higher apoptotic activity dose-dependently. Interestingly, there was the appearance of vacuoles in the cytoplasms and increased levels of LC3 I and II indicative of the induction of autophagy [Lytvynchuk et al. 2015]. As autophagy has a role in maintaining cellular homeostasis and in caspase-independent cellular death [Lin and Baehrecke 2015], this finding may be evidence that there had been induction of autophagic death in these cells. Clearly, further studies with RPE cells should be conducted.

Only 8 cadaver samples from AMD patients were used in this study and with the *Col18a1*$^{-/-}$ mice we also faced difficulties with obtaining sufficient sample materials. Human specimes are hard to obtain due to legislative and ethical reasons. We received the harvested murine eyes prefixed. Unfortunately, there were some problems with the fixation, leading to some samples being damaged.

To further evaluate the possibilities of *Col18a1*$^{-/-}$ mice as an AMD model, a quantitative analysis of the proteins of interest by Western blotting and mRNA quantification would have provided further information. Unfortunately, *Col18a1*$^{-/-}$ cell lines are not commercially available. We considered but then rejected the possibility of microsurgically isolating the RPE from these mice. Microsurgical isolation, even if performed extremely carefully, would invariably lead to the presence of some extra (i.e. non-RPE) tissue in the sample leading to experimental artefacts in any data. Information about the presence of the proteins of interest from patients with Knobloch syndrome would also provide additional information about the applicability of our findings.

8.3 FUTURE DIRECTIONS

At present, we can only offer treatment to about one in ten AMD patients and even in these cases, the treatment is not curative. A fundamental comprehension of the pathogenesis of AMD is needed in order to develop effective and curative treatments.

The current data indicates that a dysfunction of autophagy is an essential component in the pathogenesis AMD. The information gathered in this thesis project will hopefully act as a springboard for future studies with larger sample volumes allowing more extensive assay of relevant targets. Clearly more data from studies utilizing human samples would be especially illuminating.

To end on a positive note, several trials with promising therapeutics are currently in clinical trials and hopefully at least some of them will emerge as future therapies for AMD.

9 Conclusions

I SQSTM1/p62 is a good marker of impaired autophagy. Impaired autophagy seems to have a great role in AMD pathology.

II Cellular chaperone Hsp70 is not degraded by autophagy and it could be used as a therapy target in the treatment of AMD.

III The current standard-of-care for wet AMD (bevacizumab) does not interfere with autophagy in any level.

IV Collagen XVIII total knock-out mouse with it´s AMD-like changes in the RPE is a novel but a potential model for AMD.

10 References

Abdelmohsen K, Srikantan S, Kuwano Y, Gorospe M. miR-519 reduces cell proliferation by lowering RNA-binding protein HuR levels. Proc Natl Acad Sci U S A. 2008;105:20297–302.

Abdelmohsen K, Srikantan S, Yang X, et al. Ubiquitin-mediated proteolysis of HuR by heat shock. EMBO J. 2009;28:1271–82.

Age-Related Eye Disease Study Research Group. Risk factors associated with age-related macular degeneration. A case-control study in the age-related eye disease study: Age-Related Eye Disease Study Report Number 3. Ophthalmology. 2000; 107(12):2224-32.

Age-Related Eye Disease Study Research Group. A randomized, placebo-controlled, clinical trial of high-dose supplementation with vitamins C and E and beta carotene for age-related cataract and vision loss: AREDS report no. 9. Arch Ophthalmol. 2001; 119(10):1439-52.

Age-Related Eye Disease Study 2 Research Group. Lutein + zeaxanthin and omega-3 fatty acids for age-related macular degeneration: the Age-Related Eye Disease Study 2 (AREDS2) randomized clinical trial. JAMA. 2013; 309(19):2005-15. doi: 10.1001/jama.2013.4997.

Ahlberg J, Marzella L, Glaumann H. Uptake and degradation of proteins by isolated rat liver lysosomes. Suggestion of a microautophagic pathway of proteolysis. Lab Invest. 1982; 47(6):523-32.

Aikio M, Hurskainen M, Brideau G, et al. Collagen XVIII short isoform is critical for retinal vascularization, and overexpression of the Tsp-1 domain affects eye growth and cataract formation. Invest Ophthalmol Vis Sci. 2013;54(12):7450-62. doi: 10.1167/iovs.13-13039.

Akeo K, Curran SA, Dorey CK. Superoxide dismutase activity and growth of retinal pigment epithelial cells are suppressed by 20% oxygen in vitro. Curr Eye Res. 1988;7(10):961-7.

Algvere PV, Seregard S. Age-related maculopathy: pathogenetic features and new treatment modalities. Acta Ophthalmologica Scandinavica. 2002; 80:136-43.

Algvere PV, Kvanta A, Seregard S. Drusen maculopathy: a risk factor for visual deterioration. Acta Ophtalmol. 2016. doi: 10.1111/aos.13011.

Amadio M, Scapagnini G, Laforenza U, et al. Post-transcriptional regulation of HSP70 expression following oxidative stress in SH-SY5Y cells: the potential involvement of the RNA-binding protein HuR. Curr Pharm Des. 2008;14:2651–8.

Amadio M, Pascale A, Wang J, et al. nELAV proteins alteration in Alzheimer's disease brain: a novel putative target for amyloid-beta reverberating on AbetaPP processing. J Alzheimers Dis. 2009;16:409–19.

Ambati J, Anand A, Fernandez S, et al. An animal model of age-related macular degeneration in senescent Ccl-2- or Ccr-2-deficient mice. Nat Med. 2003; 9(11):1390-7.

Ambati J, Atkinson JP, Gelfand BD. Immunology of age-related macular degeneration. Nat Rev Immunol. 2013; 13(6):438-51. doi: 10.1038/nri3459.

Ardeljan D, Chan CC. Aging is not a disease: distinguishing age-related macular degeneration from aging. Prog Retin Eye Res. 2013; 37:68-89. doi: 10.1016/j.preteyeres.2013.07.003.

Arjamaa O, Nikinmaa M, Salminen A, Kaarniranta K. Regulatory role of HIF-1alpha in the pathogenesis of age-related macular degeneration (AMD). Ageing Res Rev. 2009; 8(4):349-58. doi: 10.1016/j.arr.2009.06.002.

Arjamaa O, Minn H. Resistance, not tachyphylaxis or tolerance. Br J Ophtalmol. 2012; 96(8):1153-4. doi: 10.1136/bjophthalmol-2012-301823

Aronson JF. Human retinal pigment cell culture. In Vitro. 1983;19(8):642-50.

Arstila AU, Trump BF. Autophagocytosis: origin of membrane and hydrolytic enzymes. Virchows Arch B Cell Pathol. 1969; 2(1):85-90.

Avery RL, Pearlman J, Pieramici DJ, et al. Intravitreal bevacizumab (Avastin) in the treatment of proliferative diabetic retinopathy. Ophthalmology. 2006;113(10):1695.e1-15.

Bakri SJ, Cameron JD, McCannel CA, et al. Absence of histologic retinal toxicity of intravitreal bevacizumab in a rabbit model. Am J Ophthalmol. 2006;142(1):162-4

Beatty S, Koh H, Phil M, et al. The role of oxidative stress in the pathogenesis of age-related macular degeneration. Surv Ophthalmol. 2000; 45: 115–134.

Becker S, Jayaram H, Limb GA. Recent Advances towards the Clinical Application of Stem Cells for Retinal Regeneration. Cells. 2012;1(4):851-73. doi: 10.3390/cells1040851.

Behl T, Kotwani A. Possible role of endostatin in the antiangiogenic therapy of diabetic retinopathy. Life Sci. 2015;135:131-7. doi: 10.1016/j.lfs.2015.06.017.

Bellhorn RW, King CD, Aguirre GD, et al. Pigmentary abnormalities of the macula in rhesus monkeys: clinical observations. Invest Ophthalmol Vis Sci. 1981 Dec;21(6):771-81.

Bergmann M, Schütt F, Holz FG, Kopitz J. Inhibition of the ATP-driven proton pump in RPE lysosomes by the major lipofuscin fluorophore A2-E may contribute to the pathogenesis of age-related macular degeneration. FASEB J. 2004; 18(3):562-4.

Bhutto IA, Kim SY, McLeod DS, et al. Localization of collagen XVIII and the endostatin portion of collagen XVIII in aged human control eyes and eyes with age-related macular degeneration. Invest Ophthalmol Vis Sci. 2004;45(5):1544-52.

Biarnés M, Monés J, Alonso J, Arias L. Update on geographic atrophy in age-related macular degeneration. Optom Vis Sci. 2011; 88(7):881-9. doi: 10.1097/OPX.0b013e31821988c1.

Bierhaus A, Humpert PM, Morcos M, et al. Understanding RAGE, the receptor for advanced glycation end products. J Mol Med. 2005; 83: 876–886.

Bird AC, Bressler NM, Bressler SB, et al. An international classification and grading system for age-related maculopathy and age-related macular degeneration. The International ARM Epidemiological Study Group. Surv Ophthalmol. 1995; 39(5):367-74.

Bird AC. Therapeutic targets in age-related macular disease. J Clin Invest. 2010; 120(9):3033-41. doi: 10.1172/JCI42437.

Bjørkøy G, Lamark T, Brech A, et al. p62/SQSTM1 forms protein aggregates degraded by autophagy and has a protective effect on huntingtin-induced cell death. J Cell Biol. 2005;171:603–14.

Blasiak J, Petrovski G, Veréb Z, et al. Oxidative stress, hypoxia, and autophagy in the neovascular processes of age-related macular degeneration. Biomed Res Int. 2014; 2014:768026. doi: 10.1155/2014/768026.

Bonelli MA, Alfieri RR, Desenzani S, et al. Proteasome inhibition increases HuR level, restores heat-inducible HSP72 expression and thermotolerance in WI-38 senescent human fibroblasts. Exp Gerontol. 2004;39:423–32.

Boulton M, Moriarty P, Jarvis-Evans J, Marcyniuk B. Regional variation and age-related changes of lysosomal enzymes in the human retinal pigment epithelium. Br J Ophthalmol. 1994; 78(2):125-9.

Bowes Rickman C, Farsiu S, Toth CA, Klingeborn M. Dry age-related macular degeneration: mechanisms, therapeutic targets, and imaging. Invest Ophthalmol Vis Sci. 2013; 54(14):ORSF68-80. doi: 10.1167/iovs.13-12757.

Boyault C, Zhang Y, Fritah S, et al. HDAC6 controls major cell response pathways to cytotoxic accumulation of protein aggregates. Genes Dev. 2007;21(17):2172-81.

Braak H, Thal DR, Tredici KD. Nerve cells immunoreactive for p62 in select hypothalamic and brainstem nuclei of controls and Parkinson's disease cases. J Neural Transm. 2011;118:809–819.

Brechner RJ, Rosenfeld PJ, Babish JD, Caplan S. Pharmacotherapy for neovascular age-related macular degeneration: ananalysis of the 100% 2008 Medicare fee-for-service Part B claims file. Am J Ophthalmol. 2011; 151:887–895e1.

Bressler NM. Antiangiogenic approaches to age-related macular degeneration today. Ophthalmology 2009; 116(10):S15–23.
Bukau, B, Horwich, AL. The Hsp70 and Hsp60 chaperone machines. Cell. 1998; 92:351–366.

Brunk UT and Terman A. Lipofuscin: mechanisms of age-related accumulation and influence on cell function. Free Radic Biol Med. 2002;33:611-9. doi:10.1016/S0891-5849(02)00959-0

Buschini E, Piras A, Nuzzi R, Vercelli A. Age related macular degeneration and drusen: neuroinflammation in the retina. Prog Neurobiol. 2011; 95(1):14-25. doi: 10.1016/j.pneurobio.2011.05.011.

Caglayan AO, Baranoski JF, Aktar F, et al. Brain malformations associated with Knobloch syndrome--review of literature, expanding clinical spectrum, and identification of novel mutations. Pediatr Neurol. 2014;51(6):806-813.e8. doi: 10.1016/j.pediatrneurol.2014.08.025.

Cahn RD and Cahn MB. Heritability of cellular differentiation: clonal growth and expression of differentiation in retinal pigment cells in vitro. Proc Natl Acad Sci. 1966;55(1):106-14.

Calderwood SK, Murshid A, Prince T. The shock of aging: molecular chaperones and the heat shock response in longevity and aging–a mini-review. Gerontology. 2009;55:550-558.

Cashman SM, Desai A, Ramo K, Kumar-Singh R. Expression of complement component 3 (C3) from an adenovirus leads to pathology in the murine retina. Invest Ophthalmol Vis Sci. 2011 May 18;52(6):3436-45. doi: 10.1167/iovs.10-6002.

Casten RJ, Rovner BW, Tasman W. Age-related macular degeneration and depression: a review of recent research. Curr Opin Ophthalmol. 2004; 15:181–3.

CATT Research Group, Martin DF, Maguire MG, Ying GS, et al. Ranibizumab and bevacizumab for neovascular age-related macular degeneration. N Engl J Med. 2011;364:1897–1908.

Chen CL, Liang CM, Chen YH, et al. Bevacizumab modulates epithelial-to-mesenchymal transition in the retinal pigment epithelial cells via connective tissue growth factor up-regulation.Acta Ophthalmol. 2012;90(5):e389-98. doi: 10.1111/j.1755-3768.2012.02426.x

Cheung LK and Eaton A. Age-Related Macular Degeneration. Pharmacotherapy 2013; 33(8):838–55. doi: 10.1002/phar.1264.

Chew EY, Clemons TE, Agrón E, et al., (Age-Related Eye Disease Study Research Group). Long-term effects of vitamins C and E, β-carotene, and zinc on age-related macular degeneration: AREDS report no. 35. Ophthalmology. 2013;120(8):1604-11.e4. doi: 10.1016/j.ophtha.2013.01.021.

Ciechanover A. Intracellular protein degradation: from a vague idea thru the lysosome and the ubiquitin-proteasome system and onto human diseases and drug targeting. Biochim Biophys Acta. 2012; 1824(1):3-13. doi: 10.1016/j.bbapap.2011.03.007.

Cleasby GW, Nakanishi AS, Norris JL. Prophylactic photocoagulation of the fellow eye in exudative senile maculopathy. A preliminary report. Mod Probl Ophthalmol. 1979; 20:141-7.

Coffey PJ, Gias C, McDermott CJ, et al. Complement factor H deficiency in aged mice causes retinal abnormalities and visual dysfunction. Proc Natl Acad Sci U S A. 2007 Oct 16;104(42):16651-6.

Congdon N, O'Colmain B, Klaver CC, et al.; Eye Diseases Prevalence Research Group. Causes and prevalence of visual impairment among adults in the United States. Arch Ophthalmol. 2004 Apr; 122(4):477-85.

Cousins SW, Espinosa-Heidmann DG, Alexandridou A, et al. The role of aging, high fat diet and blue light exposure in an experimental mouse model for basal laminar deposit formation. Exp Eye Res. 2002; 75(5):543-53.

da Silva KP, Borges JC. The molecular chaperone Hsp70 family members function by a bidirectional heterotrophic allosteric mechanism. Protein Pept Lett. 2011; 18:132-142.

De Los Rios P, Ben-Zvi A, Slutsky O, et al. Hsp70 chaperones accelerate protein translocation and the unfolding of stable protein aggregates by entropic pulling. Proc Natl Acad Sci U S A. 2006 Apr 18;103(16):6166-71.

de Jong PT. Age related macular degeneration. N Engl J Med. 2006;355:1474–1485.

Decanini A, Nordgaard CL, Feng X, et al. Changes in select redox proteins of the retinal pigment epithelium in age-related macular degeneration. Am J Ophthalmol. 2007; 143:607-615.

Del Monte MA, Maumenee IH. New technique for in vitro culture of human retinal pigment epithelium. Birth Defects Orig Artic Ser. 1980;16(2);327-38.

Ding JD, Johnson LV, Herrmann R, et al. Anti-amyloid therapy protects against retinal pigmented epithelium damage and vision loss in a model of age-related macular degeneration. Proc Natl Acad Sci U S A. 2011; 108(28):E279-87. doi: 10.1073/pnas.1100901108.

Ding WX, Yin XM. Sorting, recognition and activation of the misfolded protein degradation pathways through macroautophagy and the proteasome. Autophagy. 2008; 4(2):141-50.

Dixon JA, Oliver SC, Olson JL, Mandava N. VEGF Trap-Eye for the treatment of neovascular age-related macular degeneration. Expert Opin Investig Drugs. 2009; 18(10):1573–80.

Dokladny K, Zuhl MN, Mandell M, et al. Regulatory coordination between two major intracellular homeostatic systems: heat shock response and autophagy. J Biol Chem. 2013; 288(21):14959-72. doi: 10.1074/jbc.M113.462408.

Dokladny K, Myers OB, Moseley PL. Heat shock response and autophagy - cooperation and control. Autophagy. 2015; 11(2):200-13. doi: 10.1080/15548627.2015.1009776.

Drolet DW, Nelson J, Tucker CE, et al. Pharmacokinetics and safety of an anti-vascular endothelial growth factor aptamer (NX1838) following injection into the vitreous humor of rhesus monkeys. Pharm Res. 2000;17(12):1503-10.

Dunn KC, Aotaki-Keen AE, Putkey FR, Hjelmeland LM. ARPE-19, a human retinal pigment epithelium cell line with differentiated properties. Exp Eye Res. 1996;62(2):155-69.

Ferrara N, Damico L, Shams N, et al. Development of ranibizumab, an anti-vascular endothelial growth factor antigen binding fragment, as therapy for neovascular age-related macular degeneration. Retina 2006; 26:859–70.

Ferrington DA, Gregerson DS. Immunoproteasomes: structure, function and antigen presentation. Prog Mol Biol Transl Sci. 2012; 109:75e112.

Ferrington DA, Sinha D, Kaarniranta K. Defects in retinal pigment epithelial cell proteolysis and the pathology associated with age-related macular degeneration. Prog Retin Eye Res. 2015. pii: S1350-9462(15)00069-5. doi: 10.1016/j.preteyeres.2015.09.002.

Fine SL, Berger JW, Maguire MG, Ho AC. Age-related macular degeneration. N Engl J Med. 2000; 342:483–92.

Finnemann SC, Leung LW, Rodriguez-Boulan E. The lipofuscin component A2E selectively inhibits phagolysosomal degradation of photoreceptor phospholipid by the retinal pigment epithelium. Proc Natl Acad Sci U. S. A. 2002;99:3842–3847.

Fletcher EL, Jobling AI, Greferath U, et al. Studying age-related macular degeneration using animal models. Optom Vis Sci. 2014;91(8):878-86.

Folkman J. Antiangiogenesis in cancer therapy -endostatin and its mechanisms of action. Exp Cell Res. 2006;312(5):594-607.

Francis PJ, Appukuttan B, Simmons E, et al. Rhesus monkeys and humans share common susceptibility genes for age-related macular disease. Hum Mol Genet. 2008;17:2673-80. doi: 10.1093/hmg/ddn167

Frennesson CI, Bek T, Jaakkola A, Nilsson SE. Prophylactic Laser Treatment Study Group. Prophylactic laser treatment of soft drusen maculopathy: a prospective, randomized Nordic study. Acta Ophthalmol. 2009; 87(7):720-4. doi: 10.1111/j.1755-3768.2008.01396.x.

Friedman DS, O'Colmain BJ, Munoz B, et al. Prevalence of age related macular degeneration in the United States. Arch Ophthalmol. 2004;122:564–572.

Fritsche LG, Chen W, Schu M, et al. Seven new loci associated with age-related macular degeneration. Nat Genet. 2013;45(4):433-9, 439e1-2. doi: 10.1038/ng.2578.

Frost LS, Mitchell CH, Boesze-Battaglia K. Autophagy in the eye: implications for ocular cell health. Exp Eye Res. 2014; 124:56-66. doi: 10.1016/j.exer.2014.04.010.

Fukai N, Eklund L, Marneros AG, et al. Lack of collagen XVIII/endostatin results in eye abnormalities. EMBO J. 2002;21(7):1535-44.

Geetha T, Vishwaprakash N, Sycheva M, Babu JR. Sequestosome 1/p62: across diseases. Biomarkers. 2012;17:99–103.

Geh KM, Anderson DH, Johnson LV, Hageman GS. Age related macular degeneration emerging pathogenetic and therapeutic concepts. Ann Med. 2006;38:450–471.

Goettsch S, Bayer P. Structural attributes in the conjugation of ubiquitin, SUMO and RUB to protein substrates. Front Biosci. 2002; 7:a148-62.

Gold B, Merriam JE, Zernant J, et al; AMD Genetics Clinical Study Group. Variation in factor B (BF) and complement component 2 (C2) genes is associated with age-related macular degeneration. Nat Genet. 2006; 38(4):458-62.

Goldstein G, Scheid M, Hammerling U, et al. Isolation of a polypeptide that has lymphocyte-differentiating properties and is represented universally in living cells. Proc Natl Acad Sci. 1975;72(1):11-15.

Gordois A, Pezzullo L, Cutler H, et al. An estimation of the worldwide economic and health burden of visual impairment. Glob Public Health. 2012;7:465–481.

Gordon S. Phagocytosis: An Immunobiologic Process. Immunity. 2016;44:463-75. doi: 10.1016/j.immuni.2016.02.026.

Gouras P, Ivert L, Landauer N, et al. Drusenoid maculopathy in rhesus monkeys (Macaca mulatta): effects of age and gender. Graefes Arch Clin Exp Ophthalmol. 2008;246:1395-402.

Gross-Jendroska M, Owens SL, Flaxel CJ, et al. Prophylactic laser treatment to fellow eyes of unilateral retinal pigment epithelial tears. Am J Ophthalmol. 1998; 126(1):77-81.

Guinez C, Mir AM, Dehennaut V, et al. Protein ubiquitination is modulated by O-GlcNAc glycosylation. FASEB J. 2008; 22:2901-2911.

Gurskaya NG, Verkhusha VV, Shcheglov AS, et al. Engineering of a monomeric green-to-red photoactivatable fluorescent protein induced by blue light. Nat Biotechnol. 2006;24:461–465.

Hageman GS, Luthert PJ, Victor Chong NH, et al. An integrated hypothesis that considers drusen as biomarkers of immune-mediated processes at the RPE-Bruch's membrane interface in aging and age-related macular degeneration. Prog. Retin. Eye Res. 2001; 20:705–732.

Hanus J, Zhao F, Wang S. Current therapeutic developments in atrophic age-related macular degeneration. Br J Ophthalmol. 2016; 100(1):122-7. doi: 10.1136/bjophthalmol-2015-306972.

Hartl FU, Bracher A, Hayer-Hartl M. Molecular chaperones in protein folding and proteostasis. Nature. 2011; 475(7356):324-32. doi: 10.1038/nature10317.

Hershko A, Ciechanover A, Heller H, et al. Proposed role of ATP in protein breakdown: conjugation of protein with multiple chains of the polypeptide of ATP-dependent proteolysis. Proc Natl Acad Sci U S A. 1980 Apr;77(4):1783-6.

Holz FG, Schütt F, Kopitz J, et al. Inhibition of lysosomal degradative functions in RPE cells by a retinoid component of lipofuscin. Invest Ophthalmol Vis Sci. 1999; 40(3):737-43.

Howes KA, Liu Y, Dunaief JL, et al. Receptor for advanced glycation end products and age-related macular degeneration. Invest Ophthalmol Vis Sci. 2004; 45: 3713–3720.

Hurskainen M, Eklund L, Hägg PO, et al. Abnormal maturation of the retinal vasculature in type XVIII collagen/endostatin deficient mice and changes in retinal glial cells due to lack of collagen types XV and XVIII. FASEB J. 2005;19(11):1564-6.

Hyman L, Neborsky R. Risk factors for age-related macular degeneration: an update. Curr Opin Ophthalmol. 2002; 13:171–5.

Ichimura Y, Kumanomidou T, Sou YS, et al. Structural basis for sorting mechanism of p62 in selective autophagy. J Biol Chem. 2008;283(33):22847-57. doi: 10.1074/jbc.M802182200.

Imamura Y, Noda S, Hashizume K, et al. Drusen, choroidal neovascularization, and retinal pigment epithelium dysfunction in SOD1-deficient mice: a model of age-related macular degeneration. Proc Natl Acad Sci U S A. 2006;103(30):11282-7.

Inan UU, Avci B, Kusbeci T, et al. Preclinical safety evaluation of intravitreal injection of full-length humanized vascular endothelial growth factor antibody in rabbit eyes. Invest Ophthalmol Vis Sci. 2007;48(4):1773-81.

Inoue H, Nojima H, Okayama H. High efficiency transformation of Escherichia coli with plasmids. Gene. 1990;96:23–28.

Ishii T, Yanagawa T, Yuki K, et al. Low micromolar levels of hydrogen peroxide and proteasome inhibitors induce the 60-kDa A170 stress protein in murine peritoneal macrophages. Biochem Biophys Res Commun. 1997;6:33–7.

IVAN Study Investigators, Chakravarthy U, Harding SP, Rogers CA, et al. Ranibizumab versus bevacizumab to treat neovascular age-related macular degeneration: one-year findings from the IVAN randomized trial. Ophthalmol. 2012 ;119:1399-411.

Izumi-Nagai K, Nagai N, Ozawa Y et al. Interleukin-6 receptor-mediated activation of signal transducer and activator of transcription-3 (STAT3) promotes choroidal neovascularization. Am J Pathol. 2007;170(6):2149-58.

Jack LS, Sadiq MA, Do DV, Nguyen QD. Emixustat and Lampalizumab: Potential Therapeutic Options for Geographic Atrophy. Dev Ophthalmol. 2016; 55:302-9. doi: 10.1159/000438954.

Jager RD, Mieler WF, Miller JW. Age related macular degeneration. N Engl J Med. 2008;358:2606–17.

Jain A, Lamark T, Sjøttem E, et al. p62/SQSTM1 is a target gene for transcription factor NRF2 and creates a positive feedback loop by inducing antioxidant response element-driven gene transcription. J Biol Chem. 2010;285:22576–91.

Janer A, Werner A, Takahashi-Fujigasaki J, et al. SUMOylation attenuates the aggregation propensity and cellular toxicity of the polyglutamine expanded ataxin-7. Hum Mol Genet. 2010; 19:181-195.

Jarrett SG, Boulton ME. Consequences of oxidative stress in age-related macular degeneration. Mol Aspects Med. 2012;33:399–417. doi: 10.1016/j.mam.2012.03.009

Javitt NB, Javitt JC. The retinal oxysterol pathway: a unifying hypothesis for the cause of age-related macular degeneration. Curr Opin Ophthalmol. 2009; 20: 151–7.

Johansson I, Monsen VT, Pettersen K, et al. The marine n-3 PUFA DHA evokes cytoprotection against oxidative stress and protein misfolding by inducing autophagy and NFE2L2 in human retinal pigment epithelial cells. Autophagy. 2015;11(9):1636-51. doi: 10.1080/15548627.2015.1061170.

Johnson LV, Ozaki S, Staples MK, et al. A potential role for immune complex pathogenesis in drusen formation. Exp. Eye Res. 2000; 70: 441–9.

Jung T, Catalgol B, Grune T. The proteasomal system. Mol Aspects Med 2009; 30:191-196.

Juuti-Uusitalo K, Vaajasaari H, Ryhänen T, et al. Efflux protein expression in human stem cell–derived retinal pigment epithelial cells. 2012; PLoS ONE 7(1): e30089. doi:10.1371/journal.pone.0030089

Kaarniranta K, Sihvola R, Salminen A, et al. Silmänpohjan ikärappeuma - vaikea ongelma sekä potilaalle että silmälääkärille. Duodecim 2003;119:935-45.

Kaarniranta K, Ryhänen T, Sironen RK, et al. Geldanamycin activates Hsp70 response and attenuates okadaic acid-induced cytotoxicity in human retinal pigment epithelial cells. Brain Res Mol Brain Res. 2005; 137(1-2):126-31.

Kaarniranta K, Seitsonen S, Paimela T, Immonen I (A). Silmänpohjan ikärappeuman patogeneesi. Duodecim 2009; 125(2):145-53.

Kaarniranta K, Salminen A, Eskelinen EL, Kopitz J (B). Heat shock proteins as gatekeepers of proteolytic pathways-Implications for age-related macular degeneration (AMD). Ageing Res Rev. 2009; 8(2):128-39.

Kaarniranta K, Salminen A. NF-kappaB signaling as a putative target for omega-3 metabolites in the prevention of age-related macular degeneration (AMD). Exp Gerontol. 2009; 44(11):685-8. doi: 10.1016/j.exger.2009.09.002

Kaarniranta K, Hyttinen J, Ryhanen T, et al. Mechanisms of protein aggregation in the retinal pigment epithelial cells. Front Biosci (Elite Ed). 2010;2:1374-84.

Kaarniranta K, Salminen A, Haapasalo A, et al. Age-related macular degeneration (AMD): Alzheimer's disease in the eye? J Alzheimers Dis. 2011;24(4):615-31. doi: 10.3233/JAD-2011-101908.

Kaarniranta K, Kauppinen A, Blasiak J, Salminen A. Autophagy regulating kinases as potential therapeutic targets for age-related macular degeneration. Future Med. Chem. 2012; 4 (17):2153–61.

Kaarniranta K, Sinha D, Blasiak J, et al. Autophagy and heterophagy dysregulation leads to retinal pigment epithelium dysfunction and development of age-related macular degeneration. Autophagy 2013; 9: 973–84.

Kaiser PK. Treatment of age-related macular degeneration with photodynamic therapy (TAP) study group. Verteporfin therapy of subfoveal choroidal neovascularization in agerelated macular degeneration: 5-year results of two randomized clinical trials with an open-label extension: TAP report no. 8. Graefes Arch Clin Exp Ophthalmol. 2006; 244:1132–42.

Kannan R, Sreekumar PG, Hinton DR. Alpha crystallins in the retinal pigment epithelium and implications for the pathogenesis and treatment of age-related macular degeneration. Biochim Biophys Acta. 2016;1860(1 Pt B):258-68. doi: 10.1016/j.bbagen.2015.05.016.

Karlsson M, Frennesson C, Gustafsson T, et al. Autophagy of iron-binding proteins may contribute to the oxidative stress resistance of ARPE-19 cells. Exp Eye Res. 2013; 116:359-365.

Katsuragi Y, Ichimura Y, Komatsu M. p62/SQSTM1 functions as a signaling hub and an autophagy adaptor. FEBS J. 2015;282(24):4672-8. doi: 10.1111/febs.13540.

Kauppinen A, Paterno JJ, Blasiak J, et al. Inflammation and its role in age-related macular degeneration. Cell Mol Life Sci. 2016. doi:10.1007/s00018-016-2147-8

Kennedy CJ, Rakoczy PE, Constable IJ. Lipofuscin of the retinal pigment epithelium: a review. Eye. 1995; 9 (6):763-71.

Khan AO, Aldahmesh MA, Mohamed JY, et al. The distinct ophthalmic phenotype of Knobloch syndrome in children. Br J Ophthalmol. 2012;96(6):890-5. doi: 10.1136/bjophthalmol-2011-301396.

Kim J, Kundu M, Viollet B, et al. AMPK and mTOR regulate autophagy through direct phosphorylation of Ulk1. Nat Cell Biol. 2011 Feb;13(2):132-41. doi: 10.1038/ncb2152

Kinnunen K, Petrovski G, Moe MC, et al. Molecular mechanisms of retinal pigment epithelium damage and development of age-related macular degeneration. Acta Ophthalmol. 2012; 90(4):299-309. doi: 10.1111/j.1755-3768.2011.02179.x.

Kirkin V, Dikic I. Role of ubiquitin- and Ubl-binding proteins in cell signaling. Curr Opin Cell Biol. 2007;19(2):199-205.

Kivinen N, Hyttinen JMT, Viiri J, et al. Hsp 70 binds reversibly to proteasome inhibitor-induced protein aggregates and evades autophagic clearance in ARPE-19 cells. J Biochemical and Pharmacological Research. 2014;2(1):1-7.

Klein BE, Klein R, Lee KE, Jensen SC. Measures of obesity and age-related eye diseases. Ophthalmic Epidemiol. 2001; 8:251–62.

Klein BE, Moss SE, Klein R, et al. Associations of visual function with physical outcomes and limitations 5 years later in an older population: the Beaver Dam eye study. Ophthalmology. 2003; 110(4):644-50.

Klein R, Peto T, Bird A, Vannewkirk MR. The epidemiology of age-related macular degeneration. Am J Ophthalmol. 2004;137:486–95.

Klein R, Cruickshanks KJ, Nash SD, et al. The prevalence of age-related macular degeneration and associated risk factors. Arch Ophthalmol. 2010; 128(6):750-8. doi: 10.1001/archophthalmol.2010.92.

Klein R, Lee KE, Gangnon RE, Klein BE. Relation of smoking, drinking, and physical activity to changes in vision over a 20-year period: the Beaver Dam Eye Study. Ophthalmology. 2014; 121(6):1220-8. doi: 10.1016/j.ophtha.2014.01.003

Klettner A. The induction of heat shock proteins as a potential strategy to treat neurodegenerative disorders. Drug News Perspect. 2004; 17:299-306.

Klettner A, Roider J. Comparison of bevacizumab, ranibizumab, and pegaptanib in vitro: efficiency and possible additional pathways. Invest Ophthalmol Vis Sci. 2008;49(10):4523-7. doi: 10.1167/iovs.08-2055

Klettner A, Roider J. Treating age-related macular degeneration - interaction of VEGF-antagonists with their target. Mini Rev Med Chem. 2009; 9(9):1127-35.

Klettner AK, Kruse ML, Meyer T, et al. Different properties of VEGF-antagonists: Bevacizumab but not Ranibizumab accumulates in RPE cells. Graefes Arch Clin Exp Ophthalmol. 2009;247(12):1601-8. doi: 10.1007/s00417-009-1136-0

Klettner A, Möhle F, Roider J. Intracellular bevacizumab reduces phagocytotic uptake in RPE cell. Graefes Arch Clin Exp Ophthalmol. 2010;248(6):819-24. doi:10.1007/s00417-010-1317-x

Klettner A, Kauppinen A, Blasiak J, et al. Cellular and molecular mechanisms of age-related macular degeneration: from impaired autophagy to neovascularization. Int J Biochem Cell Biol. 2013; 45(7):1457-67. doi: 10.1016/j.biocel.2013.04.013.

Klettner A. VEGF-A and its inhibitors in age-related macular degeneration – pharmacokinetic differences and their retinal and systemic implications. J Biochemical and Pharmacological Research. 2014; 2(1):8-20.

Klionsky DJ, Elazar Z, Seglen PO, Rubinsztein DC. Does bafilomycin A1 block the fusion of autophagosomes with lysosomes? Autophagy. 2008;4:849–50.

Klionsky DJ, Abdalla FC, Abeliovich H, et al. Guidelines for the use and interpretation of assays for monitoring autophagy. Autophagy. 2012;8:445–544.

Klionsky DJ, Schulman BA. Dynamic regulation of macroautophagy by distinctive ubiquitin-like proteins. Nat Struct Mol Biol. 2014;21(4):336-45. doi: 10.1038/nsmb.2787.

Klionsky D, Abdelmohsen K, Abe A, et al. Guidelines for the use and interpretation of assays for monitoring autophagy (3rd edition). Autophagy. 2016; 12(1):1-222.

Knaevelsrud H, Simonsen A. Fighting disease by selective autophagy of aggregate-prone proteins. FEBS Lett. 2010;584(12):2635-45. doi: 10.1016/j.febslet.2010.04.041.

Knobloch WH, Layer JM. Retinal Detachment and Encephalocele. J Pediatr Ophthalmol. 1971;8(3):181–184.

Koh V, Tan C, Tan PT, et al. Myopic Maculopathy and Optic Disc Changes in Highly-Myopic Young Asian Eyes and Impact on Visual Acuity. Am J Ophthalmol. 2016 Feb 2. pii: S0002-9394(16)30026-5. doi: 10.1016/j.ajo.2016.01.005.

Komatsu M, Waguri S, Koike M, et al. Homeostatic levels of p62 control cytoplasmic inclusion body formation in autophagy-deficient mice. Cell. 2007;131:1149–1163.

Komatsu M, Ichimura Y. Physiological significance of selective degradation of p62 by autophagy. FEBS Lett. 2010;584, 1374–1378.

Komatsu M, Kurokawa H, Waguri S, et al. The selective autophagy substrate p62 activates the stress responsive transcription factor Nrf2 through inactivation of Keap1. Nat Cell Biol. 2010 Mar;12(3):213-23. doi: 10.1038/ncb2021

Korolchuk VI, Mansilla A, Menzies FM, Rubinsztein DC (A). Autophagy inhibition compromises degradation of ubiquitin-proteasome pathway substrates. Mol Cell. 2009 Feb 27;33(4):517-27. doi: 10.1016/j.molcel.2009.01.021.

Korolchuk VI, Menzies FM, Rubinsztein DC (B). A novel link between autophagy and the ubiquitin-proteasome system. Autophagy. 2009; 5(6):862-3.

Koskela A, Reinisalo M, Petrovski G, et al. Nutraceutical with Resveratrol and Omega-3 Fatty Acids Induces Autophagy in ARPE-19 Cells. Nutrients. 2016;8(5). pii: E284. doi: 10.3390/nu8050284.

Krohne TU, Kaemmerer E, Holz FG, Kopitz J (A). Lipid peroxidation products reduce lysosomal protease activities in human retinal pigment epithelial cells via two different mechanisms of action. Exp Eye Res. 2010;90(2):261-6. doi: 10.1016/j.exer.2009.10.014.

Krohne TU, Holz FG, Kopitz J (B). Apical-to-basolateral transcytosis of photoreceptor outer segments induced by lipid peroxidation products in human retinal pigment epithelial cells. Invest Ophthalmol Vis Sci. 2010;51:553–60.

Krohne TU, Stratmann NK, Kopitz J, Holz FG (C). Effects of lipid peroxidation products on lipofuscinogenesis and autophagy in human retinal pigment epithelial cells. Exp Eye Res. 2010; 90(3):465-71. doi: 10.1016/j.exer.2009.12.011.

Kurz T, Karlsson M, Brunk UT, et al. ARPE-19 retinal pigment epithelial cells are highly resistant to oxidative stress and exercise strict control over their lysosomal redox-active iron. Autophagy. 2009;5:494–501.

Kuusisto E, Salminen A, Alafuzoff I (A). Ubiquitin-binding protein p62 is present in neuronal and glial inclusions in human tauopathies and synucleinopathies. Neuroreport. 2001;12:2085–90.

Kuusisto E, Suuronen T, Salminen A (B). Ubiquitin-binding protein p62 expression is induced during apoptosis and proteosomal inhibition in neuronal cells. Biochem Biophys Res Commun. 2001; 280:223–8.

Kuusisto E, Salminen A, Alafuzoff I. Early accumulation of p62 in neurofibrillary tangles in Alzheimer's disease: possible role in tangle formation. Neuropathol Appl Neurobiol. 2002;28: 228–37.

Käypä hoito. Kostea silmäpohjan ikärappeuma (AMD). Duodecim 2016.

Lakshmanachetty S, Koster MI. Emerging Roles for Collagen XV and XVIII in Cancer Progression. Exp Dermatol. 2016. doi: 10.1111/exd.12960.

Lee JJ, Kim YM, Jeong J, et al. Ubiquitin-associated (UBA) domain in human Fas associated factor 1 inhibits tumor formation by promoting Hsp70 degradation. PLoS One. 2012; 7:e40361.

Li Y, Wang YS, Shen XF, et al. Alterations of activity and intracellular distribution of the 20S proteasome in ageing retinal pigment epithelial cells, Exp. Gerontol. 2008; 43:1114–22.
Liang XH, Kleeman LK, Jiang HH, et al. Protection against fatal Sindbis virus encephalitis by beclin, a novel Bcl-2-interacting protein. J Virol. 1998;72(11):8586-96.

Liang J, Shao SH, Xu ZX, et al. The energy sensing LKB1-AMPK pathway regulates p27(kip1) phosphorylation mediating the decision to enter autophagy or apoptosis, Nat Cell Biol. 2007;9:218–224.

Lilienbaum A. Relationship between the proteasomal system and autophagy, Int. J. Biochem. Mol Biol. 2013; 4:1–26.

Lin L, Baehrecke EH. Autophagy, cell death, and cancer. Mol Cell Oncol. 2015; 2(3):e985913. doi: 10.4161/23723556.2014.985913.

Lüke M, Januschowski K, Warga M, et al., (Tuebingen Bevacizumab Study Group). The retinal tolerance to bevacizumab in co-application with a recombinant tissue plasminogen activator. Br J Ophthalmol. 2007;91(8):1077-82.

Luthra S, Narayanan R, Marques LE, et al. Evaluation of in vitro effects of bevacizumab (Avastin) on retinal pigment epithelial, neurosensory retinal, and microvascular endothelial cells. Retina. 2006;26(5):512-8.

Luthra S, Sharma A, Dong J, et al. Effect of bevacizumab (Avastin (TM)) on mitochondrial function of in vitro retinal pigment epithelial, neurosensory retinal and microvascular endothelial cells. Indian J Ophthalmol. 2013;61(12):705-10. doi: 10.4103/0301-4738.124750.

Lytvynchuk L, Sergienko A, Lavrenchuk G, Petrovski G. Antiproliferative, Apoptotic, and Autophagic Activity of Ranibizumab, Bevacizumab, Pegaptanib, and Aflibercept on Fibroblasts: Implication for Choroidal Neovascularization. J Ophthalmol. 2015;2015:934963. doi: 10.1155/2015/934963.

Macular Photocoagulation Study Group. Laser photocoagulation of subfoveal recurrent neovascular lesions in age-related macular degeneration. Arch Ophthalmol. 1991; 109:1232–41.

Mannagh J, Arya DV, Irvine AR. Tissue culture of human retinal pigment epithelium. Investg Ophthalmol. 1973;12:52-64.

Mannermaa E, Urtti A, Kaarniranta K. Lasiaiseen annosteltavat silmänpohjan ikärappeuman uudet lääkkeet. Duodecim 2007; 123:2229-37.

Mannermaa E, Vellonen KS, Ryhänen T, et al. Efflux protein expression in human retinal pigment epithelium cell lines. Pharm Res. 2009;26(7):1785-91. doi: 10.1007/s11095-009-9890-6.

Maquire MG, Bressler SB, Bressler NM, et al. Risk factors for choroidal neovascularization in the second eye of patients with juxtafoveal or subfoveal choroidal neovascularization secondary to age-related macular degeneration: Macular Photocoagulation Study Group. Arch Ophthalmol. 1997; 115:741-7.

Marneros AG, Keene DR, Hansen U, et al. Collagen XVIII/endostatin is essential for vision and retinal pigment epithelial function. EMBO J. 2004;23(1):89-99.

Marneros AG, Olsen BR. Physiological role of collagen XVIII and endostatin. FASEB J. 2005;19(7):716-28

Matsui Y, Takagi H, Qu X, et al. Distinct roles of autophagy in the heart during ischemia and reperfusion: roles of AMP-activated protein kinase and Beclin 1 in mediating autophagy. Circ Res. 2009;100:914–922.

Matsuyama K, Ogata N, Matsuoka M, et al. Plasma levels of vascular endothelial growth factor and pigment epithelium-derived factor before and after intravitreal injection of bevacizumab. Br J Ophthalmol. 2010;94(9):1215-8. doi: 10.1136/bjo.2008.156810

Mei W, Dong C, Hui C, et al. Gambogenic acid kills lung cancer cells through aberrant autophagy. PLoS One. 2014; 9(1):e83604. doi: 10.1371/journal.pone.0083604.

Meley D, Bauvy C, Houben-Weerts JH, et al. AMP-activated protein kinase and the regulation of autophagic proteolysis. J Biol Chem. 2006;281:34870–34879.

Miguel NC, Matsuda M, Portes AL, et al. In vitro effects of bevacizumab treatment on newborn rat retinal cell proliferation, death, and differentiation. Invest Ophthalmol Vis Sci. 2012;53(12):7904-11. doi: 10.1167/iovs.12-10283.

Mishra A, Godavarthi SK, Maheshwari M, et al. The ubiquitin ligase E6-AP is induced and recruited to aggresomes in response to proteasome inhibition and may be involved in the ubiquitination of Hsp70-bound misfolded proteins. J Biol Chem. 2009; 284:10537-10545.

Mitter SK, Rao HV, Qi X, et al. Autophagy in the retina: a potential role in age-related macular degeneration. Adv Exp Med Biol. 2012; 723:83-90. doi: 10.1007/978-1-4614-0631-0_12.

Mitter SK, Song C, Qi X, et al. Dysregulated autophagy in the RPE is associated with increased susceptibility to oxidative stress and AMD. Autophagy. 2014;10(11):1989-2005. doi: 10.4161/auto.36184.

Mizushima N, Levine B, Cuervo AM, Klionsky DJ. Autophagy fights disease through cellular self-digestion. Nature. 2008; 451(7182):1069-75. doi: 10.1038/nature06639.

Mizushima N, Komatsu M. Autophagy: renovation of cells and tissues. Cell. 2011;147:728–741.

Moseley PL. Heat shock proteins and the inflammatory response. Ann N Y Acad Sci. 1998;856:206-13.

Mullins RF, Russell SR, Anderson DH, Hageman GS. Drusen associated with aging and age-related macular degeneration contain proteins common to extracellular deposits associated with atherosclerosis, elastosis, amyloidosis, and dense deposit disease. FASEB J. 2000;14:835–46.

Muragaki Y, Timmons S, Griffith CM, et al. Mouse Col18a1 is expressed in a tissue-specific manner as three alternative variants and is localized in basement membrane zones. Proc Natl Acad Sci U S A. 1995;92(19):8763-7.

Nagaoka U, Kim K, Jana NR, et al. Increased expression of p62 in expanded polyglutamine-expressing cells and its association with polyglutamine inclusions. J Neurochem. 2004;91:57–68.

Nakaso K, Yoshimoto Y, Nakano T, et al. Transcriptional activation of p62/A170/ZIP during the formation of the aggregates: possible mechanisms and the role in Lewy body formation in Parkinson's disease. Brain Res. 2004;1012(1-2):42-51.

Nguyen TM, Subramanian IV, Xiao X, et al. Endostatin induces autophagy in endothelial cells by modulating Beclin 1 and beta-catenin levels. J Cell Mol Med. 2009;13(9B):3687-98. doi: 10.1111/j.1582-4934.2009.00722.x.

O'Brien CE, Wyss-Coray T. Sorting through the roles of beclin 1 in microglia and neurodegeneration. J Neuroimmune Pharmacol. 2014;(3):285-92. doi: 10.1007/s11481-013-9519-8.

O'Brien CE, Bonanno L, Zhang H, Wyss-Coray T. Beclin 1 regulates neuronal transforming growth factor-β signaling by mediating recycling of the type I receptor ALK5. Mol Neurodegener. 2015;10:69. doi: 10.1186/s13024-015-0065-0.

Ohlmann AV, Ohlmann A, Welge-Lüssen U, May CA. Localization of collagen XVIII and endostatin in the human eye. Curr Eye Res. 2005;30(1):27-34.

Ojamo M. Näkövammarekisterin vuosikirja 2014. Aleksipaino Group Oy. Helsinki.

O'Reilly MS, Boehm T, Shing Y, et al.Endostatin: an endogenous inhibitor of angiogenesis and tumor growth. Cell. 1997;88:277–285.

Ortega N, Werb Z. New functional roles for non-collagenous domains of basement membrane collagens. J Cell Sci. 2002;115(Pt 22):4201-14.

Oskolkova OV, Afonyushkin T, Leitner A, et al. ATF4-dependent transcription is a key mechanism in VEGF up-regulation by oxidized phospholipids: critical role of oxidized sn-2 residues in activation of unfolded protein response. Blood. 2008; 112: 330–9.

Paimela T, Ryhänen T, Mannermaa E, et al. The effect of 17beta-estradiol on IL-6 secretion and NF-kappaB DNA-binding activity in human retinal pigment epithelial cells. Immunol Lett. 2007; 110: 139–144.

Paimela T, Hyttinen JMT, Viiri J, et al. Celastrol regulates innate immunity response via NF-kB and Hsp70 in human retinal pigment epithelial cells. Pharmacol Res. 2011; 64:501-508.

Paine MG, Babu JR, Seibenhener ML, Wooten MW. Evidence for p62 aggregate formation: role in cell survival. FEBS Lett. 2005;579(22):5029-34.

Pankiv S, Clausen TH, Lamark T, et al. p62/SQSTM1 binds directly to Atg8/LC3 to facilitate degradation of ubiquitinated protein aggregates by autophagy. Biol Chem. 2007;282:24131–45.

Pankiv S, Lamark T, Bruun JA, et al. Nucleocytoplasmic shuttling of p62/SQSTM1 and its role in recruitment of nuclear polyubiquitinated proteins to promyelocytic leukemia bodies. J Biol Chem. 2010;285(8):5941-53. doi: 10.1074/jbc.M109.039925.

Park D, Jeong H, Lee MN, et al. Resveratrol induces autophagy by directly inhibiting mTOR through ATP competition. Sci Rep. 2016;6:21772. doi: 10.1038/srep21772.

Pascale A, Govoni S. The complex world of post-transcriptional mechanisms: is their deregulation a common link for diseases? Focus on ELAV-like RNA-binding proteins. Cell Mol Life Sci. 2012;69:501–17.

Pascolini D, Mariotti SP, Pokharel GP, et al. Global update of available data on visual impairment: a compilation of population-based prevalence studies. Ophthalmic Epidemiol 2002; 2004:67–115.

Pascolini D, Mariotti SP, Pokharel GP, et al. Global update of available data on visual impairment: a compilation of population based prevalence studies. Ophthalmic Epidemiol. 2004;11:67–115.

Pennesi ME, Neuringer M, Courtney RJ. Animal models of age related macular degeneration. Mol Aspects Med. 2012; 33(4):487-509. doi: 10.1016/j.mam.2012.06.003.

Pfeffer BA, Philp NJ. Cell culture of retinal pigment epithelium: Special Issue. Exp Eye Res. 2014; 126:1-4. doi: 10.1016/j.exer.2014.07.010.

Piippo N, Korkmaz A, Hytti M, et al. Decline in cellular clearance systems induces inflammasome signaling in human ARPE-19 cells. Biochim Biophys Acta. 2014;1843:3038–3046. doi: 10.1016/j.bbamcr.2014.09.015.

Pickart CM. Mechanisms underlying ubiquitination. Annu Rev Biochem. 2001; 70:503-33.

Pickford F, Masliah E, Britschgi M, et al. The autophagy-related protein beclin 1 shows reduced expression in early Alzheimer disease and regulates amyloid beta accumulation in mice. J Clin Invest. 2008;118(6):2190-9. doi: 10.1172/JCI33585.

Piri N, Kwong JMK, Gu L, Caprioli J. Heat shock Proteins in the retina: Focus on HSP70 and alpha crystallins in ganglion cell survival. Prog Retin Eye Res. 2016;52:22-46. doi: 10.1016/j.preteyeres.2016.03.001.

Qian J, Lu Q, Tao Y, Jiang YR. Vitreous and plasma concentrations of apelin and vascular endothelial growth factor after intravitreal bevacizumab in eyes with proliferative diabetic retinopathy. Retina. 2011;31(1):161-8. doi: 10.1097/IAE.0b013e3181e46ad8.

Qin L, Wang Z, Tao L, Wang Y. ER stress negatively regulates AKT/TSC/mTOR pathway to enhance autophagy. Autophagy. 2010;6(2):239-47.

Rakoczy PE, Mann K, Cavaney DM, et al. Constable, Detection and possible functions of a cysteine protease involved in digestion of rod outer segments by retinal pigment epithelial cells, Invest. Ophthalmol. Vis. Sci. 1994;35:4100–08.

Ramkumar HL, Zhang J, Chan C-C. Retinal ultrastructure of murine models of dry age-related macular degeneration (AMD). Prog Retin Eye Res. 2010;29(3):169-90.

Ratnapriya R, Chew EY. Age-related macular degeneration – clinical review and genetics update. Clin Genet. 2013: 84: 160–6.

Ravid T, Hochstrasser M. Diversity of degradation signals in the ubiquitin-proteasome system. Nat Rev Mol Cell Biol. 2008; 9(9):679-90. doi: 10.1038/nrm2468.

Rein DB, Wittenborn JS, Zhang X, et al. Forcasting age-related macular degenerationthrough the year 2050: the potential impact of new treatments. Arch Ophthalmol 2009;127:533–40.

Rodgers KJ, Ford JL, Brunk UT. Heat shock proteins: keys to healthy ageing? Redox Rep. 2009; 14:147-153.

Rodríguez-Muela N, Koga H, García-Ledo L, et al. Balance between autophagic pathways preserves retinal homeostasis. Aging Cell. 2013;12(3):478-88. doi: 10.1111/acel.12072.

Rogov V, Dotsch V, Johansen T, Kirkin V. Interactions between autophagy receptors and ubiquitin-like proteins form the molecular basis for selective autophagy. Mol Cell. 2014;53:167–178.

Roth F, Bindewald A, Holz FG. Key pathophysiological pathways in age-related macular disease. Graefe's Arch Clin Exp Ophthalmol. 2004; 242:710-6.

Rudnicka AR, Jarrar Z, Wormald R, et al. Age and gender variations in age-related macular degeneration prevalence in populations of European ancestry: a meta-analysis. Ophthalmology. 2012; 119:571–80.

Ryhänen T, Hyttinen JM, Kopitz J, et al. Crosstalk between Hsp70 molecular chaperone, lysosomes and proteasomes in autophagy-mediated proteolysis in human retinal pigment epithelial cells. J Cell Mol Med. 2009; 13(9B):3616-31. doi: 10.1111/j.1582-4934.2008.00577.x.

Salminen A, Kaarniranta K. Regulation of the aging process by autophagy. Trends Mol Med. 2009;15:217–24.

Salminen A, Kaarniranta K, Haapasalo A, et al. Emerging role of p62/sequestosome-1 in the pathogenesis of Alzheimer's disease. Prog Neurobiol. 2012;96(1):87-95. doi: 10.1016/j.pneurobio.2011.11.005.

Salminen A, Kaarniranta K. AMP-activated protein kinase (AMPK) controls the aging process via an integrated signaling network. Ageing Res Rev. 2012;11:230–41.

Salminen A, Kaarniranta K, Kauppinen A, et al. Impaired autophagy and APP processing in Alzheimer's disease: The potential role of Beclin 1 interactome. Prog Neurobiol. 2013;106-107:33-54. doi: 10.1016/j.pneurobio.2013.06.002.

Samari HR, Seglen PO. Inhibition of hepatocytic autophagy by adenosine, aminoimidazole-4-carboxamide riboside, and N6-mercaptopurine riboside. Evidence for involvement of amp-activated protein kinase. J Biol Chem. 1998;273:23758–23763.

Sambrook J, Fritsch EF, Maniatis T. Extraction and purification of plasmid DNA: In: Molecular Cloning. A Laboratory Manual. 2nd Edition. Plainwiew, NY, USA, Cold Spring Harbor Press. 1990:1.25-1.28.

Sarks JP, Sarks SH, Killingsworth MC. Evolution of soft drusen in age-related macular degeneration. 1994; 8:269-83.

Schaljo B, Kratochvill F, Gratz N, et al. Tristetraprolin is required for full anti-inflammatory response of murine macrophages to IL-10. J Immunol. 2009;183:1197–1206.

Schmidt-Erfurth UM, Pruente C. Management of neovascular age-related macular degeneration. Prog Retin Eye Res. 2007;26(4):437-51.

Schmidt-Erfurth U, Kaiser PK, Korobelnik JF, et al. Intravitreal aflibercept injection for neovascular age-related macular degeneration: ninety-six-week results of the VIEW studies. Ophthalmology. 2014;121(1):193-201. doi: 10. 1016/j.ophtha.2013.08.011.

Schnichels S, Hagemann U, Januschowski K, et al. Comparative toxicity and proliferation testing of aflibercept, bevacizumab and ranibizumab on different ocular cells. Br J Ophthalmol. 2013;97(7):917-23. doi: 10.1136/bjophthalmol-2013-303130

Schutt F, Ueberle B, Schnolzer M, et al. Proteome analysis of lipofuscin in human retinal pigment epithelial cells. FEBS Lett. 2002; 528:217-221.

Schwartz SD, Regillo CD, Lam BL, et al. Human embryonic stem cell-derived retinal pigment epithelium in patients with age-related macular degeneration and Stargardt's macular dystrophy: follow-up of two open-label phase 1/2 studies. Lancet. 2015;385(9967):509-16. doi: 10.1016/S0140-6736(14)61376-3.

Scott LJ, Goa KL. Verteporfin. Drugs Aging. 2000; 16(2):139-46.

Seddon JM, Cote J, Rosner B. Progression of age-related macular degeneration: association with dietary fat, transunsaturated fat, nuts, and fish intake. Arch Ophthalmol 2003;121:1728–37.

Sertié AL, Sossi V, Camargo AA, et al. Collagen XVIII, containing an endogenous inhibitor of angiogenesis and tumor growth, plays a critical role in the maintenance of retinal structure and in neural tube closure (Knobloch syndrome). Hum Mol Genet. 2000;9(13):2051-8.

Shahar J, Avery RL, Heilweil G, et al. Electrophysiologic and retinal penetration studies following intravitreal injection of bevacizumab (Avastin). Retina. 2006;26(3):262-9.

Shamsi FA, Boulton M. Inhibition of RPE lysosomal and antioxidant activity by the age pigment lipofuscin. Invest Ophthalmol Vis Sci. 2001;42:3041–6.

Shang F, Taylor A. Roles for the ubiquitin-proteasome pathway in protein quality control and signaling in the retina: implications in the pathogenesis of age-related macular degeneration. Mol Aspects Med. 2012; 33(4):446-66. doi: 10.1016/j.mam.2012.04.001.

Sin HP, Liu DT, Lam DS. Lifestyle modification, nutritional and vitamins supplements for age-related macular degeneration. Acta Ophthalmol. 2012. 10.1111/j.1755-3768.2011.02357.x.

Singerman LJ, Masonson H, Patel M, et al. Pegaptanib sodium for neovascular age-related macular degeneration: third-year safety results of the VEGF Inhibition Study in Ocular Neovascularisation (VISION) trial. Br J Ophthalmol. 2008; 92(12):1606-11. doi: 10.1136/bjo.2007.132597.

Sniderman LC, Koenekoop RK, O'Gorman AM, et al. Knobloch syndrome involving midline scalp defect of the frontal region. Am J Med Genet. 2000;90(2):146-9.

Sorkio A, Hongisto H, Kaarniranta K, et al. Structure and barrier properties of human embryonic stem cell-derived retinal pigment epithelial cells are affected by extracellular matrix protein coating. 2014;20(3-4):622-34. doi: 10.1089/ten.TEA.2013.0049.

Sparrow JR, Fishkin N, Zhou J, et al.A2E, a byproduct of the visual cycle. Vision Res. 2003;43:2983-90.

Spitzer MS, Yoeruek E, Sierra A, et al. Comparative antiproliferative and cytotoxic profile of bevacizumab (Avastin), pegaptanib (Macugen) and ranibizumab (Lucentis) on different ocular cells. Graefes Arch Clin Exp Ophthalmol. 2007;245(12):1837-42.

Srikantan S, Gorospe M. HuR function in disease. Front Biosci (Landmark Ed). 2012;17:189-205.

Strauss O. The retinal pigment epithelium in visual function. Physiol Rev. 2005; 85(3):845-81.

Sunness JS, Rubin GS, Applegate CA, et al. Visual function abnormalities and prognosis in eyes with age-related geographic atrophy of the macula and good visual acuity. Ophthalmology 1997; 104:1677–91.

Suzuki K, Kirisako T, Kamada Y, et al. The pre-autophagosomal structure organized by concerted functions of APG genes is essential for autophagosome formation. EMBO J. 2001;20(21):5971-81.

Tanaka K, Ii K, Ichihara A, et al. A high molecular weight protease in the cytosol of rat liver. I. Purification, enzymological properties, and tissue distribution. J Biol Chem. 1986; 261(32):15197-203.

Tanida I, Ueno T, Kominami E. LC3 and autophagy. Methods Mol Biol. 2008;445:77-88. doi: 10.1007/978-1-59745-157-4_4.

Tate DJ Jr, Miceli MV, Newsome DA. Phagocytosis and H2O2 induce catalase and metallothionein gene expression in human retinal pigment epithelial cells. Invest Ophthalmol Vis Sci. 1995; 36(7):1271-9.

Tenenbaum SA, Lager PJ, Carson CC, Keene JD. Ribonomics: identifying mRNA subsets in mRNP complexes using antibodies to RNA-binding proteins and genomic arrays. Methods. 2002;26:191–8.

Terman A, Kurz T, Navratil M, et al. Mitochondrial turnover and aging of long-lived postmitotic cells: the mitochondrial–lysosomal axis theory of aging, Antioxid Redox Signal. 2010;12:503–535.

The CATT Research Group. Ranibizumab and bevacizumab for neovascular age-related macular degeneration. N Engl J Med. 2011;364:1897-908.

Thornton J, Edwards R, Mitchell P, et al. Smoking and age-related macular degeneration: a review of association. Eye. 2005; 19:935–44.

Tokarz P, Kauppinen A, Kaarniranta K, Blasiak J. Oxidative DNA damage and proteostasis in age-related macular degeneration. J Biochem Pharmacol Res. 2013; 1:106-113.

Tolentino MJ, Dennrick A, John E, Tolentino MS. Drugs in Phase II clinical trials for the treatment of age-related macular degeneration. Expert Opin Investig Drugs. 2014;22:1-17.

Toops KA, Tan LX, Jiang Z, et al. Cholesterol-mediated activation of acid sphingomyelinase disrupts autophagy in the retinal pigment epithelium. Mol Biol Cell. 2015;26(1):1-14. doi: 10.1091/mbc.E14-05-1028.

Tufail A, Patel PJ, Egan C, et al.; ABC Trial Investigators. Bevacizumab for neovascular age related macular degeneration (ABC Trial): multicentre randomised double masked study. BMJ. 2010; 340:c2459. doi: 10.1136/bmj.c2459.

Valapala M, Wilson C, Hose S, et al. Lysosomal-mediated waste clearance in retinal pigment epithelial cells is regulated by CRYBA1/βA3/A1-crystallin via V-ATPase-MTORC1 signaling. Autophagy. 2014;10(3):480-96. doi: 10.4161/auto.27292.

van Doorn WG, Papini A. Ultrastructure of autophagy in plant cells: a review. Autophagy. 2013;9(12):1922-36. doi: 10.4161/auto.26275.

van Horssen J, Wilhelmus MM, Heljasvaara R, et al. Collagen XVIII: a novel heparan sulfate proteoglycan associated with vascular amyloid depositions and senile plaques in Alzheimer's disease brains. Brain Pathol. 2002;12(4):456-62.

Viana R, Aguado C, Esteban I, et al. Role of AMP-activated protein kinase in autophagy and proteasome function. Biochem Biophys Res Commun. 2008;369: 964–8.

Viiri J, Hyttinen JM, Ryhänen T, et al. p62/sequestosome 1 as a regulator of proteasome inhibitor-induced autophagy in human retinal pigment epithelial cells. Mol Vis. 2010;16:1399–414.

Viiri J, Amadio M, Marchesi N, et al. Autophagy Activation Clears ELAVL1/HuR-Mediated Accumulation of SQSTM1/p62 during Proteasomal Inhibition in Human Retinal Pigment Epithelial Cells. PLoS ONE. 2013;8(7): e69563. doi:10.1371/journal.pone.0069563

Virgili G, Michelessi M, Parodi MB, et al. Laser treatment of drusen to prevent progression to advanced age-related macular degeneration. Cochrane Database of Systematic Reviews 2015, Issue 10. Art. No.: CD006537. DOI:10.1002/14651858.CD006537.pub3.

Vladan B, Panfoli I. Melatonin and abeta, macular degeneration and alzheimers disease: same disease, different outcomes? Med Hypothesis Discov Innov Ophthalmol. 2012; 1(2):24-32.

Wang AL, Boulton ME, Dunn WA Jr, et al. (A). Using LC3 to monitor autophagy flux in the retinal pigment epithelium. Autophagy. 2009;5:1190–3.

Wang AL, Lukas TJ, Yuan M, et al. (B). Autophagy and exosomes in the aged retinal pigment epithelium: possible relevance to drusen formation and age-related macular degeneration. PLoS One. 2009; 4(1):e4160. doi: 10.1371/journal.pone.0004160.

Wang AL, Lukas TJ, Yuan M, et al. (C). Autophagy, exosomes and drusen formation in age-related macular degeneration. Autophagy. 2009;5:563–4.

Wang AM, Miyata Y, Klinedinst S, et al. Activation of Hsp70 reduces neurotoxicity by promoting polyglutamine protein degradation. Nat Chem Biol. 2013; 9:112-118.

Wang L, Cano M, Handa JT. p62 provides dual cytoprotection against oxidative stress in the retinal pigment epithelium. Biochim Biophys Acta. 2014;1843(7):1248-58. doi: 10.1016/j.bbamcr.2014.03.016.

Wang L, Ebrahimi KB, Chyn M, et al. Biology of p62/sequestosome-1 in Age-Related Macular Degeneration (AMD). Adv Exp Med Biol. 2016;854:17-22. doi: 10.1007/978-3-319-17121-0_3.

Weikel KA, Fitzgerald P, Shang F, et al. Natural history of age-related retinal lesions that precede AMD in mice fed high or low glycemic index diets. Invest Ophthalmol Vis Sci. 2012; 53(2):622-32. doi: 10.1167/iovs.11-8545.

Welchman RL, Gordon C, Mayer RJ. Ubiquitin and ubiquitin-like proteins as multifunctional signals. Nat Rev Mol Cell Biol. 2005;6(8):599-609.

Williams RA, Brody BL, Thomas RG, et al. The psychosocial impact of macular degeneration. Arch Ophthalmol. 1998;116(4):514-20.

Xu H, Ren D. Lysosomal physiology. Annu Rev Physiol. 2015;77:57-80. doi: 10.1146/annurev-physiol-021014-071649.

Xu L, Lu T, Tuomi L, et al. Pharmacokinetics of ranibizumab in patients with neovascular age-related macular degeneration: a population approach. Invest Ophthalmol Vis Sci. 2013;54(3):1616-24. doi: 10.1167/iovs.12-10260.

Xu W, Ye P, Li Z, et al. Endostar, a recently introduced recombinant human endostatin, inhibits proliferation and migration through regulating growth factors, adhesion factors and inflammatory mediators in choroid-retinal endothelial cells. Mol Biol. 2010;44(4):664-70.

Yamaguchi N, Anand-Apte B, Lee M, et al. Endostatin inhibits VEGF-induced endothelial cell migration and tumor growth independently of zinc binding. EMBO J. 1999;18(16):4414-23.

Yang Q, She H, Gearing M, et al. Regulation of neuronal survival factor MEF2D by chaperone-mediated autophagy. Science. 2009;323(5910):124-7.

Yang Y, Fiskus W, Yong B, et al. Acetylated hsp70 and KAP1-mediated Vps34 SUMOylation is required for autophagosome creation in autophagy. Proc Natl Acad Sci USA. 2013; 110:6841-6846.

Yang Z, Klionsky DJ (A). Mammalian autophagy: core molecular machinery and signalling regulation. Curr Opin Cell Biol. 2010;22:124–131.

Yang Z, Klionsky DJ (B). Eaten alive: a history of macroautophagy. Nat Cell Biol. 2010;2:814–822.

Yao J, Jia L, Khan N, et al. Deletion of autophagy inducer RB1CC1 results in degeneration of the retinal pigment epithelium. Autophagy. 2015;11(6):939-53. doi: 10.1080/15548627.2015.1041699.

Yehoshua Z, de Amorim Garcia Filho CA, Nunes RP, et al. Systemic complement inhibition with eculizumab for geographic atrophy in age-related macular degeneration: the COMPLETE study. Ophthalmology. 2014; 121(3):693-701. doi: 10.1016/j.ophtha.2013.09.044.

Ylikärppä R, Eklund L, Sormunen R, et al. Lack of type XVIII collagen results in anterior ocular defects. FASEB J. 2003;17(15):2257-9.

Yu Q, Kent CR, Tytell M. Retinal uptake of intravitreally injected Hsc/Hsp70 and its effect on susceptibility to light damage. Mol Vis. 2001; 7:48-56.

Yu WH, Kumar A, Peterhoff C, et al. Autophagic vacuoles are enriched in amyloid precursor protein-secretase activities: implications for β-amyloid peptide over-production and localization in Alzheimer's disease. International Journal of Biochemistry & Cell Biology. 2004;36 36 (2004), pp. 2531–2540

Zatloukal K, Stumptner C, Fuchsbichler A, et al. p62 Is a common component of cytoplasmic inclusions in proteinaggregation diseases. Am J Pathol. 2002;160: 255–63.

Zhang J, Bai Y, Huang L, et al. Protective effect of autophagy on human retinal pigment epithelial cells against lipofuscin fluorophore A2E: implications for age-related macular degeneration. Cell Death Dis. 2015;6:e1972. doi: 10.1038/cddis.2015.330.

Zhang XJ, Chen S, Huang KX, Le WD. Why should autophagic flux be assessed? Acta Pharmacol Sin. 2013; 34(5):595-9. doi: 10.1038/aps.2012.184.

Zhu Q, Ziemssen F, Henke-Fahle S, et al. Tübingen Bevacizumab Study Group, Grisanti S. Vitreous levels of bevacizumab and vascular endothelial growth factor-A in patients with choroidal neovascularization. Ophthalmology. 2008; 115(10):1750-5, 1755.e1. doi: 10.1016/j.ophtha.2008.04.023.

Zucal C, D'Agostino V, Loffredo R, et al. Targeting the multifaceted HuR protein, benefits and caveats. Curr Drug Targets. 2015;16(5):499-515.

11 Appendix

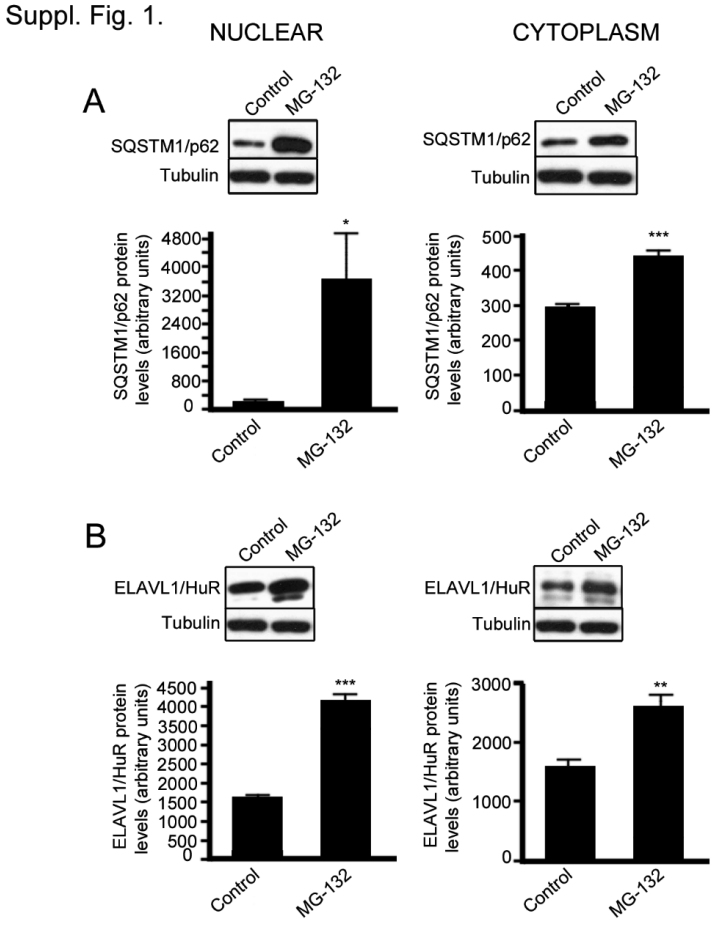

Supplemental figure 1. MG-132 induces ELAVL1/HUR and SQSTM1/p62 accumulation. A densitometric analysis of SQSTM1/p62 (A) and ELAVL1/HuR (B) proteins in the nuclear/perinuclear compartment (left panels) and in the cytoplasm (right panels) of ARPE-19 cells after exposure to MG-132 (5 μM) for 24 h. Control cells were exposed to solvent (DMSO). α-tubulin was used as a loading control. Results are expressed as means ± S.E.M.; *p<0.05, **p<0.01, ***p<0.001, control vs. treated cells, Student's t test; n=7.

Suppl. Fig. 2.

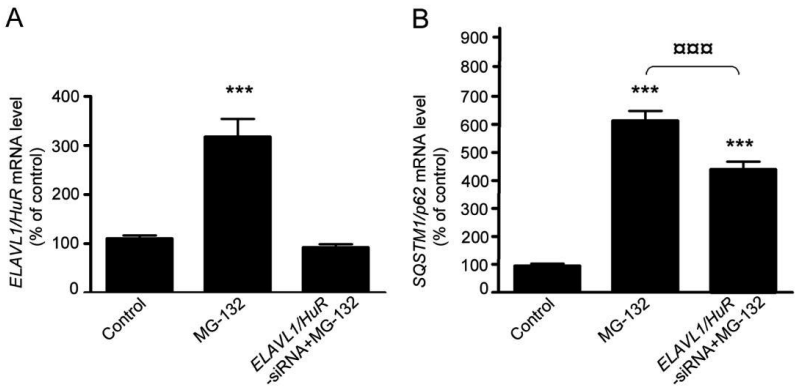

Supplemental figure 2. The 24 h MG-132-mediated upregulation of *SQSTM1/p62* mRNA expression is counteracted by the ELAVL1/HuR silencing. Determination of *ELAVL1/HuR* (A) and *SQSTM1/p62* (B) mRNA levels by real-time qPCR in the total homogenates of control (CTR), MG-132-treated cells (MG-132), and MG-132-treated ELAVL1/HuR silenced ARPE-19 cells (*ELAVL1/HuR*-siRNA+MG-132). *ELAVL1/HuR* and *SQSTM1/p62* mRNA levels in control cells were taken as 100% in (A) and (B), respectively. Control cells were exposed to solvent (DMSO). The values obtained from total cellular mRNA have been normalized to the level of *RPL6* mRNA and expressed as mean ± S.E.M. ***p<0.001 control vs. treated cells; ¤¤¤p<0.001 *ELAVL1/HuR*-siRNA+MG-132 vs. MG-132; Tukey's multiple comparison test; n = 3.

Suppl. Fig. 3.

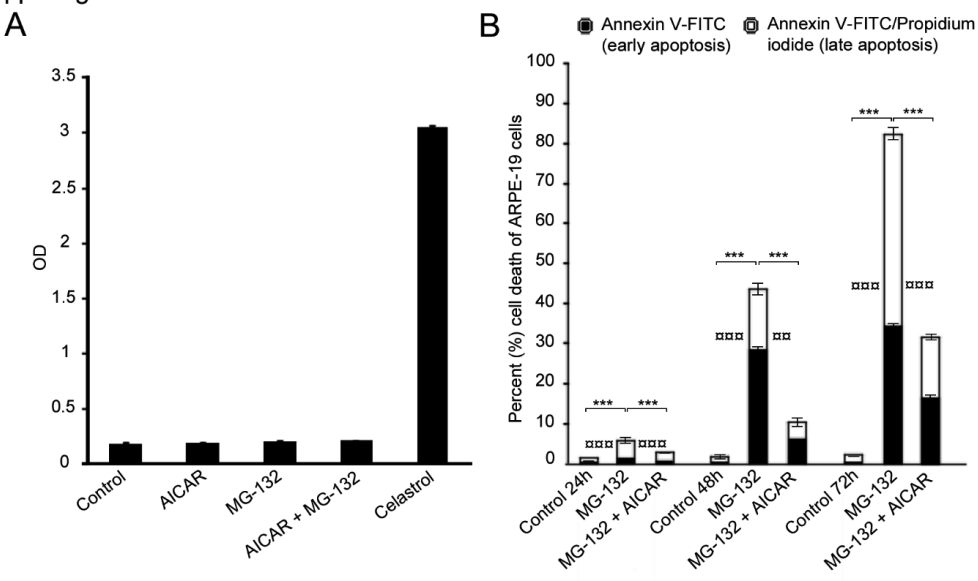

Supplemental figure 3. AICAR is well-tolerated and prevents cell death in MG-132 long-exposed ARPE-19 cells. (A): Maximum release of lactate dehydrogenase (LDH) enzyme in ARPE-19 cells treated with MG-132 5 µM and/or AICAR 2 mM for 24 h. Celastrol (10 µM) treatment is reported as a positive control since it induces maximum LDH release. Results are presented as mean optical density (OD) ± S.E.M. (n = 6, Mann-Whitney). (B): Cell death of ARPE-19 cells treated with MG-132 5 µM and/or AICAR 2 mM up to 72 h. Percent cell death of ARPE-19 cells (early apoptotic or annexin V-FITC+ cells −black bar- and late apoptotic or annexin V-FITC/propidium iodide+ cells −white bar) under different treatments. Data shown are mean+S.D. For late apoptosis ***$p<0.001$ Student's t test; n = 3. For early apoptosis ¤¤$p<0.01$, ¤¤¤$p<0.001$ Student's *t* test; n = 3.

NIKO KIVINEN

Age-related macular degeneration is the leading cause for visual impairment in aged individuals in the developed countries. Detrimental protein aggregation is a hallmark of age-related macular degeneration. This study was designed to examine the role of autophagy in the pathogenesis of age-related macular degeneration.

UNIVERSITY OF
EASTERN FINLAND

uef.fi

**PUBLICATIONS OF
THE UNIVERSITY OF EASTERN FINLAND**
Dissertations in Health Sciences

ISBN 978-952-61-2413-1
ISSN 1798-5706